SUPPLEMENTARY MATERIAL

Perchlorate-induced structural diversity in thiosemicarbazonecopper(II) complexes provides insights to understand the reactivity in acid and basic media.

Rubén Gil–García,[a] Gotzon Madariaga,*[b,c] Alondra Jiménez-Pérez,[a] Ignacio Herrán-Torres,[a] Adrián Gago-González,[a] María Ugalde,[a] Vaidas Januskaitis,[a] Joaquín Barrera-García,[a] Maite Insausti,[d] María S. Galletero,[e] Joaquín Borrás,[f] José Vicente Cuevas,[a] Rosa Pedrido,[g] Patricia Gómez-Saiz,[a] Luis Lezama,[d] and Javier García–Tojal*[a]

[a] Departamento de Química, Universidad de Burgos, 09001 Burgos, Spain

[b] Departamento de Física, Universidad del País Vasco, Aptdo. 644, 48080 Bilbao, Spain

[c] EHU Quantum Center, University of the Basque Country, UPV/EHU, E-48080 Bilbao, Spain.

[d] Servicio Central de Espectrometría de Masas, Universidad de Valencia, Av. Dr. Moliner 100, Burjassot, Valencia, Spain

[e] Servicio Central de Espectrometría de Masas, Universidad de Valencia, Av. Dr. Moliner 100, Burjassot, Valencia, Spain

[f] Departamento de Química Inorgánica, Facultad de Farmacia, Universidad de Valencia, 46100 Burjassot, Valencia, Spain

[g] Departamento de Química Inorgánica, Facultade de Química, Campus Vida, Universidade de Santiago de Compostela, 15782 Santiago de Compostela, Spain

Index

1. Title compounds of the Cu^{2+} / HL / ClO_4^- system

1. Figure captions

Figure S1.1. H-bonds (dotted red lines) for compounds ***1*** (a) and ***2*** (b). Hydrogen atoms have been omitted for clarity.

Figure S1.2. H-bonds (dotted grey lines) for compounds ***3*** (a) and ***4*** (b). Hydrogen atoms have been omitted for clarity.

Figure S1.3. H-bonds (dotted grey lines) for ***5***. Hydrogen atoms have been omitted for clarity.

Figure S1.4. π–π Stacking interactions for compounds ***1*** (a), ***2*** (b), ***3*** (c), ***4*** (d) and ***5*** (e).

Figure S1.5. Anion–π interactions for compounds ***1*** (a), ***3*** (b), ***4*** (c) and ***5*** (d).

Figure S1.6. CH–π interaction for compound ***4***.

Figure S1.7. FTIR ATR spectra of compounds ***1*** (a), ***2*** (b) and ***3*** (c).

Figure S1.8. FTIR ATR spectra of compounds ***4*** (a), and ***5*** (b).

Figure S1.9. IR spectra of HL (green), ***1*** (blue), and ***3*** (red). Rectangles highlight relevant bands in the free ligand absent or shifted in the metal complexes (green), and bands due to the perchlorate groups in the Cu(II) compounds, more intense than any of the ligand absorptions (black).

Figure S1.10. IR spectra of ***5*** (green), [Cu(HL)(NCS)](NO_3) (blue), and [{CuL(NCS)}$_2$] (red). See details in the manuscript.

Figure S1.11. ESI^+ mass spectrum of compound ***1*** in a dichloromethane / DMSO mixture solution.

Figure S1.12. ESI^+ mass spectrum of compound ***3*** in methanol.

Figure S1.13. ESI^+ mass spectrum of the $[Cu_2L_3](ClO_4)\cdot 3H_2O$ compound, analogous to complex ***4***, in methanol.

Figure S1.14. ESI^+ mass spectra of ***5*** in methanol and the corresponding blank (graphic at the bottom).

Figure S1.15. X-band EPR spectra at RT of compounds ***1*** (a), ***3*** (b), ***5*** (c) and the analogous to ***4*** with formula *$[Cu_2L_3](ClO_4)\cdot 3H_2O$* (d). The best fits are depicted in blue dotted lines, *g*-values are given in the main text (Experimental Section).

Figure S1.16. Q-band EPR spectra of compound ***5*** at RT in red; the best fit is represented with a blue dotted line, *g*-values are given in text (Experimental Section).

Figure S1.17. XRD patterns arisen from the crystal structures of compounds ***1***−***5*** (in blue) compared with powders aiming to reproduce ***4*** (*[Cu_2L_3](ClO$_4$)·3H_2O*, left column) and ***2*** (right column).

Figure S1.18. Comparison between diffractograms of powders aiming to reproduce ***4*** (*[Cu_2L_3](ClO$_4$)·3H_2O* analytical formula, in red) and ***2*** (*CuL(ClO$_4$)* analytical formula, in blue).

2. Table captions

Table S1.1. Selected bond distances (Å) and angles (°) of compounds ***1*** and ***2***.

Table S1.2. Selected bond distances (Å) and angles (°) of compounds ***3*** and ***5***.

Table S1.3. Selected bond distances (Å) and angles (°) of compound ***4***.

Table S1.4. Selected structural parameters (Å, º) and their comparison with thiosemicarbazonecopper(II) entities for tridentate deprotonated (CuL) or neutral ligands (CuHL).

Table S1.5. Selected hydrogen bonds (Å, º).

Table S1.6. π–π Stacking interactions.

Table S1.7. Anion–π interactions.

Table S1.8. CH–π interaction for compound ***4***.

Table S1.9. Selected IR bands for neutral and anionic thiosemicarbazone derivatives and proposed assignments. Bands of coligands and counterions are excluded.

3. Figures

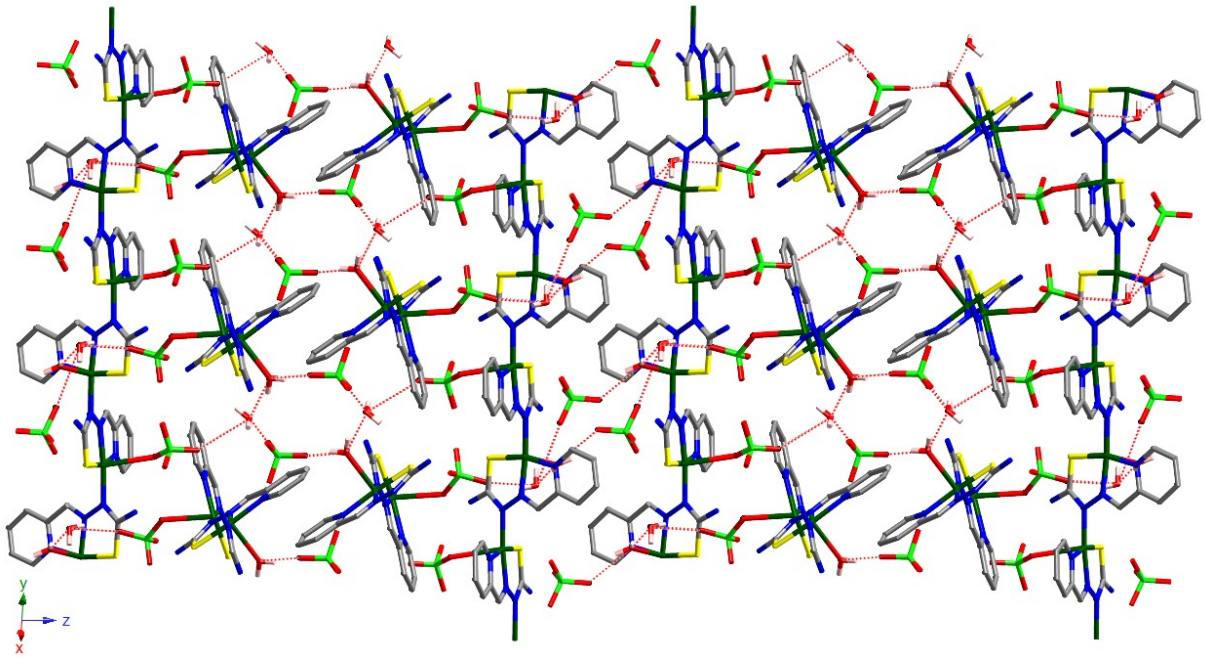

(a)

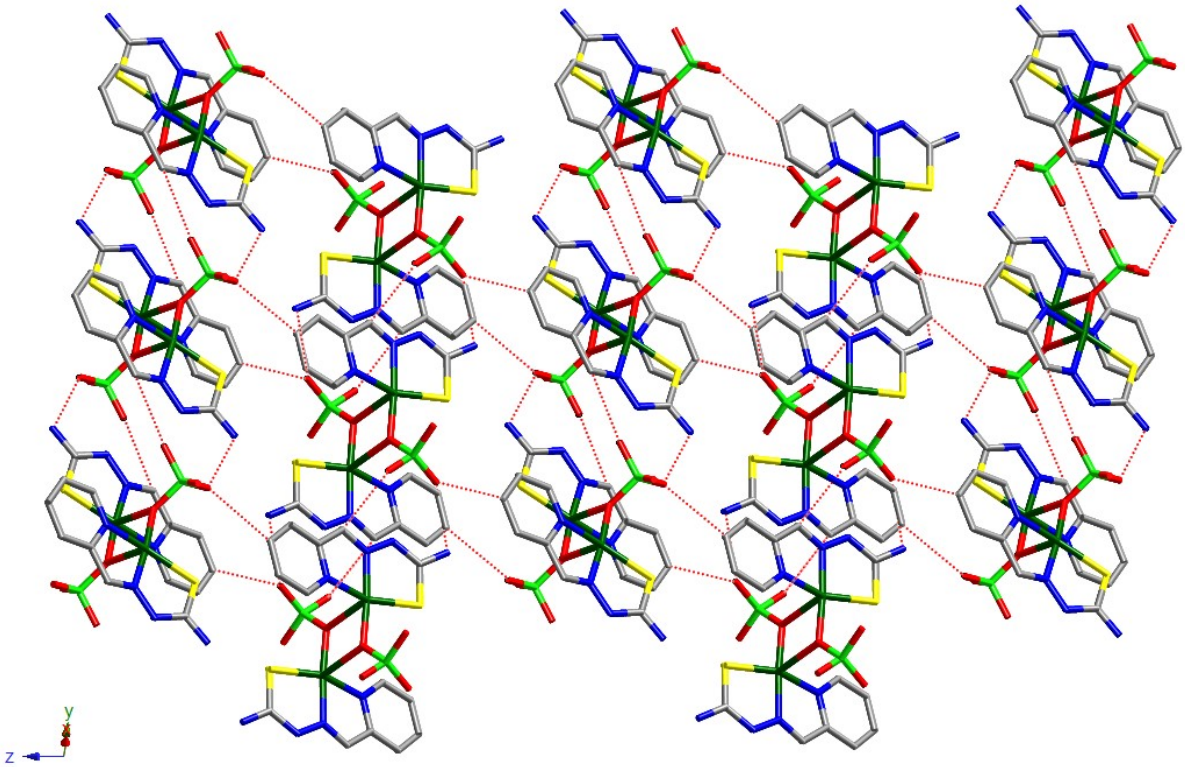

(b)

Figure S1.1. H-bonds (dotted red lines) for compounds ***1*** (a) and ***2*** (b). Hydrogen atoms have been omitted for clarity.

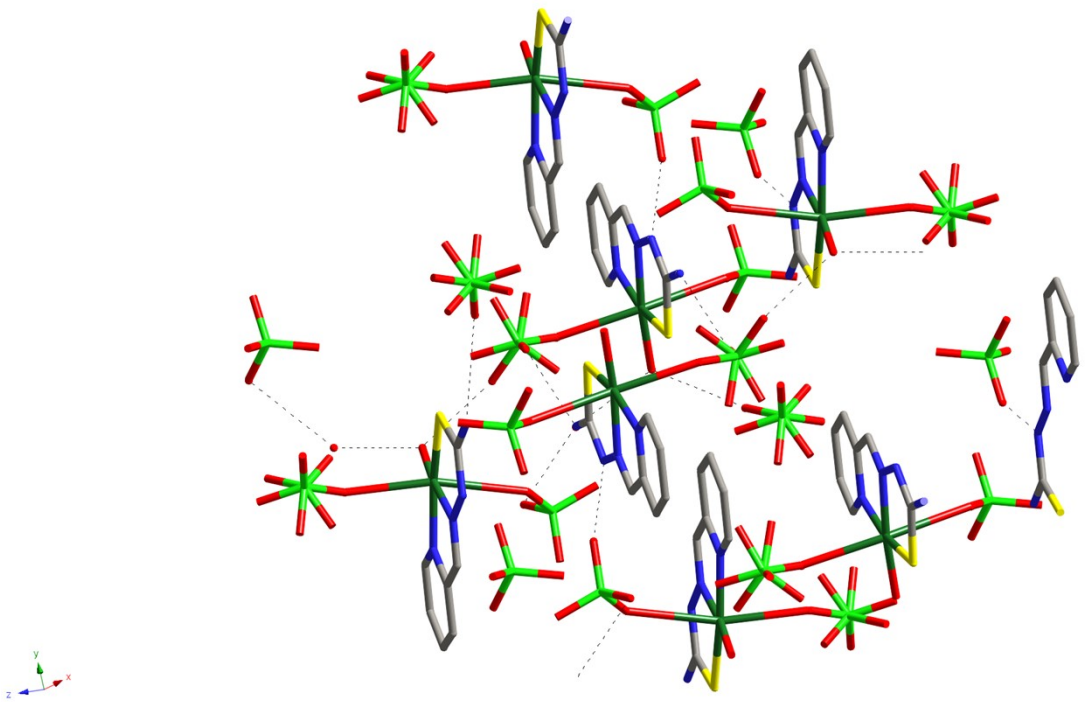

(a)

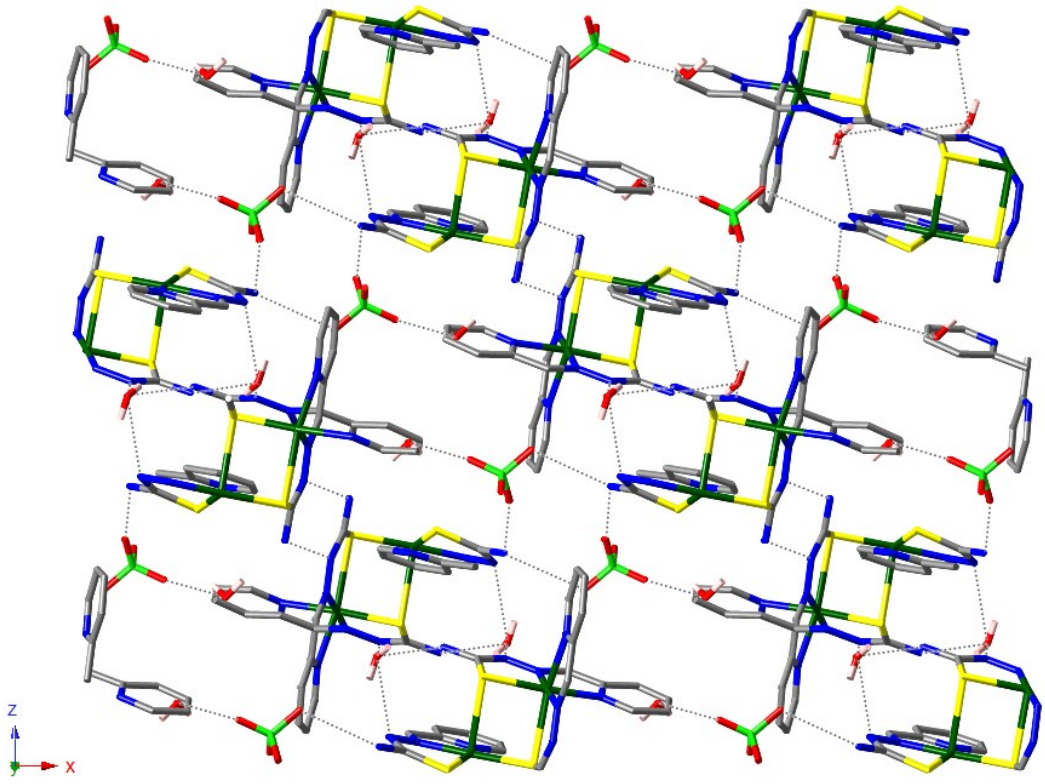

(b)

Figure S1.2. H-bonds (dotted grey lines) for compounds ***3*** (a) and ***4*** (b). Hydrogen atoms have been omitted for clarity.

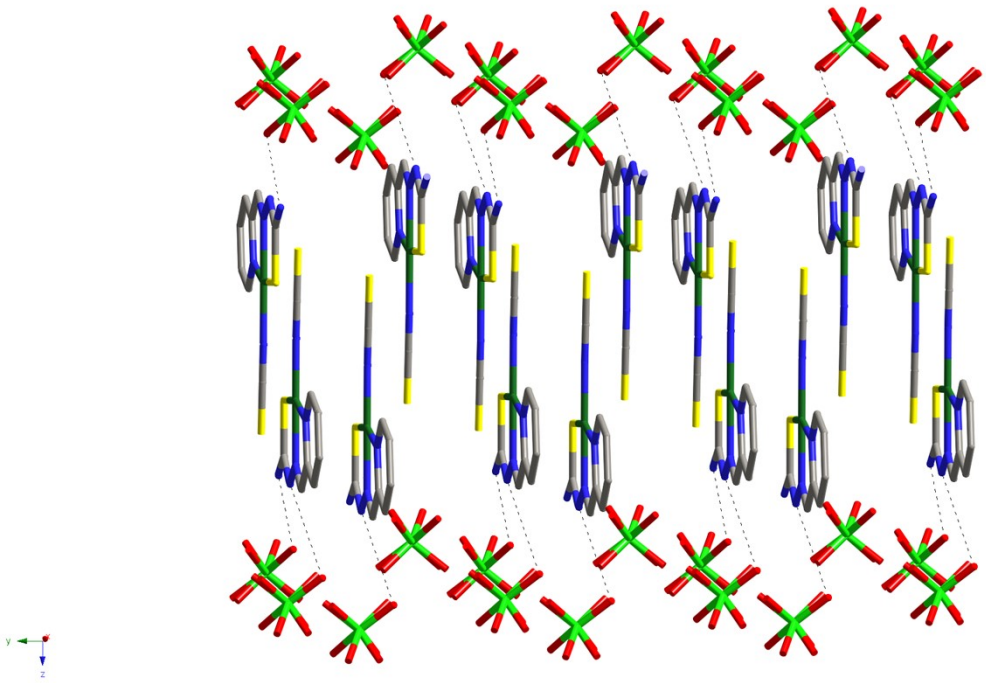

Figure S1.3. H-bonds (dotted grey lines) for ***5***. Hydrogen atoms have been omitted for clarity.

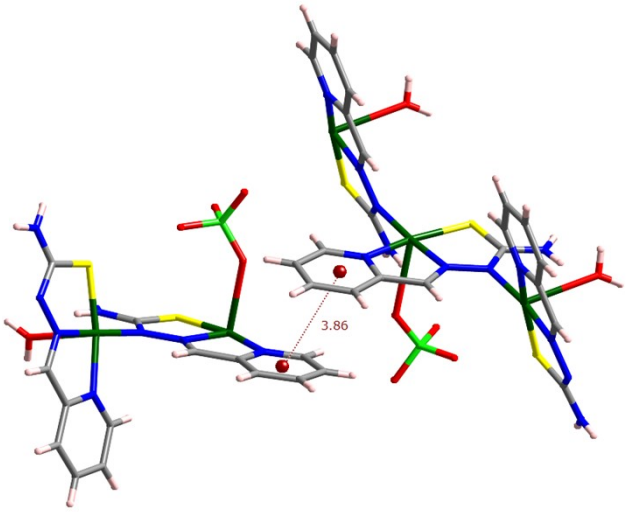

(a)

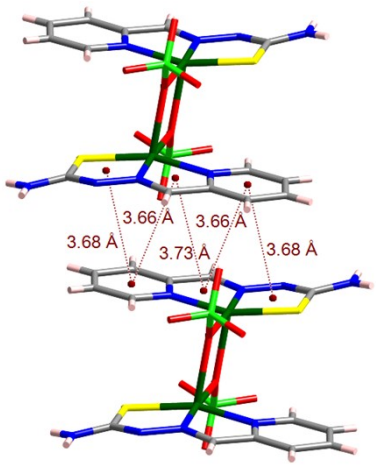

(b)

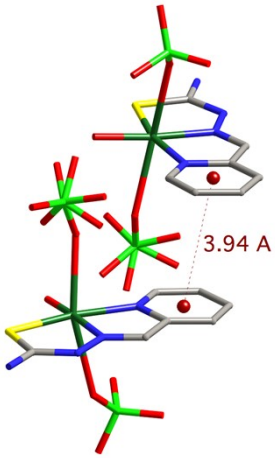

(c)

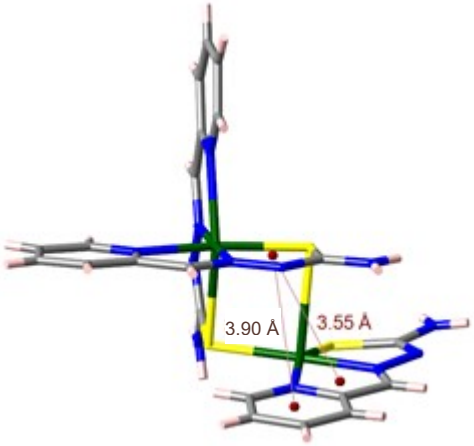

(d)

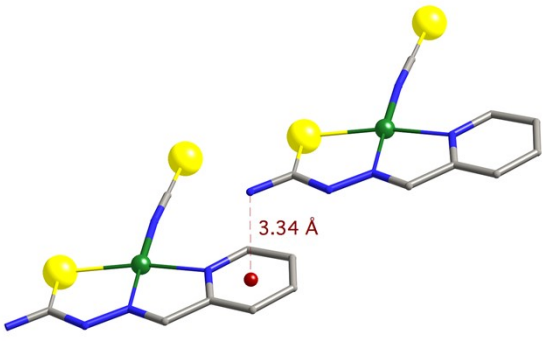

(e)

Figure S1.4. π–π Stacking interactions for compounds ***1*** (a), ***2*** (b), ***3*** (c), ***4*** (d) and ***5*** (e).

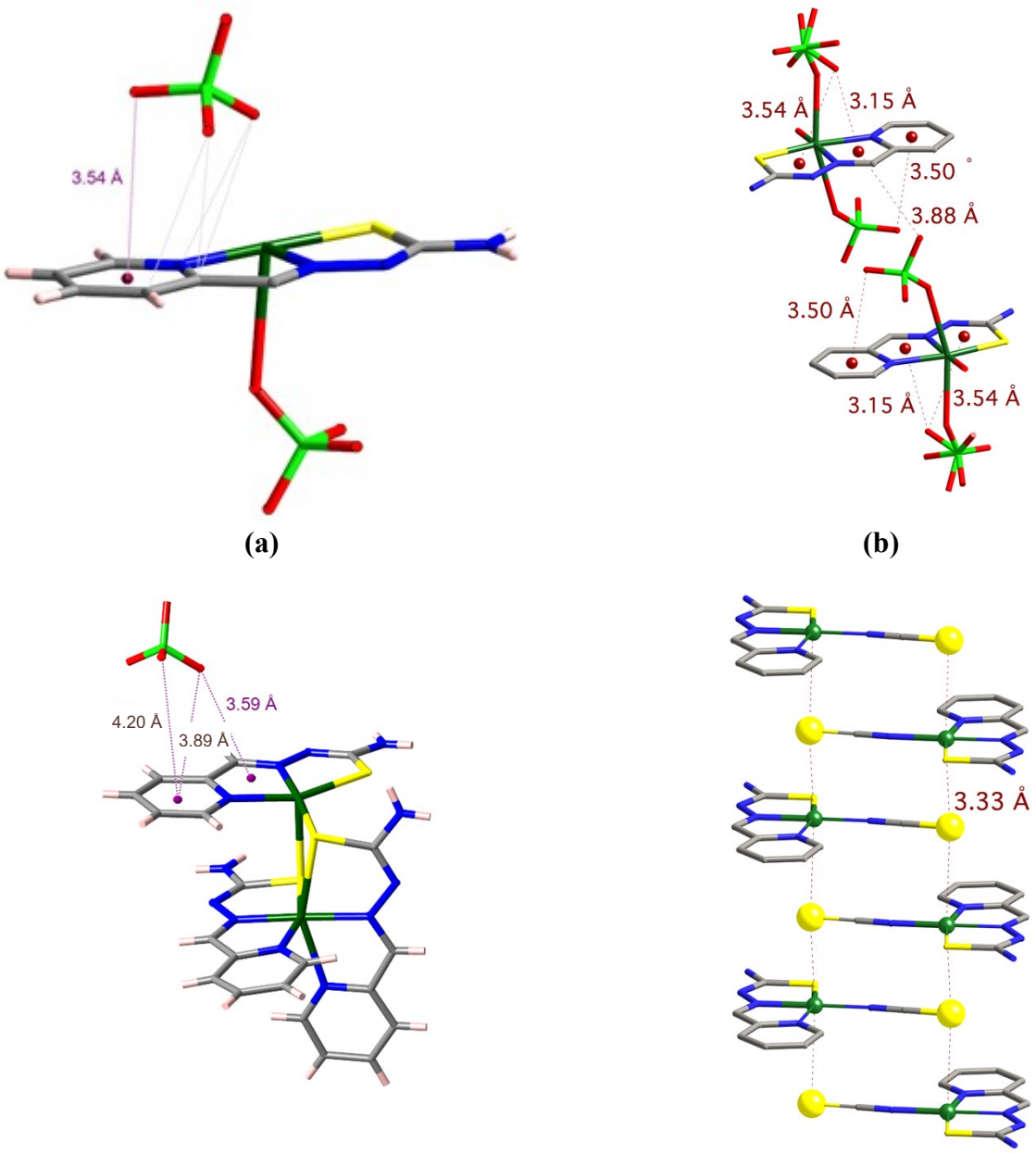

Figure S1.5. Anion–π interactions for compounds ***1*** (a), ***3*** (b), ***4*** (c) and ***5*** (d).

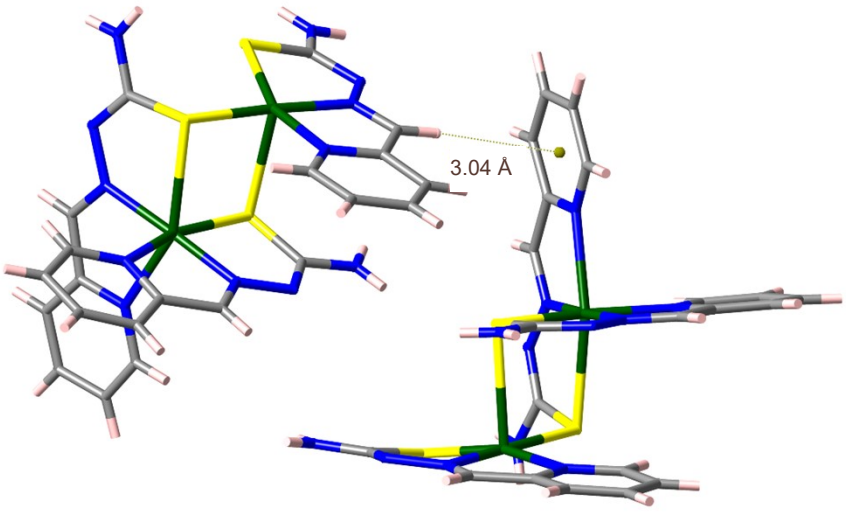

Figure S1.6. CH–π interaction for compound **4**.

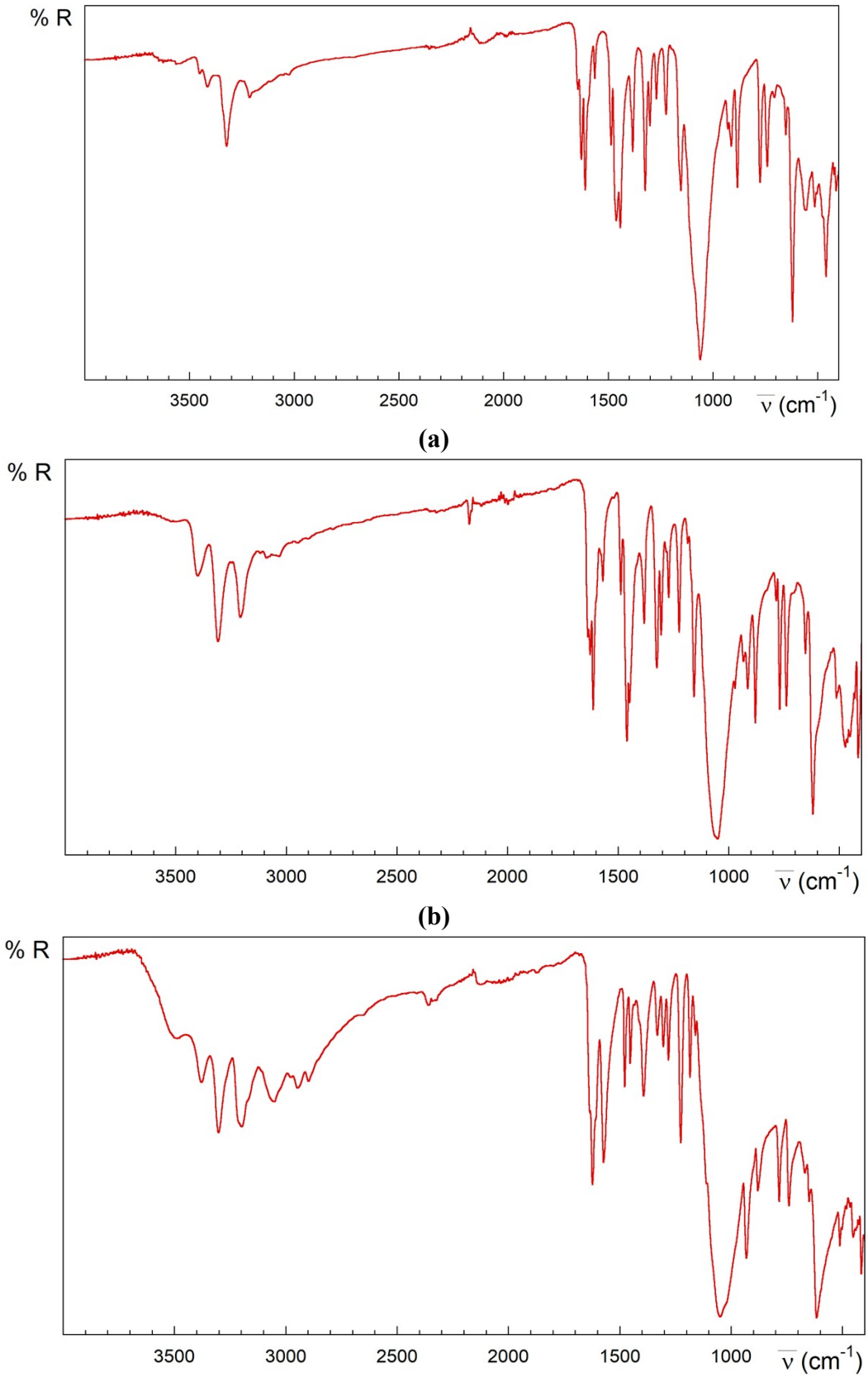

Figure S1.7. FTIR ATR spectra of compounds ***1*** (a), ***2*** (b) and ***3*** (c).

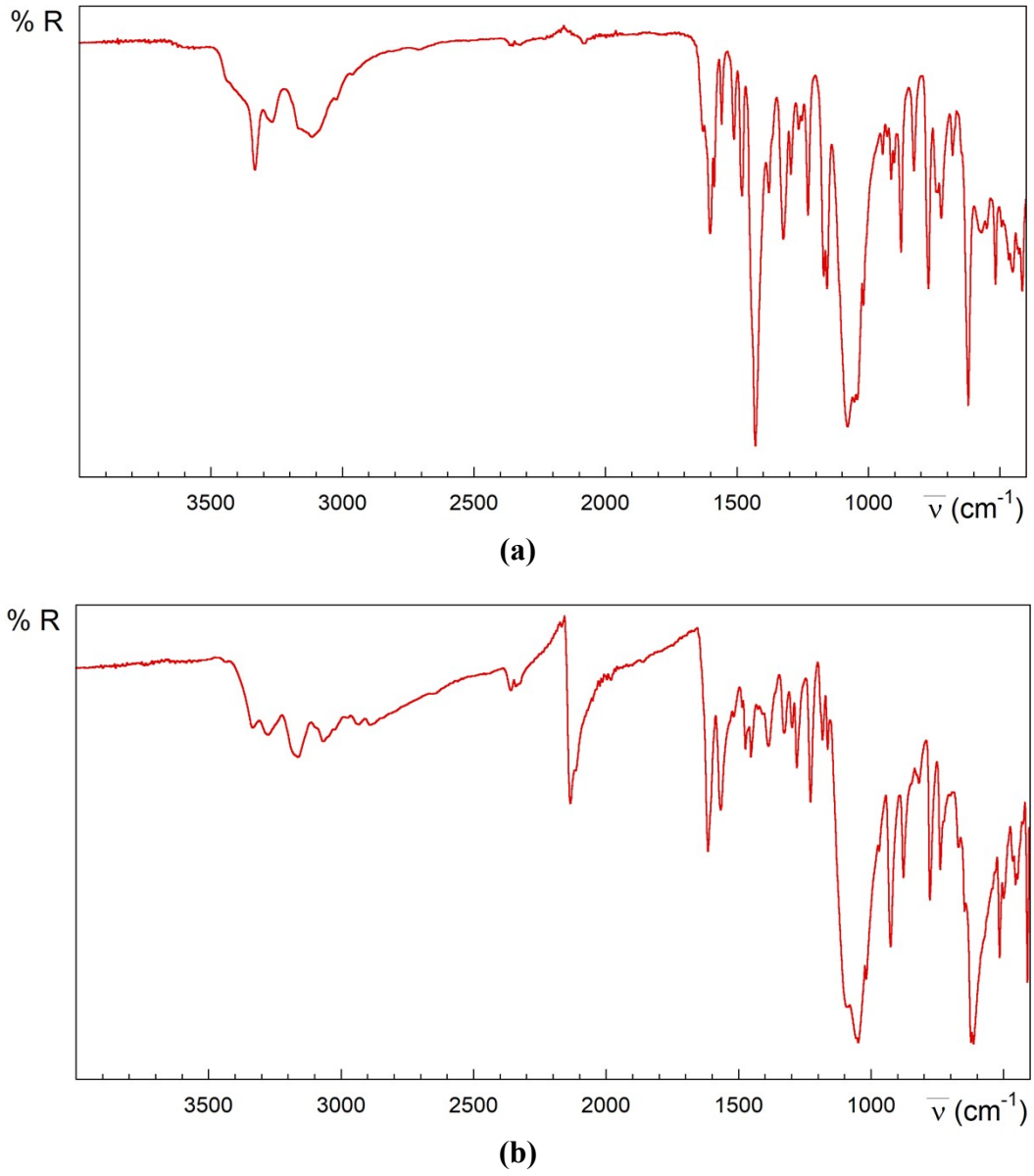

Figure S1.8. FTIR ATR spectra of compounds ***4*** (a), and ***5*** (b).

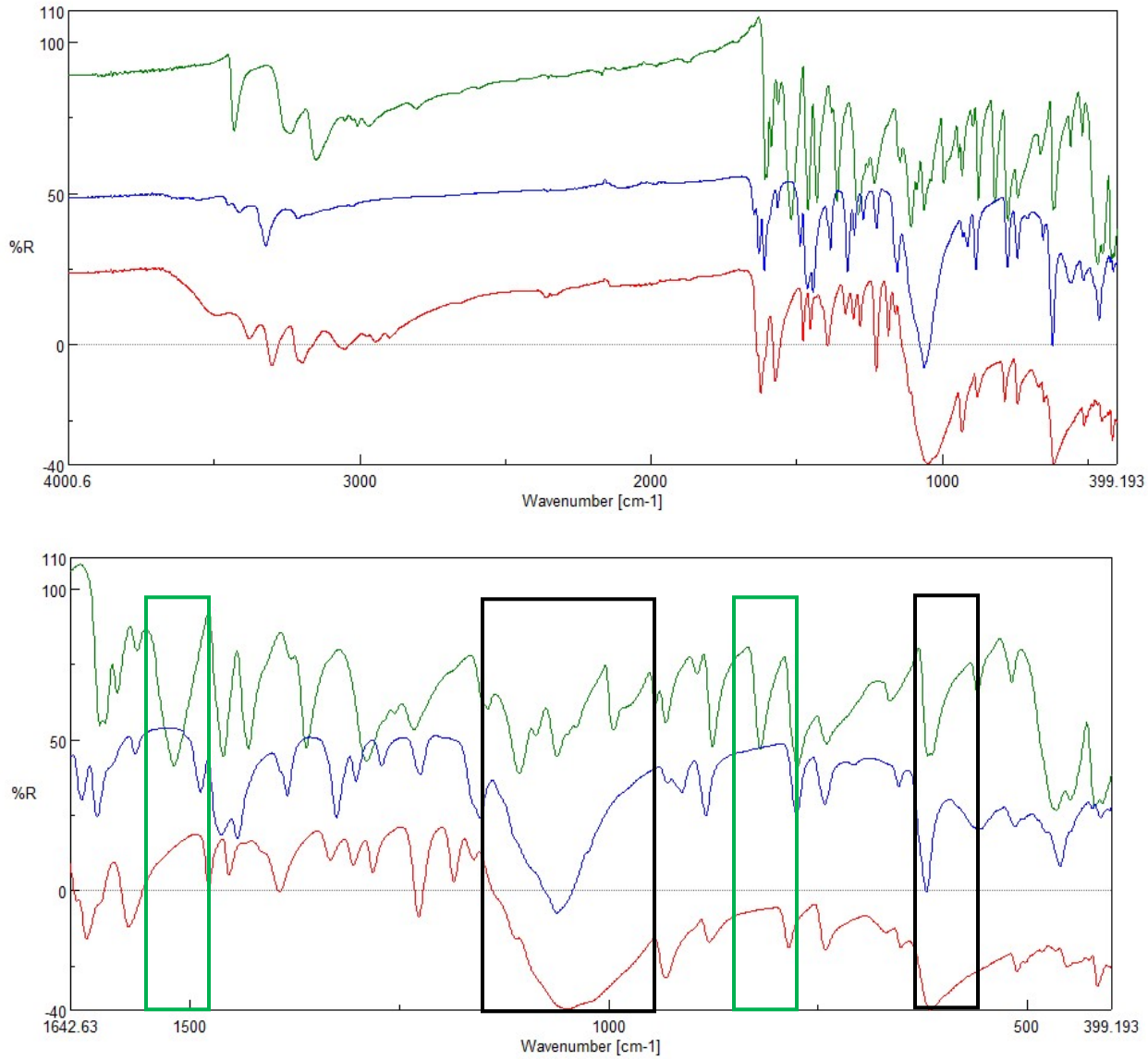

Figure S1.9. IR spectra of HL (green), ***1*** (blue), and ***3*** (red). Rectangles highlight relevant bands in the free ligand absent or shifted in the metal complexes (green), and bands due to the perchlorate groups in the Cu(II) compounds, more intense than any of the ligand absorptions (black).

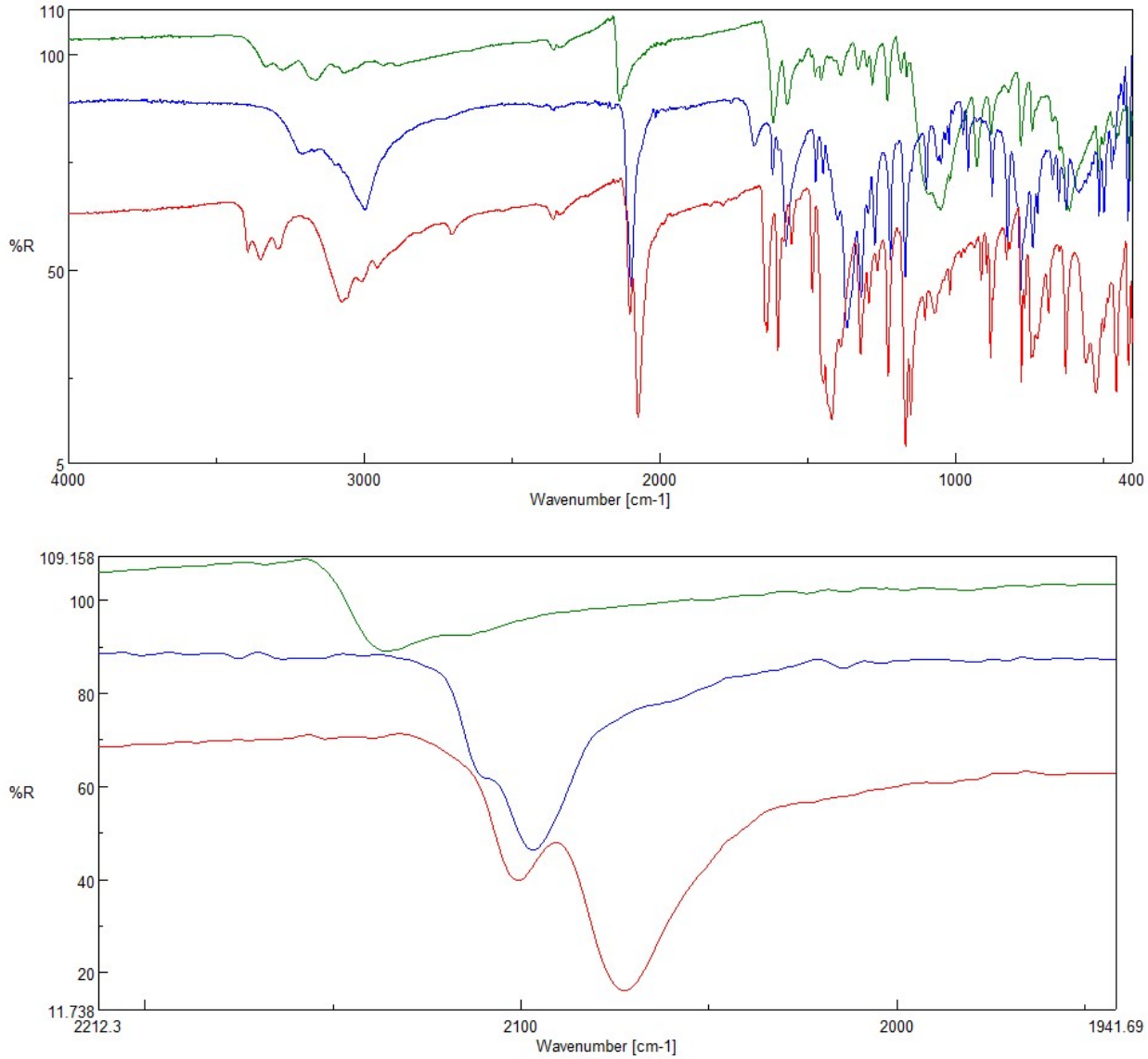

Figure S1.10. IR spectra of ***5*** (green), [Cu(HL)(NCS)](NO_3) (blue), and [{CuL(NCS)}$_2$] (red). See details in the manuscript.

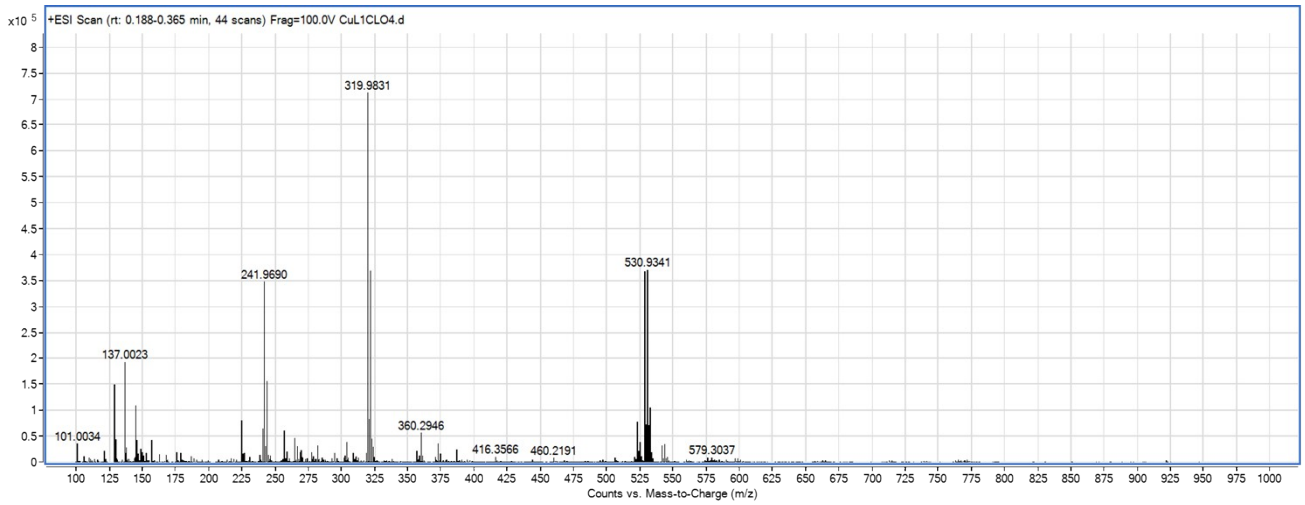

Figure S1.11. ESI$^+$ mass spectrum of compound ***1*** in a dichloromethane / DMSO mixture solution.

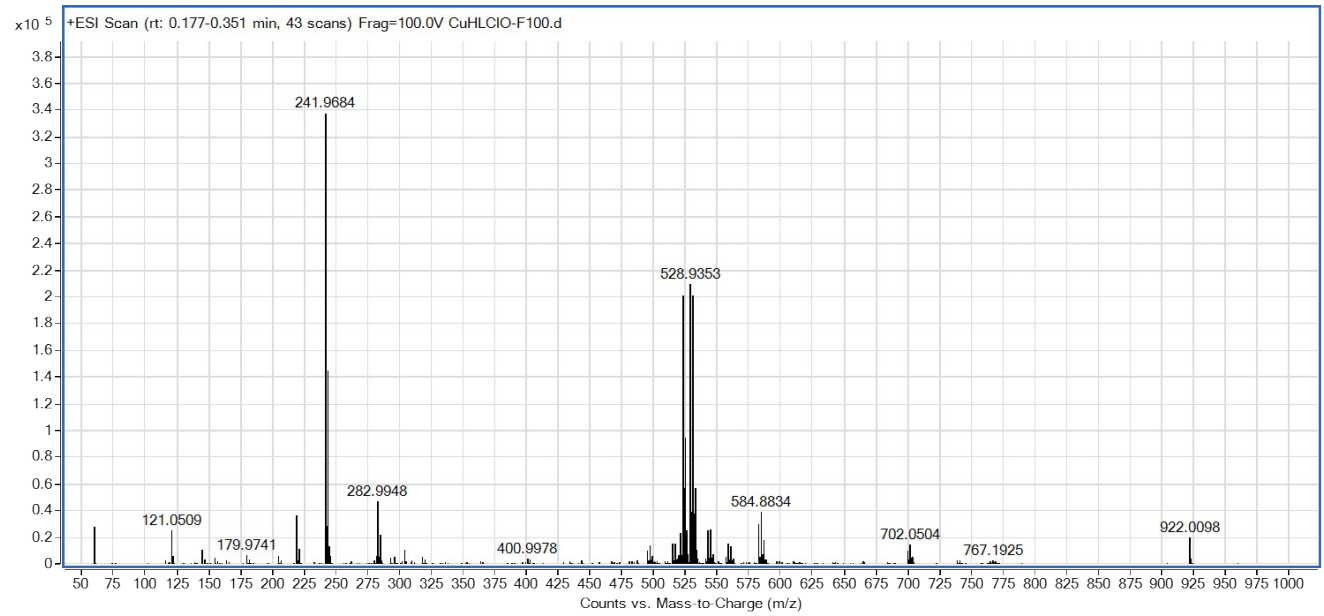

Figure S1.12. ESI$^+$ mass spectrum of compound ***3*** in methanol.

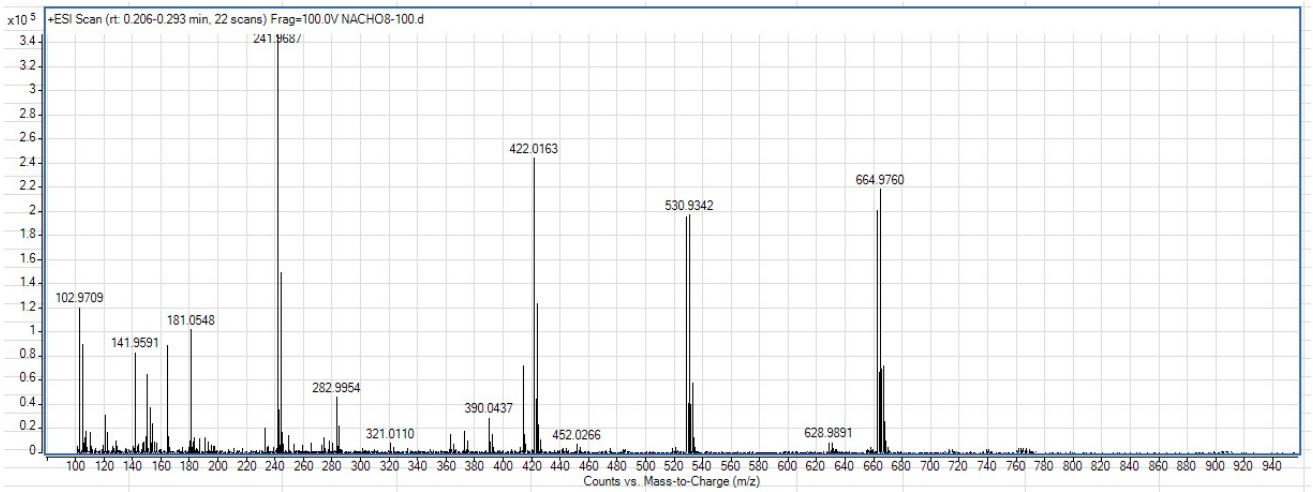

Figure S1.13. ESI$^+$ mass spectrum of the $[Cu_2L_3](ClO_4)\cdot 3H_2O$ compound, analogous to complex ***4***, in methanol.

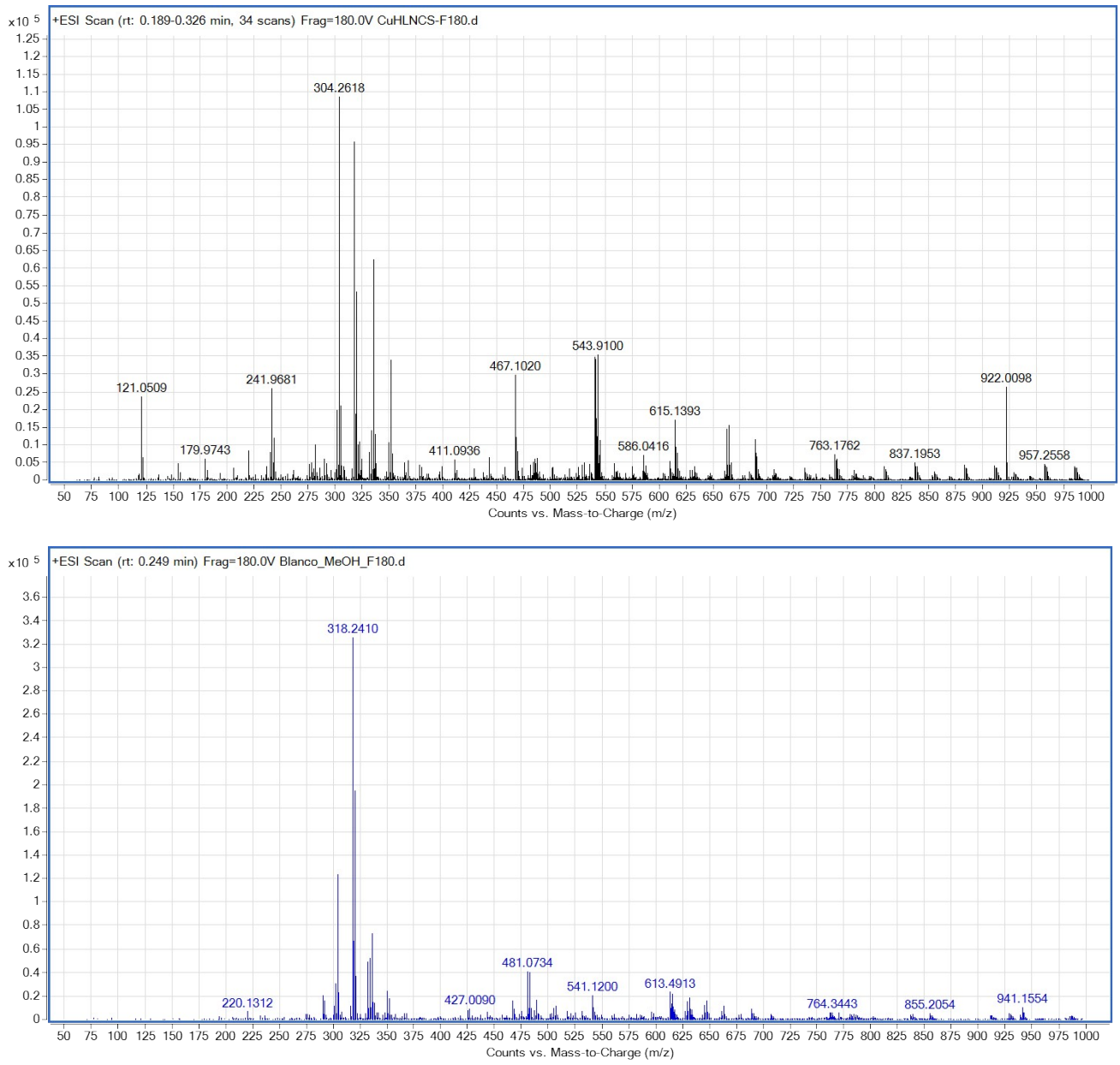

Figure S1.14. ESI$^+$ mass spectra of ***5*** in methanol and the corresponding blank (graphic at the bottom).

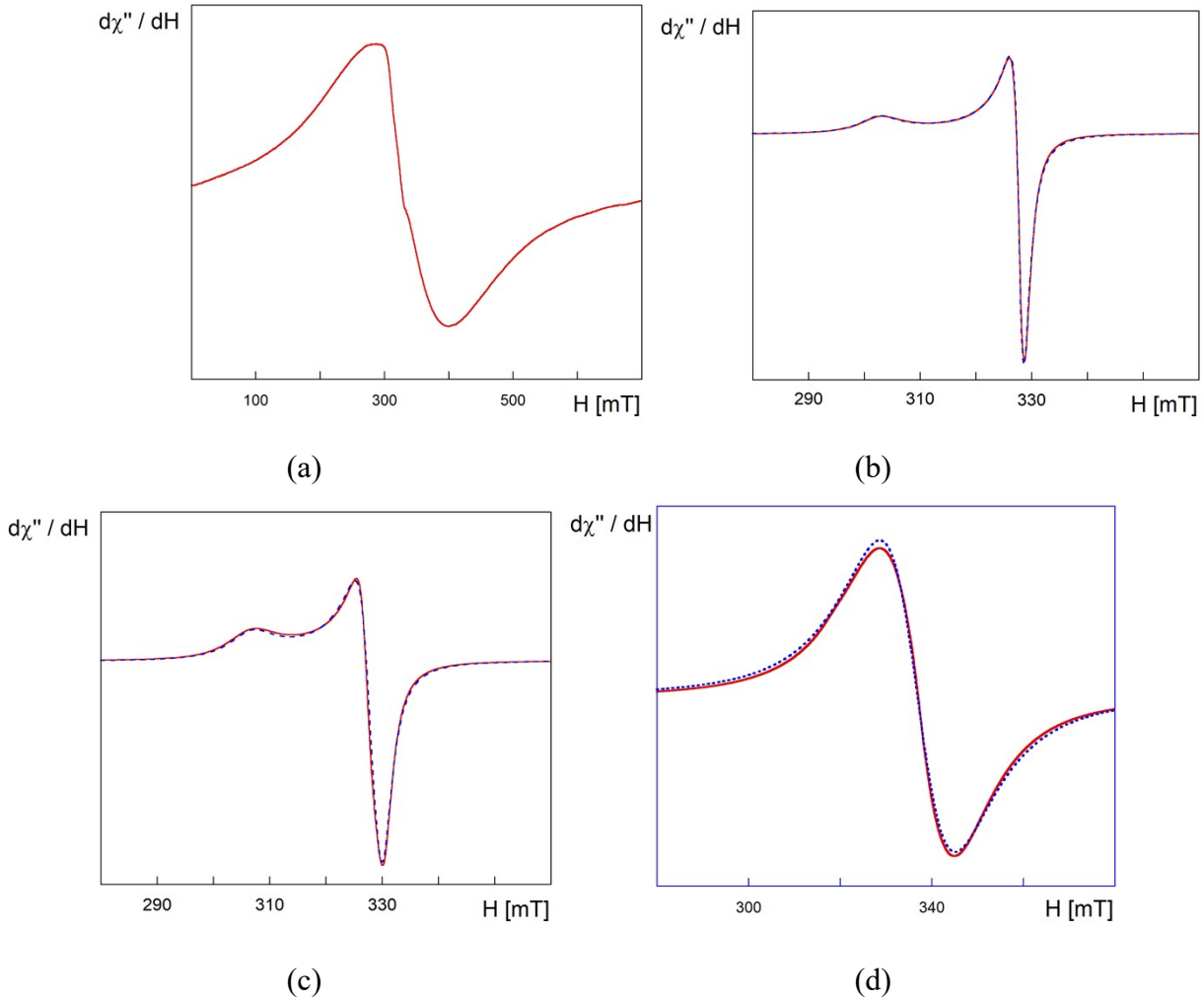

Figure S1.15. X-band EPR spectra at RT of compounds ***1*** (a), ***3*** (b), ***5*** (c) and the analogous to ***4*** with formula *[Cu_2L_3](ClO$_4$)·3H_2O* (d). The best fits are depicted in blue dotted lines, *g*-values are given in the main text (Experimental Section).

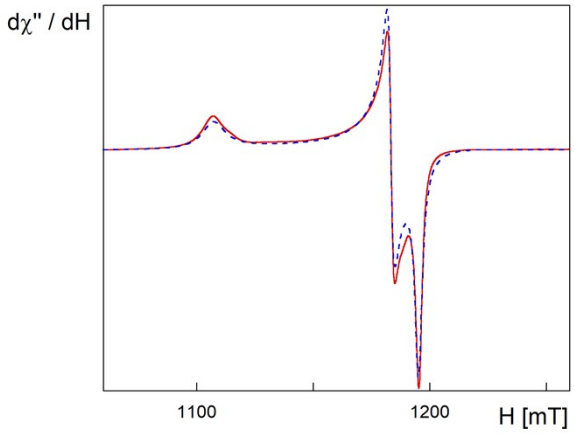

Figure S1.16. Q-band EPR spectra of compound ***5*** at RT in red; the best fit is represented with a blue dotted line, *g*-values are given in text (Experimental Section).

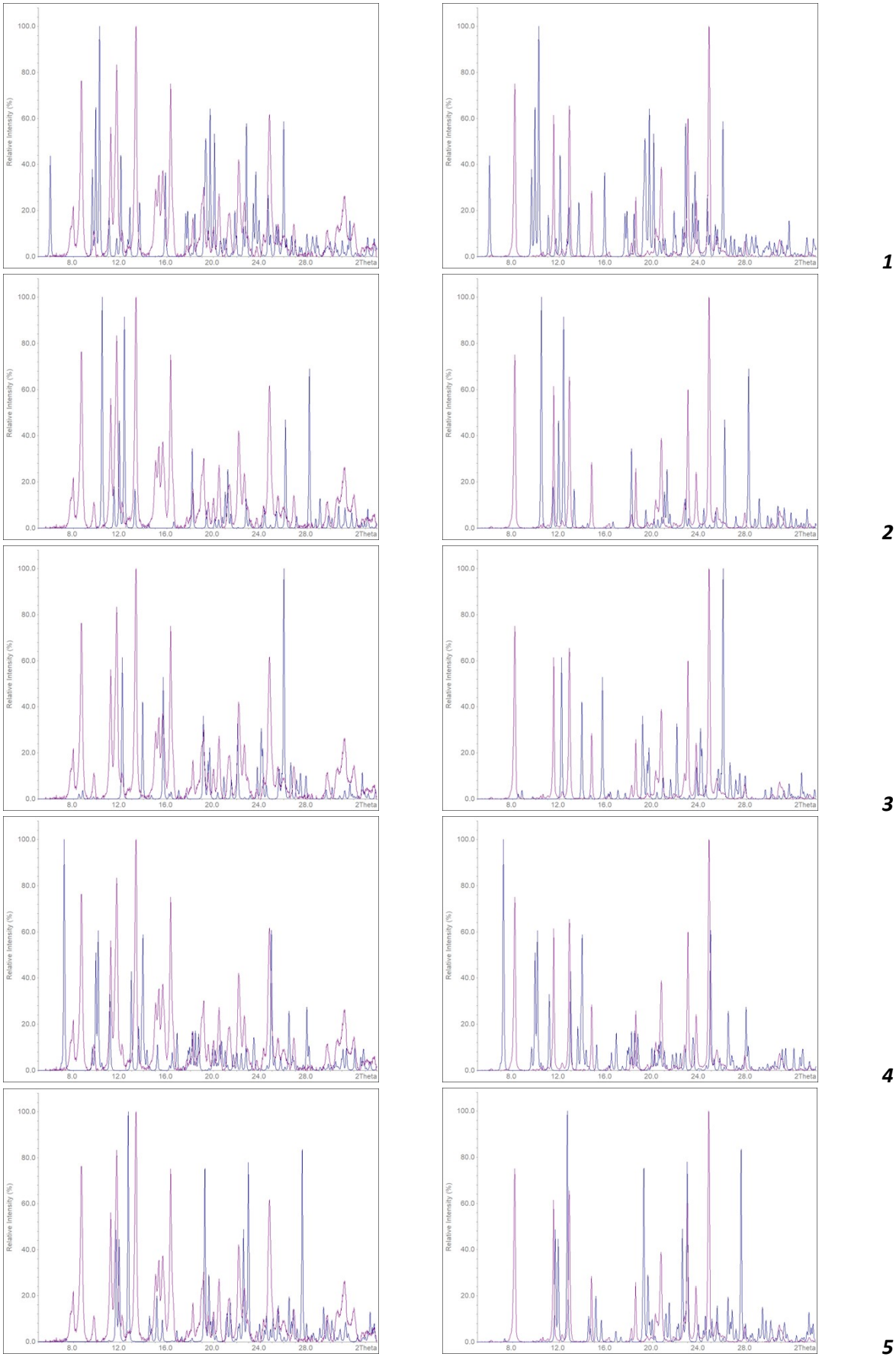

Figure S1.17. XRD patterns arisen from the crystal structures of compounds ***1***−***5*** (in blue) compared with powders aiming to reproduce ***4*** (*[Cu₂L₃](ClO₄)·3H₂O*, left column) and ***2*** (right column).

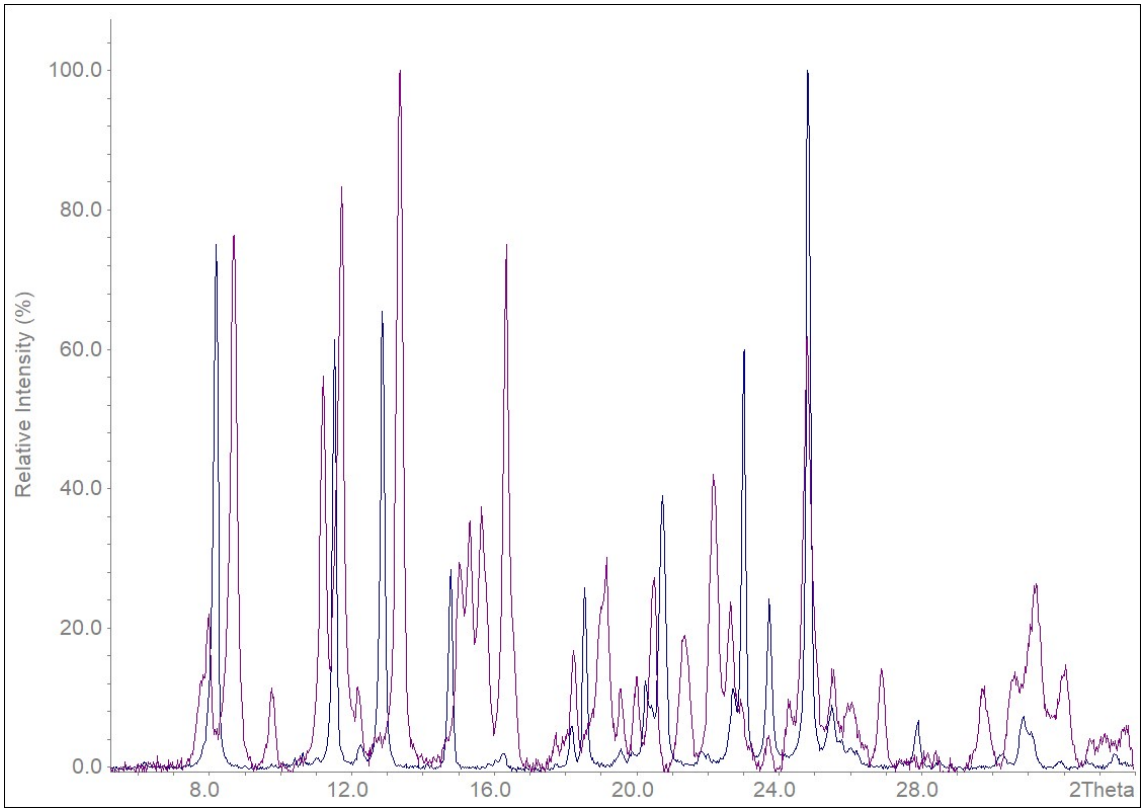

Figure S1.18. Comparison between diffractograms of powders aiming to reproduce ***4*** (*[Cu_2L_3](ClO_4)·3H_2O* analytical formula, in red) and ***2*** (*CuL(ClO_4)* analytical formula, in blue).

4. Tables

Table S1.1. Selected bond distances (Å) and angles (°) of compounds ***1*** and ***2***.

		1		**2**
		Entity 1 $[CuL(ClO_4)]$	**Entity 2** $[CuL(H_2O)]^+$	$[CuL(ClO_4)]$
Cu–N	Cu–N1	1.995(3)	2.012(3)	2.015(7)
	Cu–N2	1.975(3)	1.972(3)	1.954(6)
	Cu–N3’	2.004(3)	2.005(3)	–
Cu–S	Cu–S	2.2339(14)	2.2428(15)	2.283(3)
Cu–O	$Cu–O_{ClO4}$	2.678(3)	–	1.920(5)
	$Cu–O'_{ClO4}{}^{i}$	–	–	2.324(6)
	$Cu–O_{H2O}$	–	2.546(3)	–
C–N	C6–N2	1.277(4)	1.282(5)	1.281(10)
	C7–N3	1.339(4)	1.349(5)	1.347(10)
	C7–N4	1.328(4)	1.312(5)	1.324(10)
N–N	N2–N3	1.375(4)	1.379(4)	1.373(9)
C–S	C7–S	1.730(3)	1.726(4)	1.707(8)
N–Cu–O	$N2–Cu–O_{ClO4}$	–	–	175.3(3)
N–Cu–S	N1–Cu–S	165.70(9)	165.63(10)	160.47(19)
N–Cu–N	N2–Cu–N3’	174.65(11)	171.44(12)	–
Cu–N–N	Cu–N2–N3	122.61(18)	123.4(2)	119.9(5)
N–N–C	N2–N3–C7	111.9(2)	111.1(3)	115.7(6)
N–C–N	N3–C7–N4	118.2(3)	118.0(3)	116.4(7)
S–C–N	S–C7–N3	124.6(2)	124.7(3)	122.7(5)
	S–C7–N4	117.1(3)	117.3(3)	120.9(6)

(i = –x+1/2, –y+1/2, –z).

Table S1.2. Selected bond distances (Å) and angles (°) of compounds ***3***and ***5***.

		3 $[Cu(HL)(OClO_3)_2(OH_2)]$	**5** $[Cu(HL)(NCS)]^+$
Cu–N	Cu–N1	1.998(6)	2.013(7)
	Cu–N2	1.950(4)	1.939(5)
	Cu–N5	–	1.888(6)
Cu–S	Cu–S	2.282(2)	2.290(2)
Cu–O	$Cu–O_{ClO4}$	2.440(12)	–
	$Cu–O'_{ClO4}$	2.697(5)	–
	$Cu–O_{H2O}$	1.933(5)	–
C–N	C6–N2	1.273(7)	1.270(9)
	C7–N3	1.338(7)	1.329(10)
	C7–N4	1.314(8)	1.315(10)
N–N	N2–N3	1.355(7)	1.347(9)
C–S	C7–S	1.694(6)	1.694(7)
N–Cu–O	$N2–Cu–O_{ClO4}$	102.7(4)	–
N–Cu–S	N1–Cu–S	165.29(16)	164.3(2)
N–Cu–N	N2–Cu–N5	–	178.2(3)
Cu–N–N	Cu–N2–N3	119.9(3)	120.7(4)
N–N–C	N2–N3–C7	118.1(4)	117.7(6)
N–C–N	N3–C7–N4	117.7(5)	116.8(6)
S–C–N	S–C7–N3	120.7(5)	121.2(6)
	S–C7–N4	121.6(4)	122.0(6)

Table S1.3. Selected bond distances (Å) and angles (°) of compound **4**.

		4		
		Cu1L(1)	**Cu2L(2)**	**Cu2L(3)**
Cu–N	Cu–N1	2.043(3)	2.307(4)	2.080(4)
	Cu–N2	1.973(3)	2.046(3)	1.973(3)
Cu–S	Cu–S	2.2591(14)	2.7361(13)	2.3269(14)
	Cu–S(2)	2.2848(14)	–	–
	Cu–S(3)	2.8329(13)	–	–
C–N	C6–N2	1.278(6)	1.310(6)	1.282(6)
	C7–N3	1.327(6)	1.316(6)	1.312(6)
	C7–N4	1.340(7)	1.356(5)	1.324(6)
N–N	N2–N3	1.355(5)	1.357(5)	1.368(5)
C–S	C7–S	1.736(5)	1.755(4)	1.755(4)
N–Cu–S	N1–Cu–S	159.94(10)	153.37(10)	162.72(12)
	N2–Cu–S(2)	175.05(12)	–	–
Cu–N–N	Cu–N2–N3	122.4(3)	128.9(3)	124.7(2)
N–N–C	N2–N3–C7	112.1(4)	115.3(4)	112.9(3)
N–C–N	N3–C7–N4	117.7(5)	114.9(4)	118.0(4)
S–C–N	S–C7–N3	124.9(4)	129.4(3)	124.8(4)
	S–C7–N4	117.3(4)	115.6(3)	117.1(3)

Table S1.4. Selected structural parameters (Å, º) and their comparison with thiosemicarbazonecopper(II) entities for tridentate deprotonated (CuL) or neutral ligands (CuHL)[1].

	C7–S	Cu···N3	N2···C7	Cu–N2–N3	N2–N3–C7	S–C7–N3	S–C7–N4
1: $[CuL(ClO_4)]$ (1) and $[CuL(H_2O)]^+$ (2)							
(1)	1.730	2.953	2.249	122.6	111.9	124.6	117.1
(2)	1.726	2.964	2.250	123.4	111.1	124.7	117.3
2: $[\{CuL(ClO_4)\}_2]$							
	1.707	2.894	2.302	119.9	115.7	122.7	120.9
3: $[Cu(HL)(OClO_3)_2(OH_2)]$ H_2O							
	1.694	2.876	2.310	119.9	118.1	120.7	121.6
4: $[CuL]^+$ (1) and $[CuL_2]$ (2) and (3)							
(1)	1.736	2.932	2.224	122.4	112.1	124.9	117.3
(2)	1.755	3.084	2.259	128.9	115.3	129.4	115.6
(3)	1.755	2.973	2.234	124.7	112.9	124.8	117.1
5: $[Cu(HL)(NCS)](ClO_4)$							
	1.694	2.870	2.290	120.7	117.7	121.2	122.0
CuL	**1.71–1.77**	**2.88–2.99**	**2.20–2.28**	**118–126**	**110–115**	**123–128**	**113–121**
CuHL	**1.69–1.72**	**2.86–2.93**	**2.31–2.36**	**115–122**	**116–121**	**120–123**	**120–124**

Table S1.5. Selected hydrogen bonds (Å, º).

Compound	D–H···A	d (D–H)	d (H···A)	d (D···A)	∠ (DHA)
1	N14–H141···O1W	0.860	2.09	2.911(5)	161
	N24–H242···O22	0.860	2.29	3.064(6)	150
	O1W–H11W···O2W	0.850	2.02	2.812(7)	155(3)
	O2W–H22W···O23	0.850	2.61	3.098(8)	118(4)
	N14–H142···O12^{ii}	0.860	2.11	2.949(5)	167
	O2W–H21W···O11^{ii}	0.850	2.58(4)	3.358(8)	154(6)
	O1W–H12W···O13^{iii}	0.850	2.08(3)	2.879(6)	156(2)
	C26–H26···O14^{iv}	0.930	2.43	3.328(5)	161
	N24–H241···O21^{v}	0.860	2.33	3.071(5)	144
	N24–H241···O24^{v}	0.860	2.32	2.988(5)	135
2	N4–H4A···O13^{vi}	0.860	1.99	2.842(9)	168
	C6–H6···O14^{vi}	0.930	2.60	3.240(9)	127
	N4–H4B···O11^{v}	0.860	2.10	2.916(9)	159
	C3–H3···O13^{vii}	0.930	2.36	3.276(11)	168
3	N3– H3N3···O41^{vii}	0.860	1.91	2.739(9)	161
	O1W– H1O1···O12	0.85(6)	2.60(6)	2.981(18)	109(5)
	O1W– H1O1···O2W^{viii}	0.85(6)	1.88(7)	2.716(6)	172(5)
	O1W– H2O1···O32^{ix}	0.85(5)	2.05(5)	2.889(13)	169(7)
	O2W– H1O2···O21	0.85(2)	2.27(3)	2.998(7)	143(5)
	O2W– H1O2···O31	0.85(2)	2.39(4)	3.124(7)	145(4)
	O2W– H1O2···O12^{ix}	0.85(2)	2.52(4)	2.841(7)	104(2)
	N4– H4A···O11^{x}	0.860	2.27	2.910(7)	131
	N4– H4A···O41^{vii}	0.860	2.47	3.163(8)	139
	N4– H4B···O42^{xi}	0.860	2.12	2.968(8)	166
	C2– H2···O22^{xii}	0.930	2.54	3.30(2)	139
	C3– H3···O42^{xii}	0.930	2.49	3.347(10)	152
4	C11–H11···S12	0.930	2.80	3.348(4)	119
	C32–H32···O2	0.930	2.55	3.308(9)	139
	O2W–H1W2···O4	0.849(19)	2.20(2)	2.919(14)	142.7(18)
	N43–H43B···O1W^{xiii}	0.860	2.07	2.919(5)	168
	N41–H41A···O1^{xiii}	0.860	2.28	3.141(10)	175

	N41–H41B···O3^{xiv}	0.860	2.18	2.877(9)	138
	N42–H42A···N32^{xv}	0.860	2.38	3.163(6)	152
	O1W–H1W1···N33^{vi}	0.85(2)	2.196(10)	2.897(4)	140(3)
	O1W–H2W1···N31^{xvi}	0.844(11)	2.196(8)	2.932(5)	145.6(18)
5	N3–H3A···O1^{xvii}	0.860	2.39	3.150(11)	147
	N3–H3A···O4^{xvii}	0.860	2.19	2.980(17)	154
	N3–H3A···O1^{xviii}	0.860	2.39	3.150(11)	147
	N3–H3A···O4^{xviii}	0.860	2.19	2.980(17)	154
	N4–H4A···S2^{xix}	0.860	2.61	3.432(7)	162
	N4–H4B···O3^{iv}	0.860	2.26	2.902(12)	132
	N4–H4B···O3^{xx}	0.860	2.26	2.902(12)	132
	C3–H3···O2^{xxi}	0.930	2.42	3.316(19)	162
	C3–H3···O2^{xxii}	0.930	2.42	3.316(19)	162

Table S1.6. π–π Stacking interactions.

Compound	i	j	DC	ANG	DZ	DXY	DS	DZ'	DXY'	DS'
1	5	5[xxiii]	3.858(3)	11.19(17)	3.5604(14)	1.485	3.691	3.5604(14)	1.485	3.691
2	3	2[xxiv]	3.678(5)	9.6(3)	3.290(2)	1.645	3.637	3.436(3)	1.313	–
	3	1[xxiv]	3.661(6)	3.2(4)	3.425(3)	1.292	3.897	3.402(3)	1.352	3.672
	1	1[xxiv]	3.730(5)	0.0(3)	3.382(3)	1.571	3.959	3.383(3)	1.571	3.959
3	3	3[xxv]	3.940(5)	0.9(3)	3.430(3)	1.938	3.466	3.430(3)	1.938	3.47
4	6	7	3.902(2)	8.28(17)	3.1237(12)	2.339	3.647	3.4008(18)	1.913	–
	8	7	3.550(2)	9.32(14)	3.0600(12)	1.799	4.980	3.0851(14)	1.755	–
5	3	4[xxi]	3.341	0.00	3.285	0.609	3.69	3.285	0.609	3.298

1: Chelating ring. Considered atoms: Cu, N2, C6, C5 and N1.

2: Chelating ring. Considered atoms: Cu, N2, N3, C7 and S1.

3: Pyridine ring. Considered atoms: N1, C1, C2, C3, C4 and C5.

4: N4 atom of Thioamide fragment: N4, C7, S and N3.

5: Pyridine ring. Considered atoms: N11, C11, C12, C13, C14 and C15.

6: Pyridine ring. Considered atoms: N11, C11, C21, C31, C41 and C51.

7: Chelating ring. Considered atoms: Cu2, N33, N23, C73 and S13.

8: Chelating ring. Considered atoms: Cu1; N11, C51, C61 and N21.

DC: Distance (Å) between the centroids of the sets i and j.

ANG: Angle (º) between the least–squares planes.

DZ: Distance (Å) between the centroid of j and the least–squares plane of i.

DZ': Distance (Å) between the centroid of i and the least–squares plane of j.

DXY: Distance (Å) between the i and j centroids projected onto the least–squares plane of i.

DXY': Distance (Å) between the i and j centroids projected onto the least–squares plane of j.

DS: Distance (Å) from the centroid of j to the nearest hydrogen atom of i.

DS': Distance (Å) from the centroid of i to the nearest hydrogen atom of j.

Table S1.7. Anion–π interactions.

Compound	k	l	DC	Dkl
1	O11	2	3.95	O11···C21: 3.31; O11···C22: 3.34
	O12	3	3.54	O12···N11: 3.66; O12···C11: 3.71
3	O41	1	3.50	O41···N1: 3.61; O41···C5: 3.66
	O22	6	3.15	O22···Cu: 3.23; O22···N2: 3.30
	O22	7	3.54	O22···Cu: 3.23; O22···N2: 3.30
	$O31^{xviii}$	6	3.88	$C6\cdots O31^{xviii}$: 3.06; $C5\cdots O31^{xviii}$: 3.46
4	O2	4	3.59	$O2\cdots C61^{xii}$: 3.17; $O2\cdots C51^{xii}$: 3.28
	O2	5	3.89	$O2\cdots C51^{xii}$: 3.28; $O2\cdots C41^{xii}$: 3.45
	O4	5	4.20	$O4\cdots C41^{xii}$: 4.03; $O4\cdots C31^{xii}$: 4.19
5	Cu	S^{xxvi}	3.33	$Cu\cdots S^{xxvi}$: 3.33
	S	Cu^{xxvi}	3.33	$S\cdots Cu^{xxvi}$: 3.33

1: Pyridine ring. Considered atoms: N1, C1, C2, C3, C4 and C5.

2: Pyridine ring. Considered atoms: N21, C21, C22, C23, C24 and C25.

3: Pyridine ring. Considered atoms: N11, C11, C12, C13, C14 and C15.

4: Chelating ring. Considered atoms: Cu1, N11, C51, C61 and N21.

5: Pyridine ring. Considered atoms: N11, C11, C21, C31, C41 and C51.

6: Chelating ring. Considered atoms: Cu1, N1, C5, C6 and N2.

7: Chelating ring. Considered atoms: Cu1, N2, N3, C7 and S1.

DC: Distance (Å) between the oxygen atom of the perchlorate anion and the centroid of l.

Dkl: Distance (Å) between the oxygen atom of the perchlorate anion and the nearest atoms of l.

Table S1.8. CH–π interaction for compound **4**.

Compound	C–H···X	d (C–H)	d (H···X)	d (C···X)	∠ (CHX)
4	C61–H61···X^{xiii}	0.93	3.07	3.99	174.4

X: Centroid of the pyridinic ring. Considered atoms: N11, C11, C21, C31, C41, C51 and C61.

Symmetry transformations used to generate equivalent atoms: i = –x+1/2, –y+1/2, –z; ii = x–1/2, y–1/2, z; iii = –x+3/2, –y+1/2, –z; iv = x–1/2, y+1/2, z; v = –x+1/2, y+1/2, –z+1/2; vi = x, y+1, z; vii = x–1/2, –y+1/2, z–1/2; viii = –x+1, –y, –z+1; ix = x, –y, z+1/2; x = –x, y, –z+1/2; xi = –x, –y, –z; xii = x+1/2, –y+1/2, z+1/2; xiii = –x+1/2, y–1/2, –z+3/2; xiv = x–1/2, –y+3/2, z–1/2; xv = –x+1, –y+1, –z+1; xvi = –x+1/2, y+1/2, –z+3/2; xvii = –x+1/2, y+1/2, –z+1; xviii = –x+1/2, –y+1/2, –z+1; xix = –x, y, –z; xx = x–1/2, –y+1/2, z; xxi = x+1/2, y+1/2, z; xxii = x+1/2, –y+1/2, z; xxiii = –x+2, y, –z+1/2; xxiv = –x, –y+1, –z; xxv = –x+1, y, –z+1/2; xxvi = –x+1/2, y+1/2, –z.

Table S1.9. Selected IR bands for neutral and anionic thiosemicarbazone derivatives and proposed assignments. Bands of coligands and counterions are excluded.

Assignments	HL	$[CuL]^+$	$[Cu(HL)]^{2+}$
$\upsilon(NH_2) + \upsilon(NH)$	3435(s), 3265(m)	3445–3430(w-m), 3370–3315(w-m)	3585–3335(w-m)
$\upsilon(=CH)$	3160(m)	3200–3100(w)	3165(w)
$\upsilon(C–H)$	3010(vw), 2973(vw)		2985–2980(mw)
$\upsilon(C=N)_{az,py} + \delta(NH_2)$	1610(vs)	1650–1620(m-s), 1610–1600(s)	1665–1620(s-vs), 1605(m)
THIOAMIDE I [δ(N3–H) + δ(N4–H)]	1590(m)	1585–1555(w-m)	1590–1585(s)
[δ(N3–H) + υ(C=N)]	1525(vs)		
$Ar(C–C)_{pi} + \delta(C–H)_{\parallel pi}$	1460(vs)	1485–1480(m)	1480(m)
THIOAMIDE II [δ(N–H) + υ(C=N)]	1430(vs)	1450–1435(m-ms)	1455(w)
THiOAMIDE III [δ(N–H) + υ(C=N) + δ(N–C–S) + υ(C=S)]	1365(vs), 1295(vs), 1233(m), 1152(w), 1111(vs), 1064(m), 998(m)	1385–1000(w-m), 1170(s)	1390–1100(w-m), 1230(s)
υ(N–N)	933(m)	930–910(w-m)	950–945(w-m)
δ(=CH)	880(s)	880(m)	885(w)
THIOAMIDE IV [υ(C=S)]	820(s)		
$\gamma(C–C–C/N)_{\perp py}$	776(s), 740(m)	780–765(w)	
$(C5–C6)_{conf}$	620(m)	630–620(w)	650(w)
$\delta(C–H)_{ip,py}$	560(w), 520(w)	590–510(w)	515–510(mw)
δ(N3–H)	475(vs,b)		490(w)
δ(N4–H)	450(m)	470(w)	470(w)
$\gamma(C–H)_{oop,py}$ + $\gamma(C–C–C/N)_{\parallel py}$	420(m)	420–410(w)	420–415(d)

(vs = very strong, s = strong, m = medium, w = weak, vw = very weak, b = broad, sh = shoulder, az = azomethinic, py = pyridine ring, ip = vibration in plane, oop = vibration out of plane, conf = relative to the conformation of the thiosemicarbazone ligand around a specific bond).

5. Crystal structure of compound *5*

The modulated structure of compound ***5*** [**q**=-0.615**a***+0.345**c*** (see Fig. S1.19), superspace group *C2/m(α0γ)*] was refined using a rigid body approximation (one symmetry independent $[Cu(HL)(NCS)]^+$ ion, centered at Cu, together with its corresponding perchlorate counterion, centred at Cl) to describe the modulation with the lowest number of parameters. ADPs were restricted within the TLS rigid-body harmonic model. Such approximation was also used for the average structure to establish the R-factor level (R=0.0841 for 75 refined parameters against R=0.0497 and 139 parameters). The refined modulations are sinusoidal rigid translations and rotations:

$$T^{\mu}(x_4) = T^{\mu}_c \cos 2\pi x_4 + T^{\mu}_s \sin 2\pi x_4$$

$$R^{\mu}(x_4) = R^{\mu}_c \cos 2\pi x_4 + R^{\mu}_s \sin 2\pi x_4$$

for μ = *[Cu(HL)(NCS)]* and *ClO_4*, respectively and an occupational crenel function for the perchlorate ions (Table S1.10):

$$o^{\mu}(x_4) = 1 \text{ for } x_4 \in (x_{4,0} - \Delta/2, x_{4,0} + \Delta/2) \text{ and 0 elsewhere.}$$

Final R-factors: 0.112, 0.081 and 0.199 for all (1389) reflections, main (758) and first-order satellites (631). The displacive modulation is mainly described by a translation along **b** for both rigid bodies and rigid rotations around **a**, and (mostly for perchlorates) **c**. The resulting displacements reinforce the C–H···O hydrogen bond network. A 5x1x3 commensurate approximant (notice that **q**=-0.615**a***+0.345**c*** ≈ -3/5 **a***+1/3) **c*** of the modulated structure is shown in Fig. S1.20.

Table S1.10. Final values for the occupational and displacive parameters refined for the modulated structure of ***5***. First row fractional coordinates. Second row, in bold, translations and rotations in Å and (°), respectively.

[Cu(HL)(NCS)]	$T_{y,c}$	$T_{y,c}$	$R_{x,c}$	$R_{x,c}$	$R_{z,c}$	$R_{z,c}$
	-0.0099(3) **-0.065(2)**	0.0368(3) **0.242(2)**	0.00257(6) **2.20(5)**	-0.00078(6) **-0.67(5)**	-0.00200(9) **-1.72(8)**	-0.00336(9) **-2.89(8)**
ClO_4	$x_{4,0}$	Δ				
	0.223(3)	0.5				
	$T_{x,c}$	$T_{x,c}$	$T_{y,c}$	$T_{y,c}$	$T_{z,c}$	$T_{z,c}$
	-0.003(1) **-0.04(1)**	0.0015(4) **0.022(6)**	-0.039(1) **-0.256(7)**	-0.011(9) **-0.07(6)**	0.0019(9) **0.03(1)**	0.002(3) **0.03(5)**
	$R_{x,c}$	$R_{x,c}$	$R_{y,c}$	$R_{y,c}$	$R_{z,c}$	$R_{z,c}$
	0.000(1) **0.0(9)**	-0.004(5) **-3(4)**	-	-	0.005(1) **4.3(9)**	0.010(4) **9(3)**

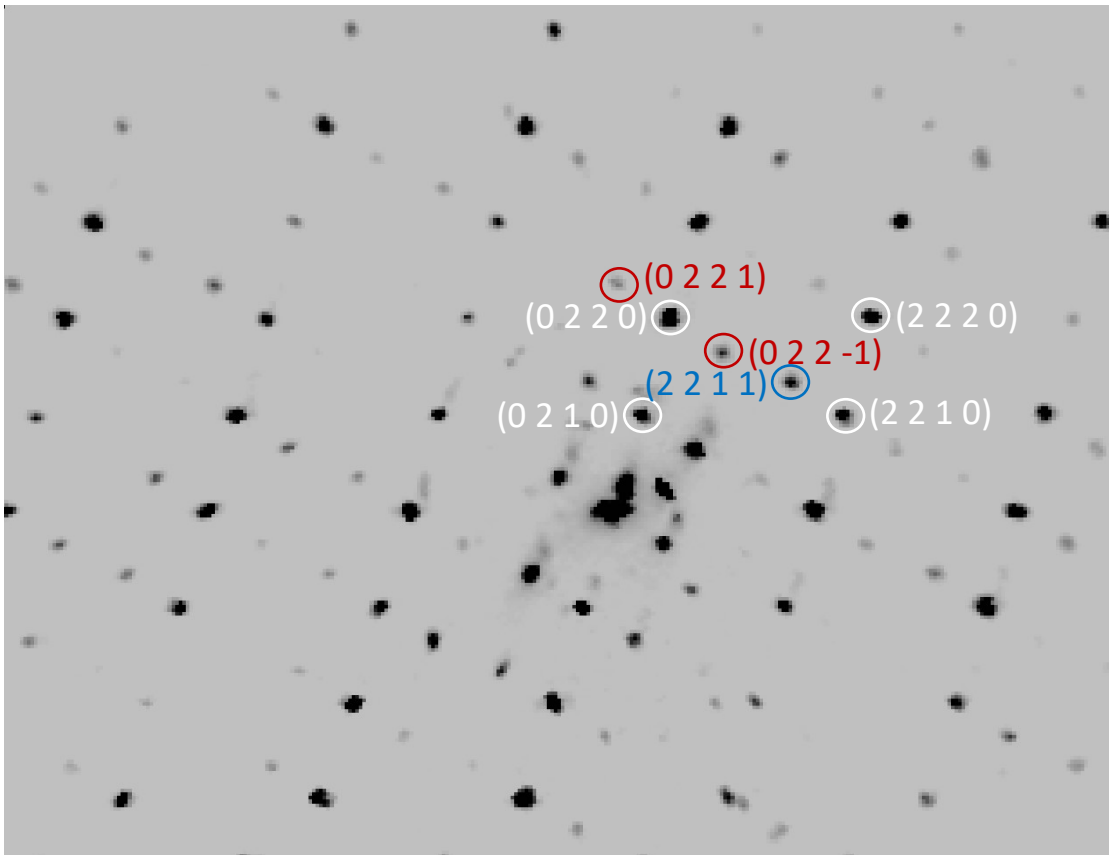

Figure S1.19. h2l reciprocal plane of ***5***, showing the presence of satellites. For clarity, some reflections are indexed on a four-dimensional scheme.

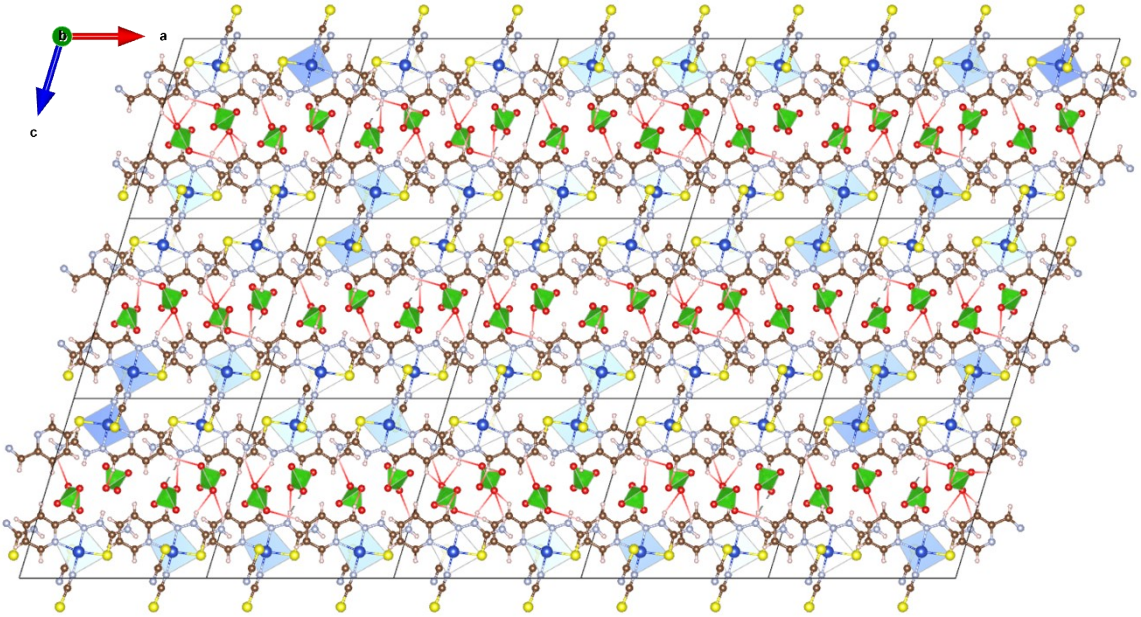

Figure S1.20. Projection along b of the 5x1x3 ordered commensurate approximant of the modulated structure of ***5***, showing the C–H···O H-bond network favoured by the modulation.

6. Magnetic measurements on compound *1*

Given that the ubiquitous compound ***1*** exhibits 1D structure with the N3 atoms acting as linkers to neighbour Cu(II) ions, we have studied the magnetic properties for comparison with the nitrato analogous.[3] The evolutions of χ_m and $\chi_m T$ with temperature for ***1*** are depicted in Fig. S1.21. The χ_m values increase on decreasing temperature to reach a broad maximum about 130 K (0.0025 cm^3/mol). Next, the susceptibility falls until a minimum at T = 15 K (0.0017 cm^3/mol). Below this point, the curve rapidly increases with decreasing temperature. This is the typical behaviour of a strong antiferromagnetic coupling in a compound with impurities, which are the responsible of an increasing susceptibility at very low temperatures. Experimental data have been unsuccessfully adjusted, being the best fit that obtained by the Bonner and Fisher's expression (Eq. (1)) for chains of equally spaced Cu(II) ions derived from the Heisenberg–van Vleck–Dirac Hamiltonian for isotropic magnetic 1D systems with S = 1/2 spins (Eq. (2)).[2,3]. The best least-square fitting was achieved for J/k = –100 K (–69.44 cm^{-1}) and calculated g = 2.19 with impurities of 0.2%.

$$\chi_m = (1-\rho)\frac{Ng^2\beta^2}{kT}\frac{0.25 + 0.0074975x + 0.075235x^2}{1 + 0.9931x + 0.172135x^2 + 0.757825x^3} + \frac{\rho Ng^2\beta^2}{4kT} \qquad \textbf{(1)}$$

where:

$$x = \frac{|2J|}{kT}, \qquad H = -2J\sum_{i=1}^{n-1} S_{Ai}\cdot S_{AiH} \qquad \textbf{(2)}$$

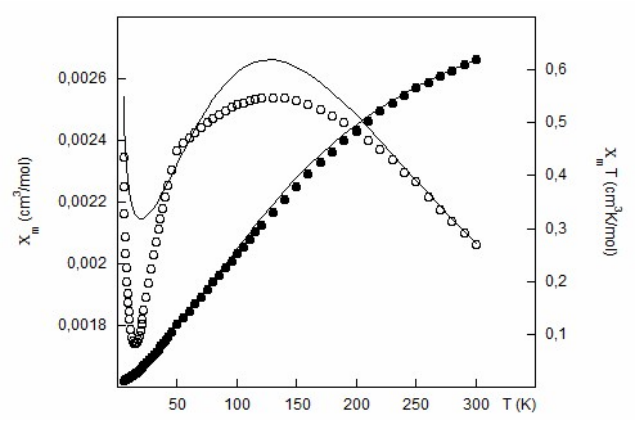

Figure S1.21. Graphics of χ_m (○○○), and $\chi_m T$ (●●●) *versus* T for compound ***1***.

7. Crystallization method for compound *4*

Crystals of compound ***4*** were serendipitously obtained in a crystallization experiment carried out with the aim to obtain AMP-Cu(II)-thiosemicarbazone compounds. The experiment is mentioned in the Experimental section of the main text. Briefly, aqueous solutions of H_2AMP (adenosine-5'-monophosphate monohydrate) and $Cu(ClO_4)_2 \cdot 6H_2O$ were mixed and basified to pH 7.6 (solution A). On the other hand, HL was dissolved in acetone (solution B). Chloroform was placed in a U-tube (solution C, see drawing and photograph given in Figure S1.22). Solution A was carefully added by one of the branches and solution B in the other. Chloroform is immiscible with the aqueous phase and acts as a separator medium that favors slow diffusion. The device was kept for several weeks and finally, crystals of ***4*** could be isolated from one of the six different layers formed in the branches.

(a) (b)

Figure S1.22. (a) The picture represents the method used for slow diffusion experiment that yielded crystals of ***4***. (b) Photograph of an analogous crystallization experiment.

2. Summary about the parallel Cu^{2+} / HL / NO_3^- system

1. Synthesis and characterization of the TSC-Cu-nitrato complexes.

The preparation of the **$[CuL(ONO_2)]_n$** compound, or **$CuL(NO_3)$** in the manuscript, has been described in different ways[4], notwithstanding the chosen method was that already used by our research group[5].

The synthesis of the **$[CuL_2]$** biscomplex was achieved following a variation of a previously reported preparative method[6]. Briefly, solid HL (4.0 mmol, 0.720 g) was placed in water (20 ml) and dissolved by stirring at moderate temperature while an aqueous NaOH solution was added to reach pH 12.0−13.0. Then, an aqueous solution of $Cu(NO_3)_2{\cdot}3H_2O$ (2.0 mmol, 0.482 g) in water (15 ml) was dropwise added. A brown precipitate immediately appeared. The reaction was kept with stirring for 3 h. The dark brown solid was filtered off, washed with water and acetone and dried in vacuum. (0.299 g, 70%). Anal. found: C, 39.44; H, 3.50; N, 26.48; S, 14.76%. Calc. for $C_{14}H_{24}CuN_8S_2$ (421.01 g/mol): C, 39.85; H, 3.34; N, 26.55; S, 15.19%. FAB^+ mass spectrometry (m/z): 180.89 $[H_2L]^+$, 241.84 $[CuL]^+$, 485.66 $[Cu_2(HL)L]^+$, 664.64 $[Cu_2L_3]^+$. ESI^+ mass spectrometry (m/z): 154.98 $[Cu(NO_3)(MeOH)]^+$, 179.97 $[CuNa(NO_3)(MeOH)]^+$, 241.84 $[CuL]^+$, 422.01 $[Cu(HL)L]^+$, 528.93 $[Cu_2L_2(HCOO)]^+$, 530.93 $[Cu_2(HL)_2(HCOO)]^+$, 628.99 $[Cu_2L_2(L^{CN})]^+$, 630.99 $[Cu_2(HL)_2(L^{CN})]^+$, 662.97 $[Cu_2L_3]^+$, 664.97 $[Cu_2(HL)_2L]^+$. UV absorptions, λmax (DMF)/nm 618 (ε/dm^3 mol^{-1} cm^{-1} 230, d-d transition), 412 (16860 charge transfer transition), 298 and 340 sh (35680, intraligand). IR bands (ATR-FTIR), ν_{max}/cm^{-1} 3475 m, 3365 w, 3267 m, 3075 m, 3062 m, 3011 m, 2988 m, 2940 w, 2353 w, 1626 m, 1614 m, 1598 m, 1590 m, 1547 m, 1475 w, 1440 h, 1397 vs, 1315 s, 1294 s, 1263 w, 1223 m, 1147 s, 1138 s, 1102 h, 1051 m, 956 w, 900 h, 881 s, 868 m, 762 m, 727 s, 679 m, 670 m, 635 w, 617 s, 540 w, 462 w, 447 s, 435 w, 418 w. X-band EPR signals at RT: g_1 = 2.194, g_2 = 2.071 and g_3 = 2.055.

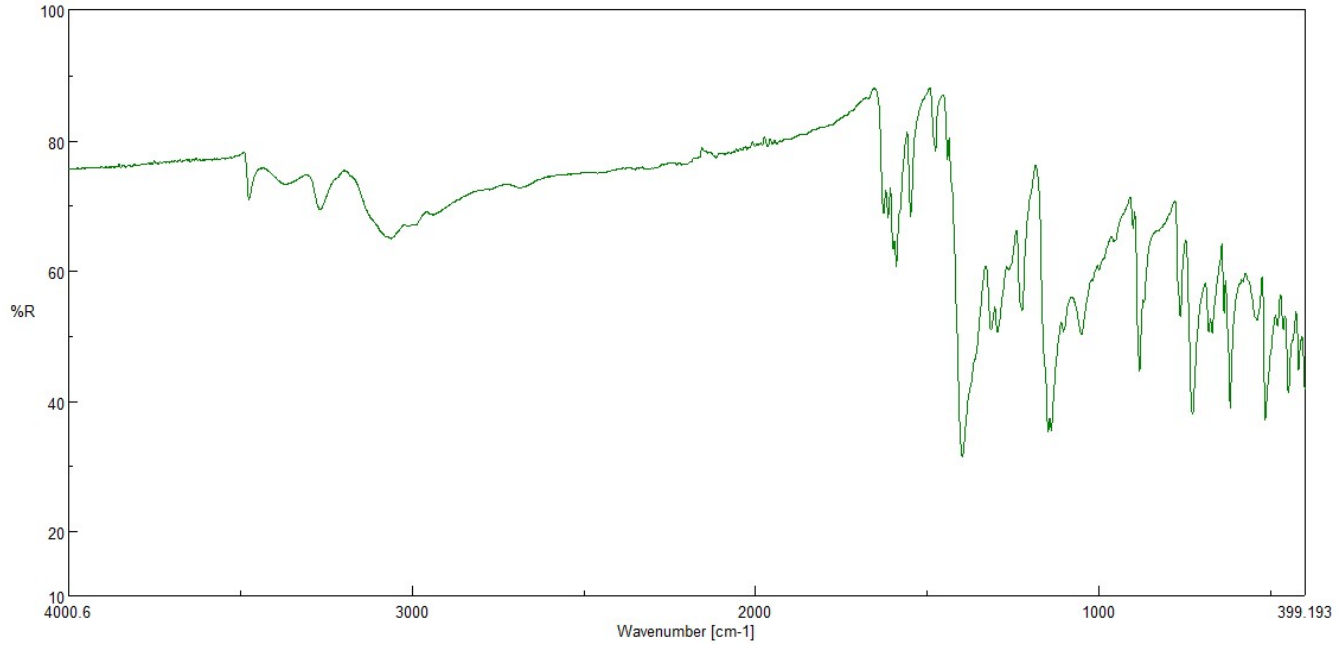

Figure S2.1. [CuL_2]. FT-IR ATR spectrum

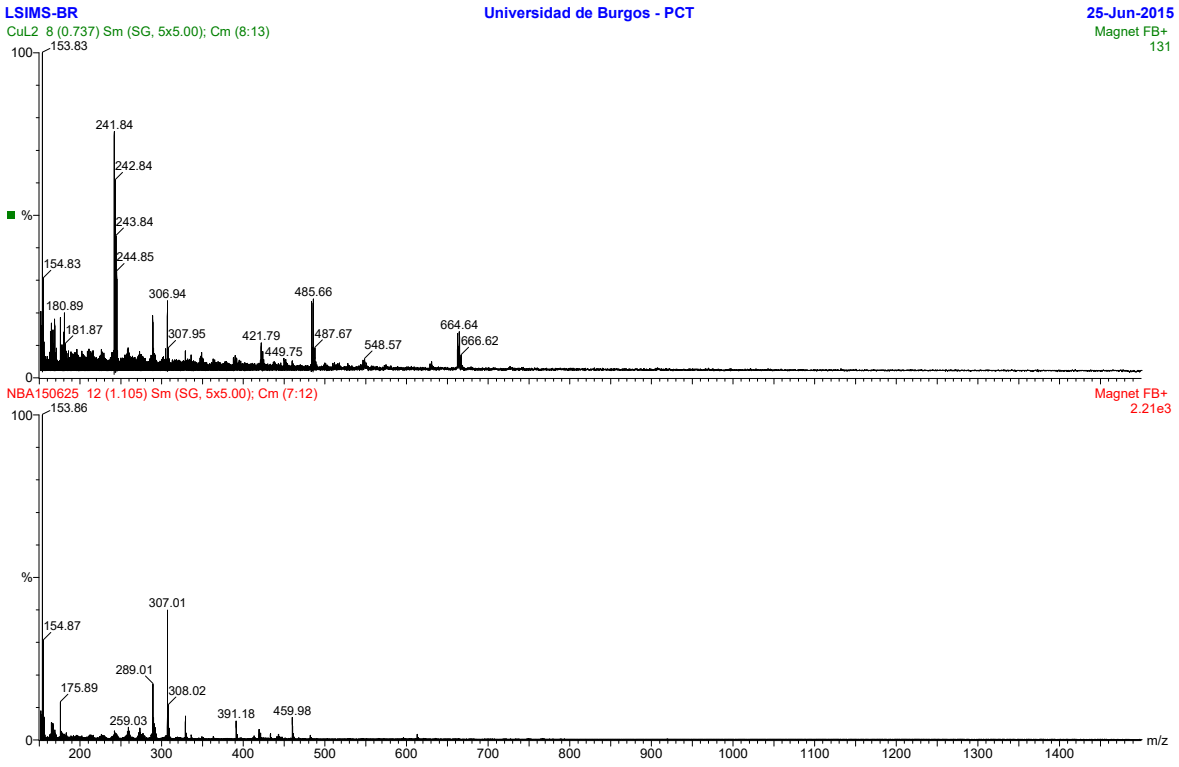

Figure S2.2. [CuL_2]. FAB^+ spectrum of the compound (above) and blank (below).

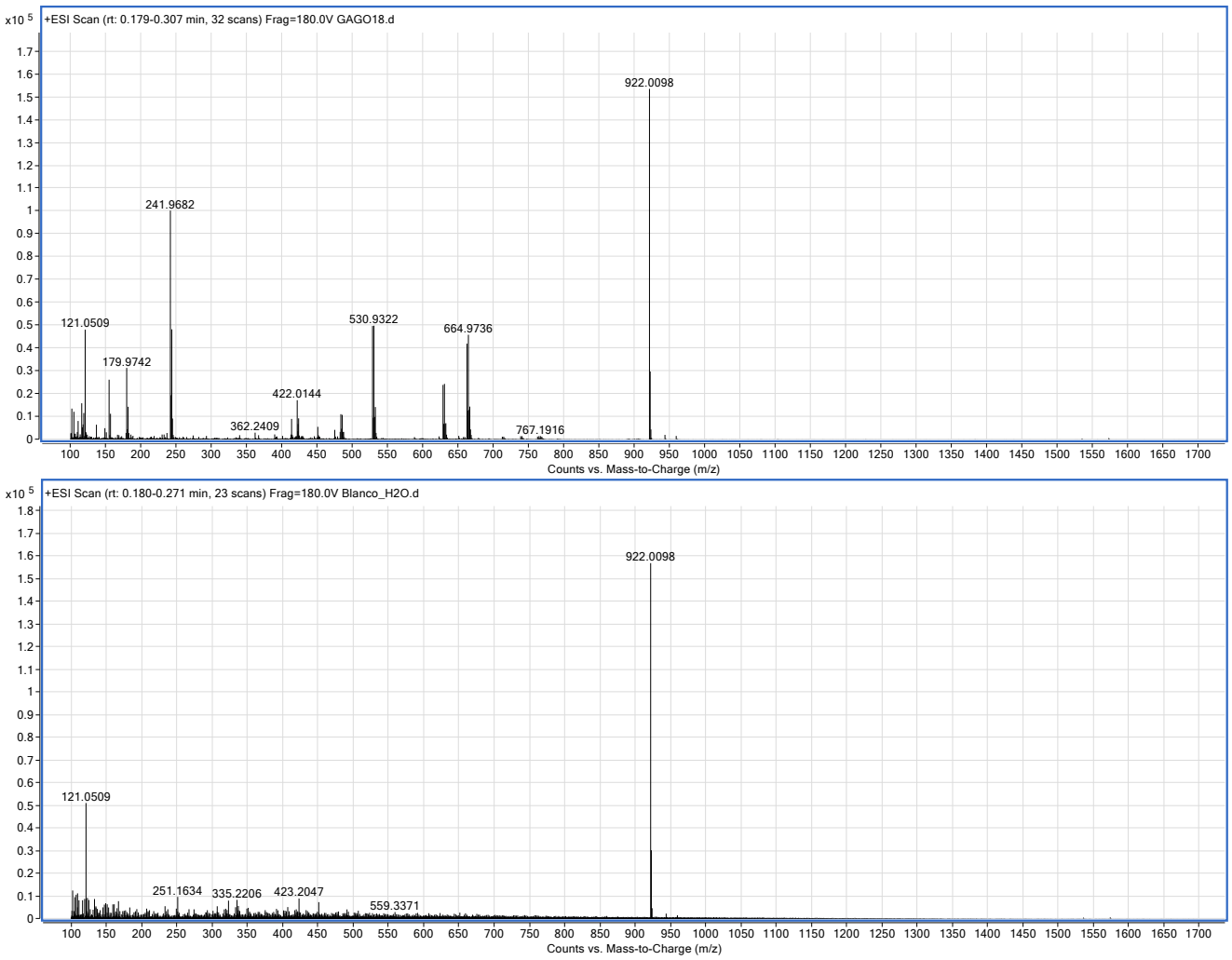

Figure S2.3. [CuL$_2$]. ESI$^+$ spectrum of the compound (above) and blank (below).

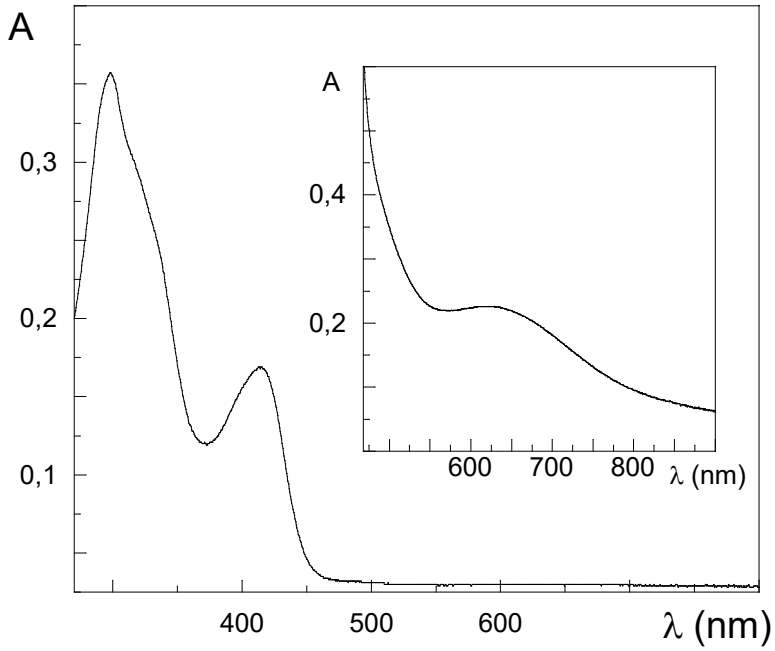

Figure S2.4. [CuL$_2$]. UV-vis spectrum of [CuL$_2$] 10^{-5} M and 10^{-3} M (inset) in DMF.

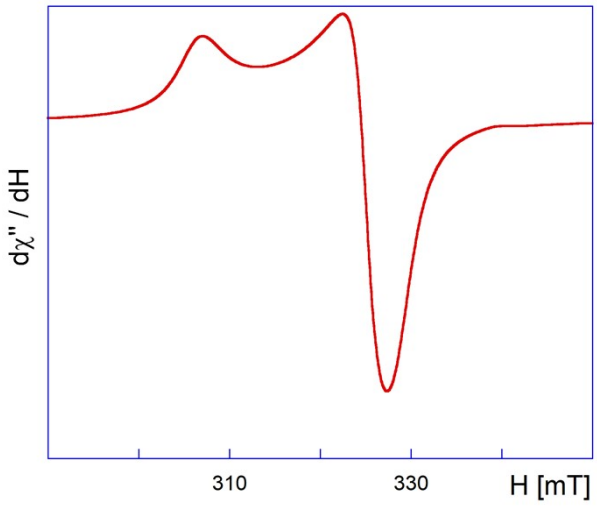

Figure S2.5. [CuL_2]. X-band EPR spectrum of a powdered sample at RT.

The synthesis of the **$Cu_2(HL)L_2(NO_3)_2(H_2O)_2$** was performed in the same way described in the main text for the analogous to ***4***. Solid HL ligand (3.0 mmol, 0.540 g) was added over a solution of $Cu(NO_3)_2{\cdot}3H_2O$ (2.0 mmol, 0.485 g) in water (20 ml) and the mixture was vigorously stirred for 1 h. Then, drops of a NaOH aqueous solution were added to pH 7 and the reaction was kept with stirring for 1 h. A dark brown solid was filtered off, washed with water and acetone, and dried over vacuum. (0.683 g, 83%). Anal. found: C, 30.74; H, 3.22; N, 23.22; S, 12.05%. Calc. for $C_{21}H_{26}Cu_2N_{14}O_8S_2$ (825.81 g/mol): C, 30.54; H, 3.17; N, 23.75; S, 11.65%. FAB^+ mass spectrometry (m/z): 241.84 $[CuL]^+$, 485.71 $[Cu_2(HL)L]^+$, 664.70 $[Cu_2L_3]^+$, 906.69 $[Cu_2(HL)_3(NO_3)_3(H_2O)_3]^+$. UV absorptions, λmax (DMF)/nm 615 (d-d transition), 411 (charge transfer transition), 297 (intraligand). IR bands (ATR-FTIR), ν_{max}/cm^{-1} 3521 w, 3365 w,sh, 3290 m, 3158 m, 3090 vw, 3056, w,sh, 2100 w,b, 1634 m, 1613 m, 1594 m, 1553 w, 1481 m, 1444 s, 1427 sh, 1408 s, 1374 s, 1335 s, 1310 s, 1291 sh, 1261 sh, 1224 s, 1165 s, 1145 vs, 1104 sh, 1053 m,sh,vb, 1015 vw, 1003 vw, 967 w, 946 w, 918 w, 875 m, 833 w,sh, 825 w, 774 m, 746 m, 727 m, 715 m, 677 w, 646 w,sh, 634 w,sh, 614 s, 555 s,b, 515 s, 469 w, 447 w, 415 m, 401 m. X-band EPR signals at RT: $g = 2.070$.

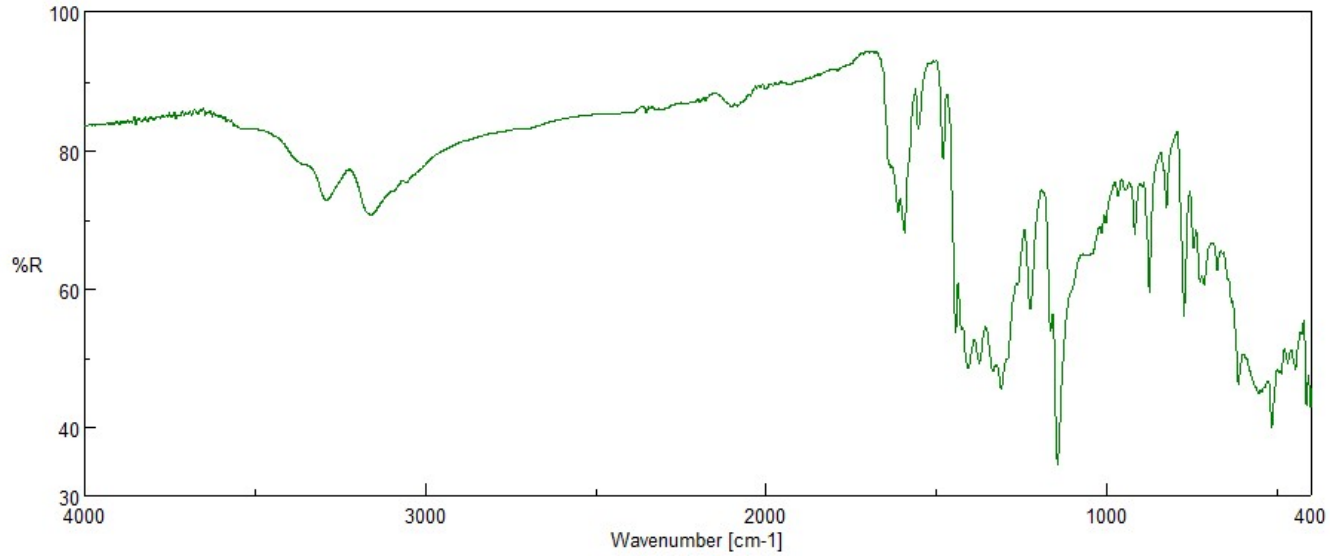

Figure S2.6. $Cu_2(HL)L_2(NO_3)_2(H_2O)_2$. FT-IR ATR spectrum

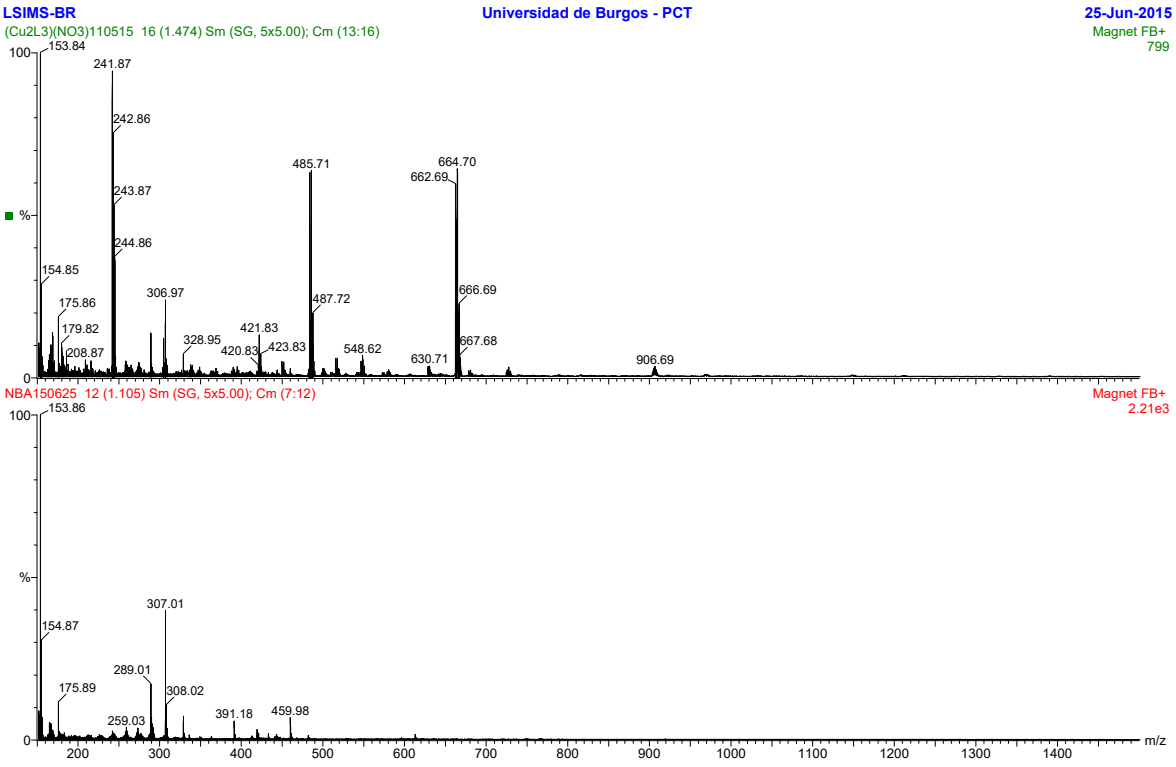

Figure S2.7. $Cu_2(HL)L_2(NO_3)_2(H_2O)_2$. FAB^+ spectrum of the compound (above) and blank (below).

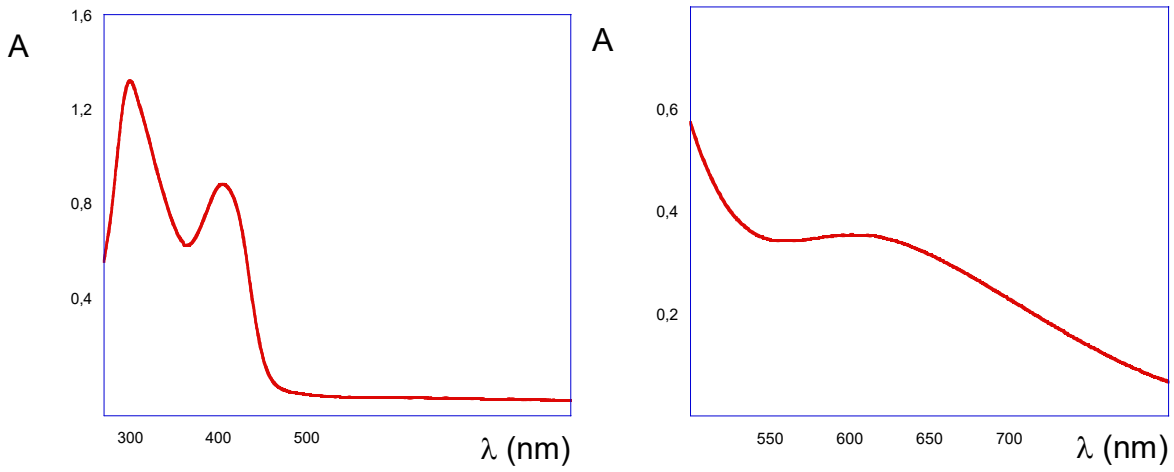

(a) (b)

Figure S2.8. $Cu_2(HL)L_2(NO_3)_2(H_2O)_2$. UV-vis spectra of 10^{-5} M (a) and 10^{-3} M (b) solutions in DMF.

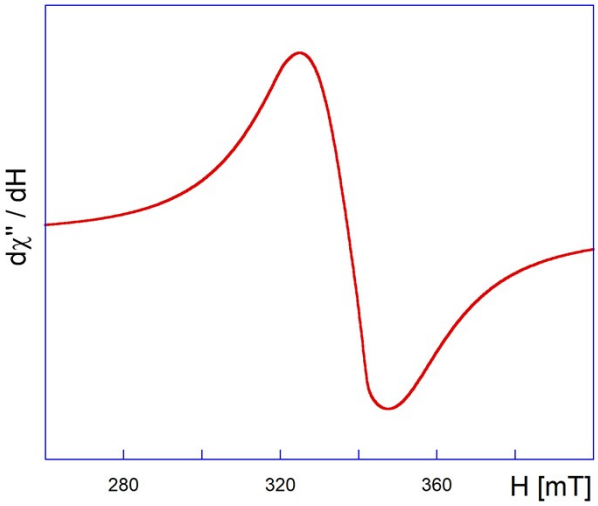

Figure S2.9. $Cu_2(HL)L_2(NO_3)_2(H_2O)_2$. X-band EPR spectrum of a powdered sample at RT.

The **CuLCl** complex was prepared only for comparison of the IR spectra. It is, actually, the $[\{CuLCl\}_2]$ dimer[7]. The method to attain it is a variation of another previously published for the analogous $[\{CuL'Cl\}_2]$ compound[8], where HL' = pyridine-2-carbaldehyde 4N-methylthiosemicarbazone. Solid HL (1.0 mmol, 0.180 g) was added to an aqueous solution of $CuCl_2$ (1.0 mmol, 0.134 g) in water (15 ml) and the reaction proceeded for 1 h. After the adjustment of pH to 4.5 by addition of NaOH, the mixture was kept with stirring for 2 h. The olive-green precipitate was filtered off, washed with water, acetone and ethyl ether and dried to vacuum. (0.245 g, 88%). Anal. found: C, 30.17; H, 2.59; N, 19.83; S, 11.85%. Calc. for $C_7H_7ClCuN_4S$ (278.22 g/mol): C, 30.22; H, 2.54; N, 20.14; S, 11.52%. FAB^+ mass spectrometry (m/z): 241.97 $[CuL]^+$, 319.98 $[CuL(DMSO)]^+$, 485.93 $[Cu_2(HL)L]^+$, 520-90 $[Cu_2L_2Cl]^+$. IR bands (ATR-FTIR), ν_{max}/cm^{-1} 3512 m, 3463 m, 3414 sh,b,m, 3270 m, 3096 b,m, 3047 vw, 1651 vw, 1627 m, 1601 m, 1582 w, 1557 m, 1483 ms, 1448 s, 1435 vs, 1423 sh,s, 1408 sh,m, 1380 m, 1316 m, 1290 m, 1267 m, 1226 ms, 1170 s, 1155 m, 1104 m, 1077 b,w, 1049 w, 1037 w, 1018 m, 980 vw, 917

sh,m, 908 s, 878 s, 781 s, 744 w, 731 s, 691 b,m, 677 m, 645 w, 625 vs, 518 w, 485 vw, 440 s, 417 s. X-band EPR signals at RT: $g_1 = 2.181$, $g_2 = 2.052$ and $g_3 = 2.033$.

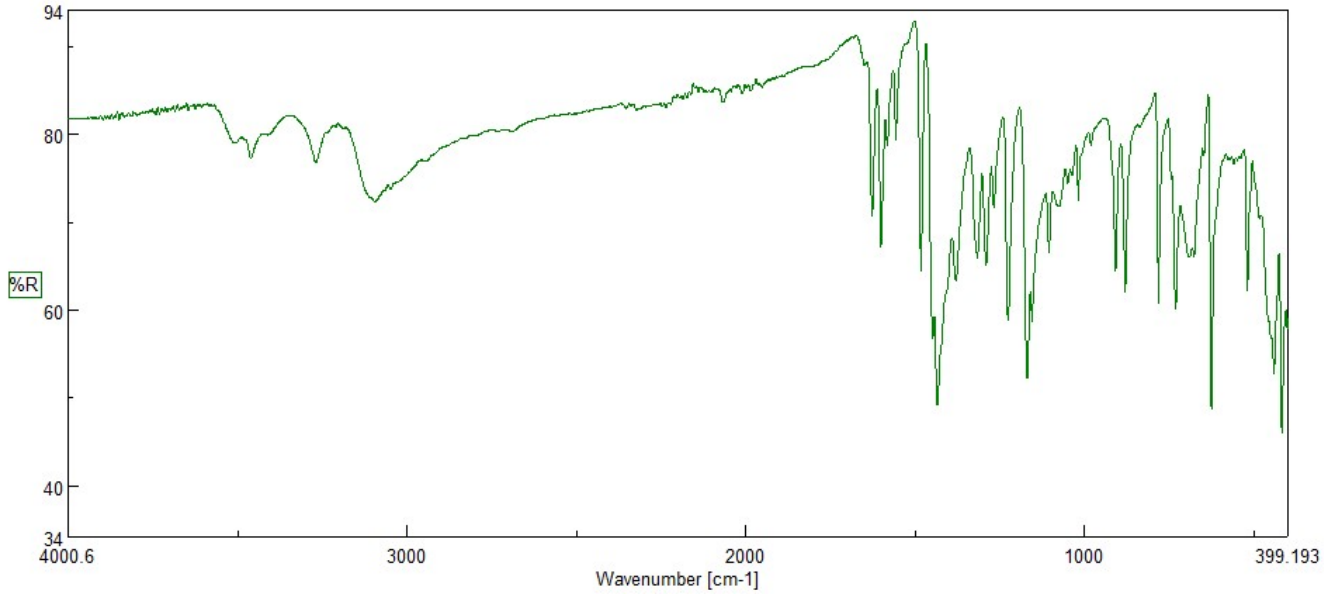

Figure S2.10. CuLCl. FT-IR ATR spectrum

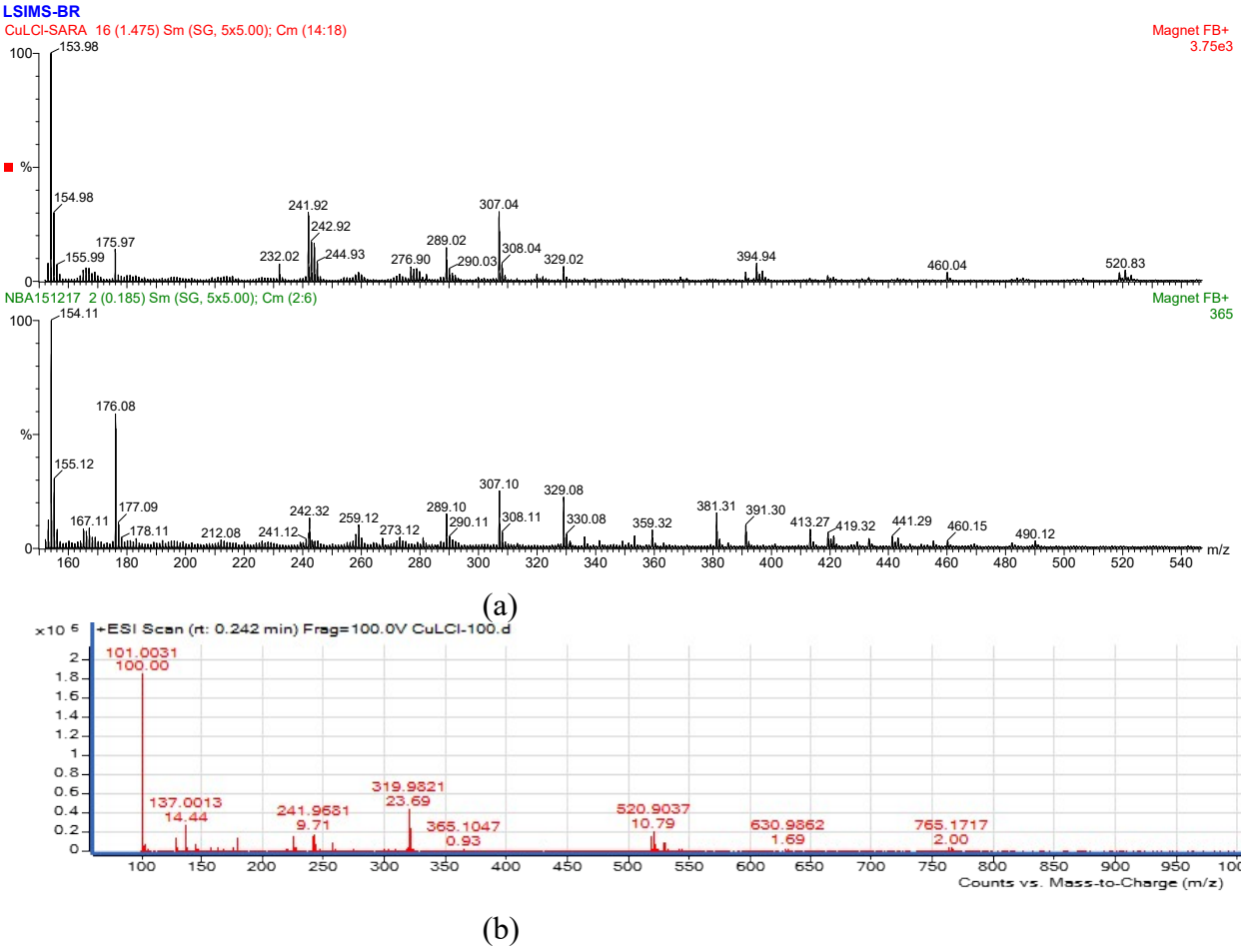

Figure S2.11. CuLCl. (a) FAB^+ spectrum of the compound (above) and blank (below). (b) ESI^+ spectrum.

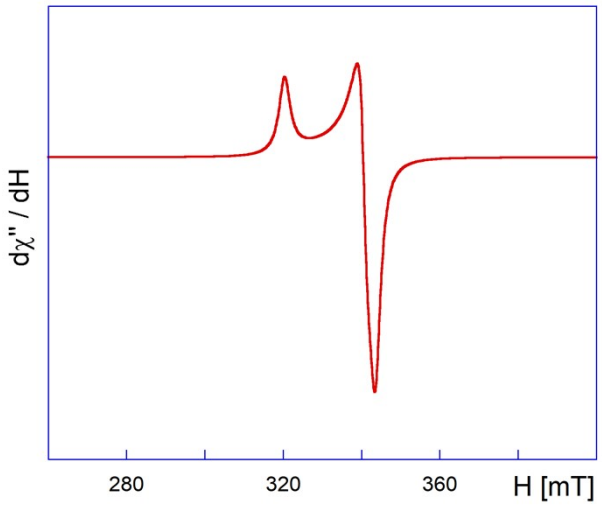

Figure S2.11. CuLCl. X-band EPR spectrum of a powdered sample at RT.

2. Complementary infrared studies for the assignment of bands.

The comparison between **[CuL(NO$_3$)]$_n$**, **[CuL$_2$]** and **CuLCl** given in Fig. S2.12 allows to attribute the very strong band with two minima at 1387 and 1323 cm^{-1}, the strong one at 1152 cm^{-1}, together with that medium at 824−822 cm^{-1}, to the vibration modes of the nitrato group. These bands are obviously absent in the spectra of **[CuL$_2$]** and **CuLCl**. This comparative insight also leads to ratify the proposed assignments of the band at 1646 cm^{-1} (compound ***1***) and 1643 cm^{-1} (**[CuL(NO$_3$)]$_n$**) as due to the imine C=N group involved in the linkage to neighbour Cu(II) ions inside the chain, because of the lack of bands of noticeable intensity in **CuLCl**, a compound without this kind of connectivity.

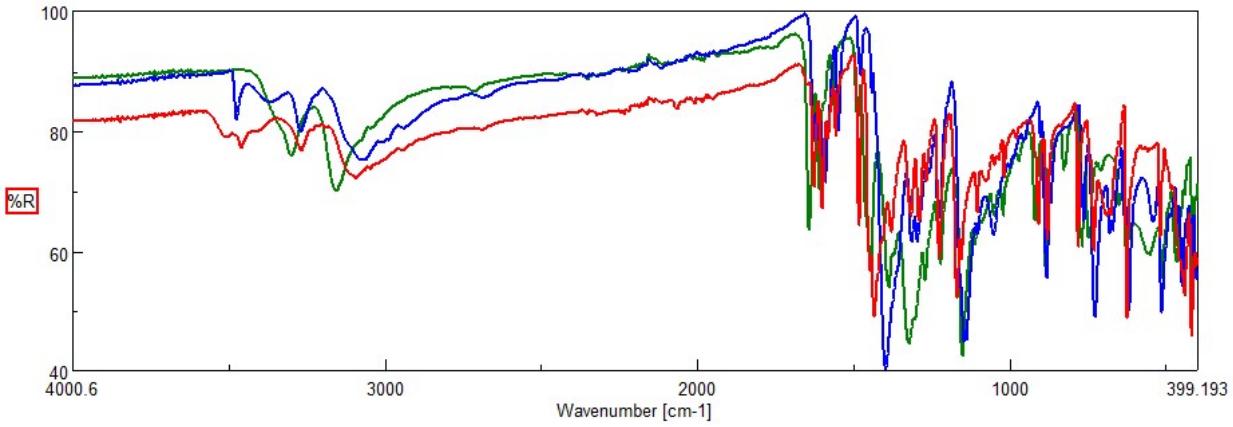

(a)

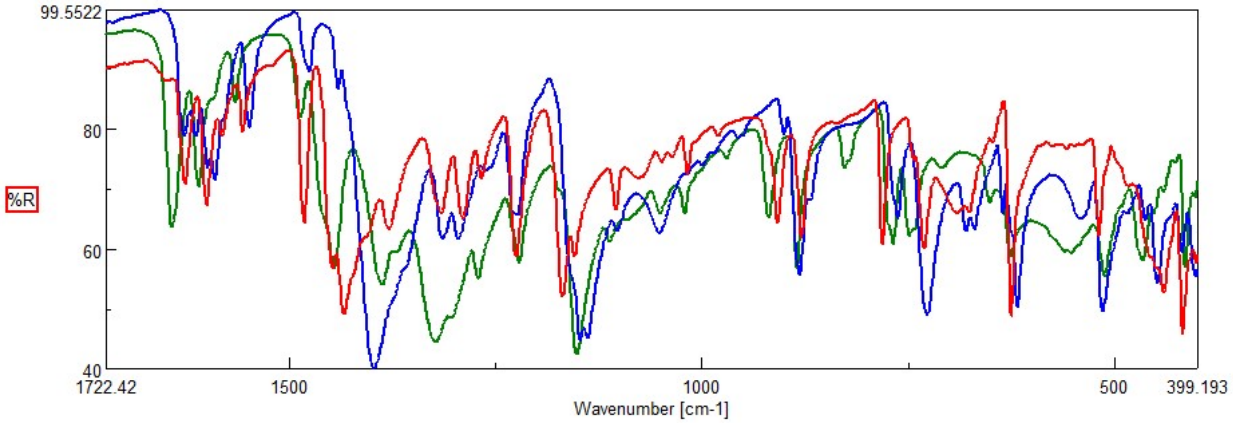

(b)

Figure S2.12. (a) IR spectra of **[CuL(NO$_3$)]$_n$** (green), **[CuL$_2$]** (blue) and **CuLCl** (red). (b) A magnification is given below.

The final comparison between compound ***1***, **[CuL(NO$_3$)]$_n$** and **CuLCl** (Fig. S2.13) reveals that the strong bands at 1448 and 1435 cm^{-1} in **CuLCl** shift to higher wavenumbers in compounds with activated hydrazinic nitrogen atom: 1443 and 1463 cm^{-1} for ***1***, and 1445 together with the shoulder around 1462 cm^{-1} in the case of **[CuL(NO$_3$)]$_n$**. Clearly, bands at 1062 (very strong and broad) and 620 cm^{-1} (sharp and strong) in ***1*** correspond to perchlorate groups.

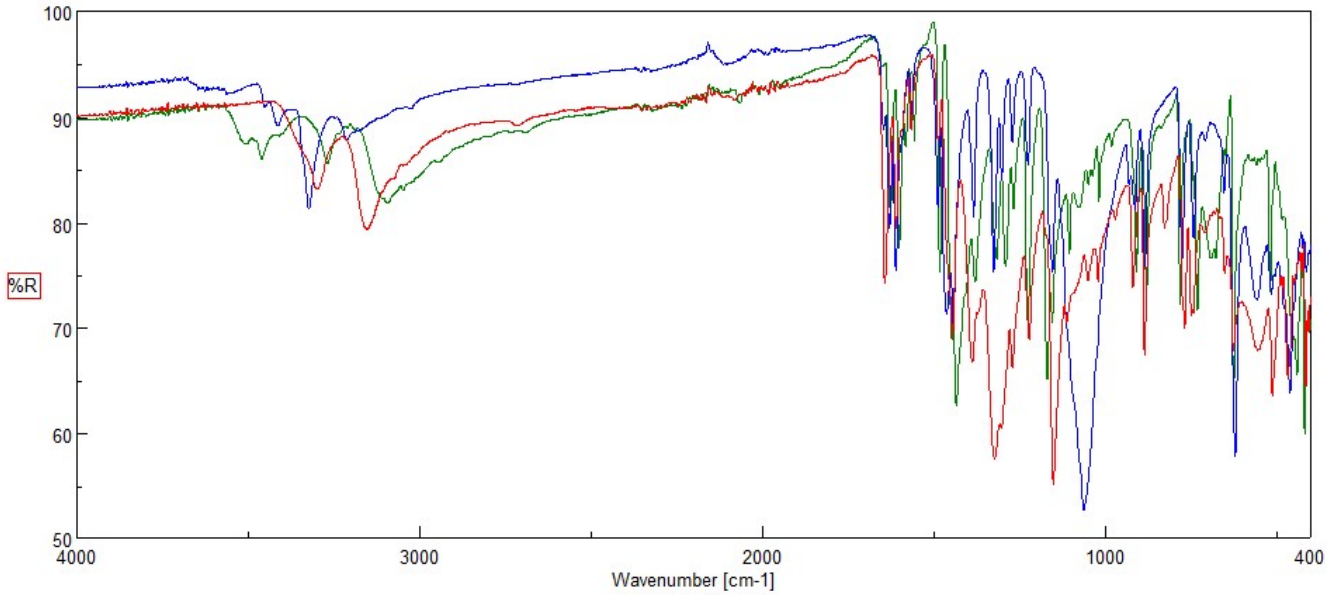

(a)

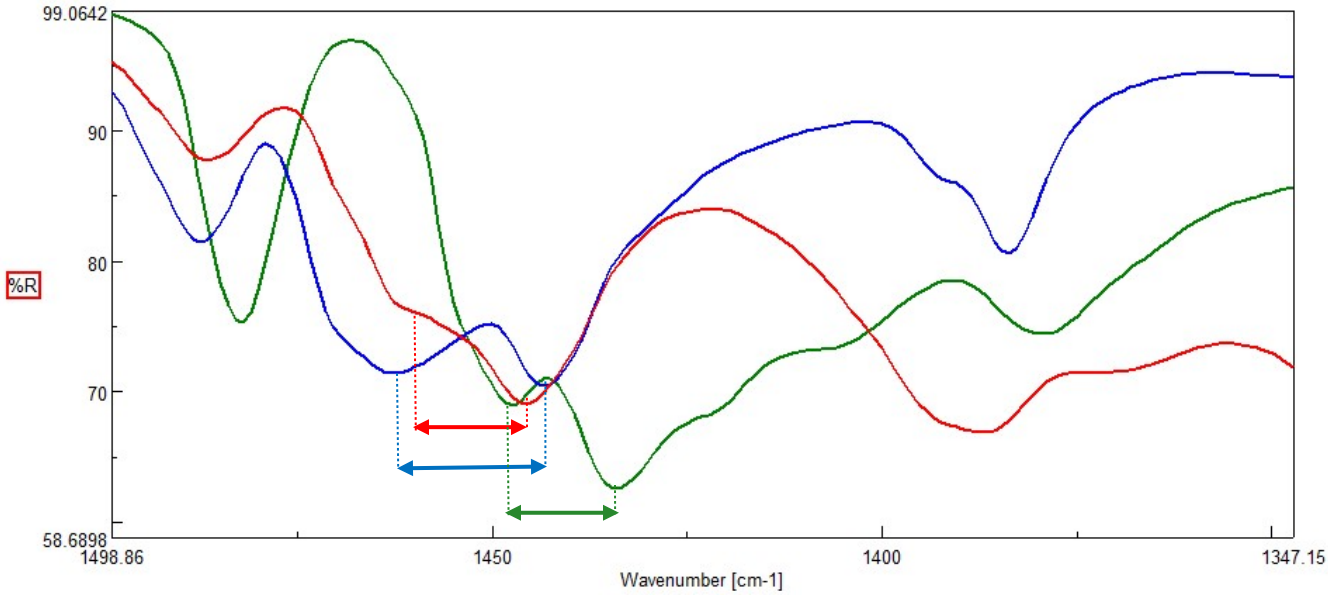

(b)

Figure S2.13. (a) IR spectra of compounds ***1*** (blue), **[CuL(NO$_3$)]$_n$** (red), and **CuLCl** (green). The arrows highlight the bands mentioned in text. (b) A magnification is given below.

3. Studies in aqueous basic media

1. Mass spectra of solutions at different pH values

ESI^+ mass spectra were measured on aqueous 10^{-3} M solutions of $CuL(NO_3)$ after addition of NaOH 0.1 M to reach pH 7.4, 9.0, 11.0 and 13.0. The obtained suspensions were kept with stirring for different times, 1 h and 24 h. Then, methanol was added to form (1:9) methanol/water mixtures and, finally, 0.1% formic acid was added just before the measurement.

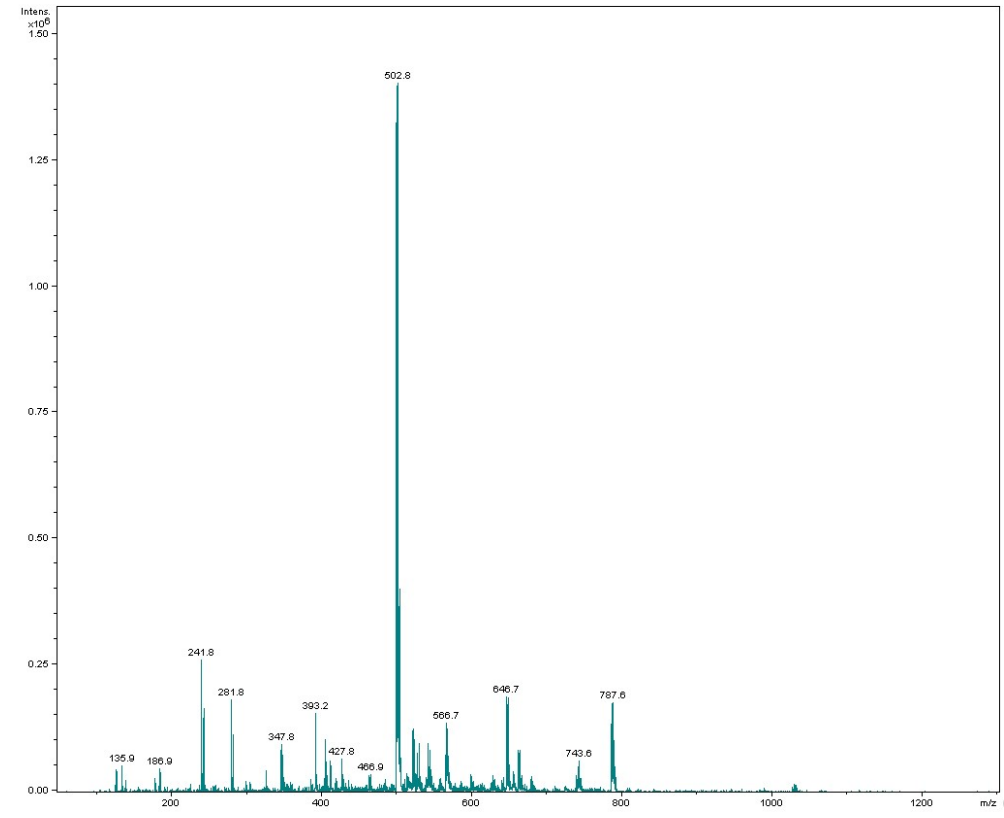

(a)

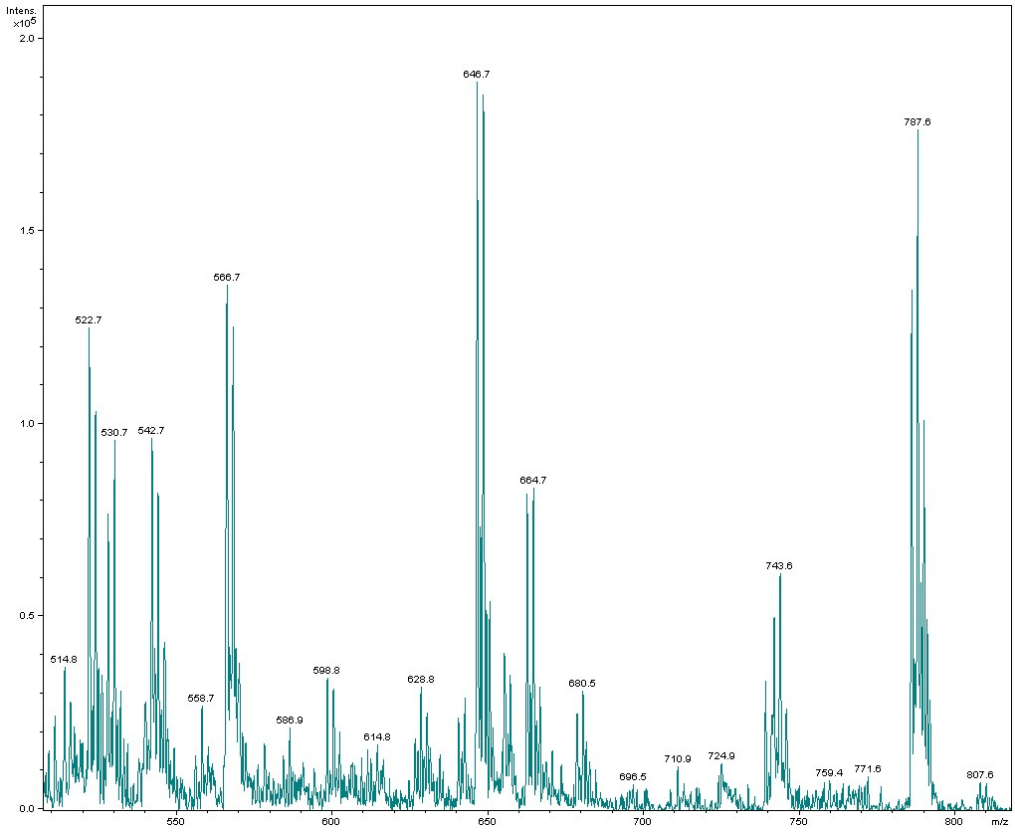

(b)

Figure S3.1. (a) ESI^+ mass spectra of an aqueous $CuL(NO_3)$ 10^{-3} M solution at pH 7.4 for 1 h. (b) Magnified region.

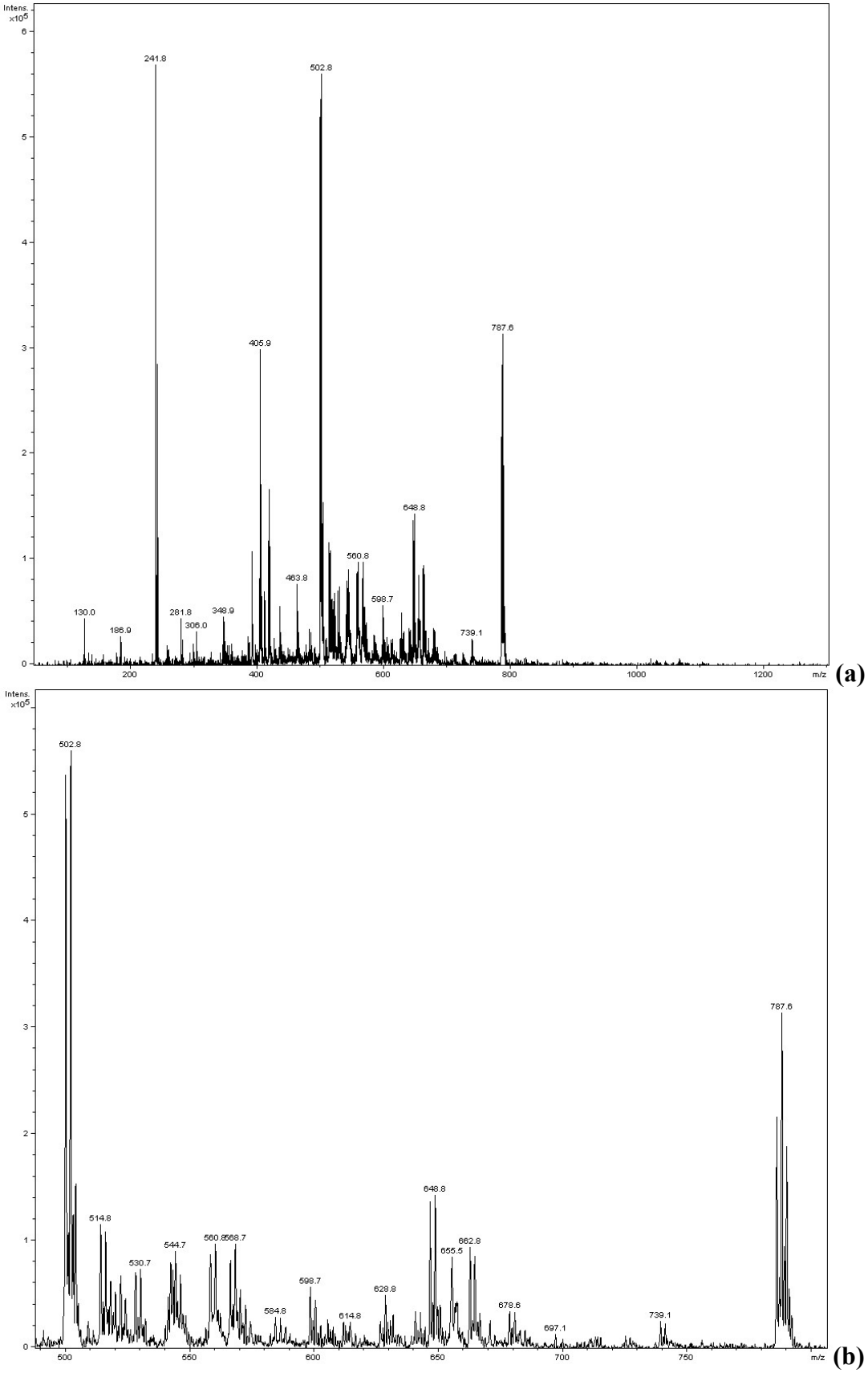

Figure S3.2. (a) ESI^+ mass spectra of $CuL(NO_3)$ 10^{-3} M solution at pH 7.4 for 24 h. (b) Magnified region.

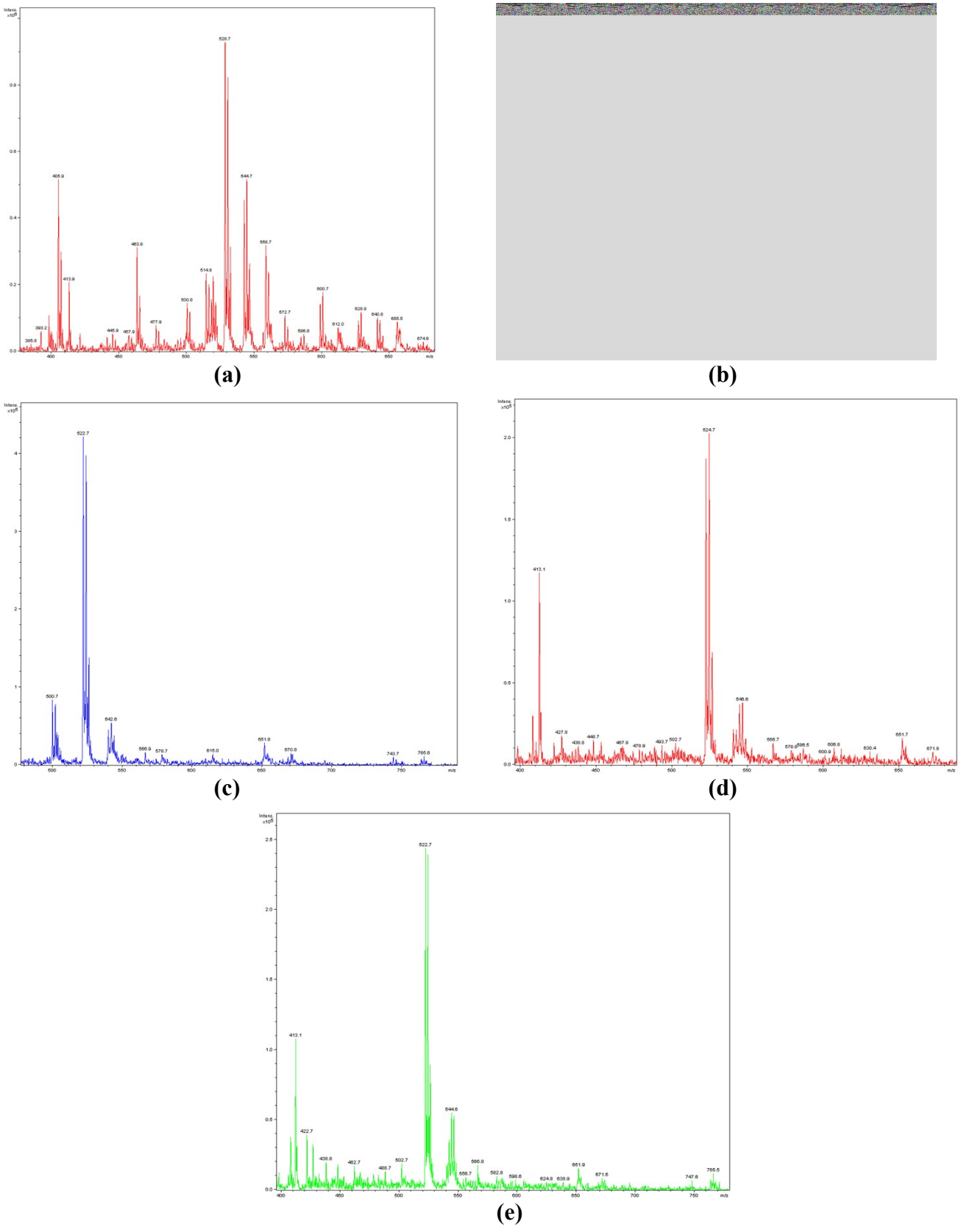

Figure S3.3. ESI$^+$ mass spectra of aqueous CuL(NO_3) 10^{-3} M solutions at pH 4.0 (a), 7.4 (b), 9.0 (c), 11.0 (d) and 13.0 (e) for 1 h.

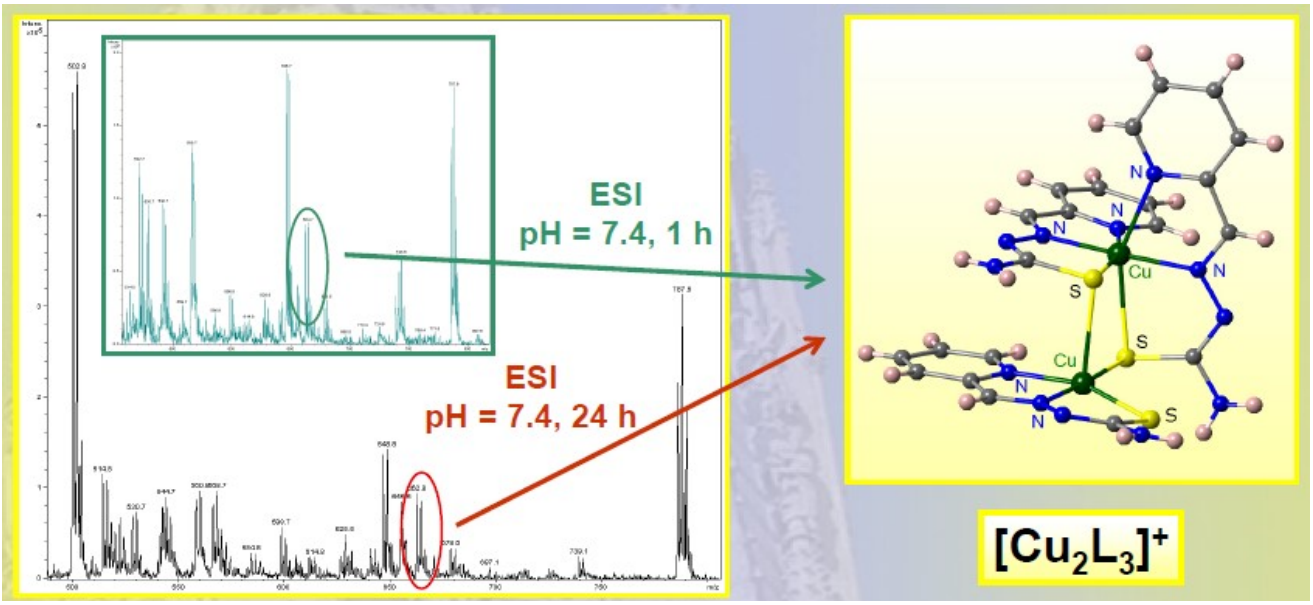

Figure S3.4. Peaks at m/z 662.8 and 664.7 in aqueous solution at pH 7.4 attributed to $[Cu_2L_3]^+$ and $[Cu_2(HL)_2L]^+$ species.

2. Studies on solid samples obtained at different pH values

In order to check if pH influences on the breakage of the TSC ligand in the Cu^{2+} / HL / NO_3^- system, IR studies were performed on the solid mixtures isolated at different pH values (2.0, 4.0, 7.4 and 9.0).

The preparation of these mixtures was as follows. Solid HL (0.216 g, 1.2 mmol) was added over a solution of $Cu(NO_3)_2 \cdot 3H_2O$ (0.242 g, 1 mmol) in water (10 mL). The suspension was kept with stirring for 2 h at room temperature. Then, drops of aqueous NaOH solutions (1 M / 0.1 M) were added to reach the required pH value (4.0, 7.4 or 9.0), and the reaction proceeded for 1 h. Finally, dark brown precipitates were filtered off, washed with acetone and ethyl ether and dried over vacuum. In one of the assays no adjustment of pH was carried out, no addition of NaOH was made, and the reaction was kept with stirring for 3 h (pH about 2.0). Once the powdered samples were obtained, ESI^+ mass spectra were measured by dissolving a portion of the solids in water, and using a water/methanol (70:30) mixture 0.1 % in formic acid as mobile phase. IR spectra were also recorded and reported in Figure S3.11.

Sample at pH = 2.0. 0.148 g. Experimental: C, 26.82; H, 2.36; N, 22.2; S, 10.08%. Calculated for $[CuL(NO_3)]\cdot 1/2H_2O$, $C_7H_8CuN_5O_{3.5}S$, C, 26.80; H, 2.57; N, 22.32; S, 10.22%.

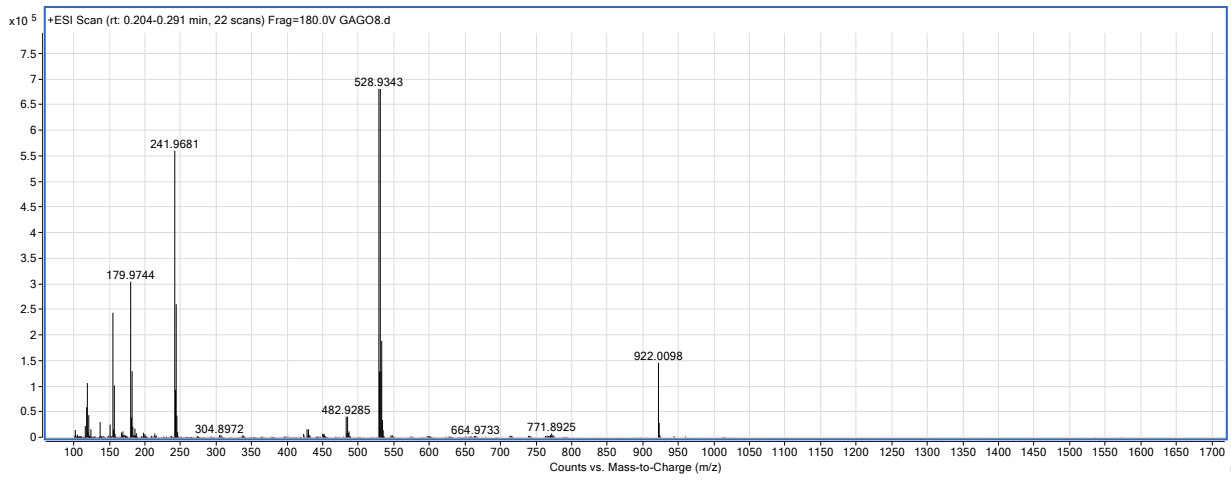

(a)

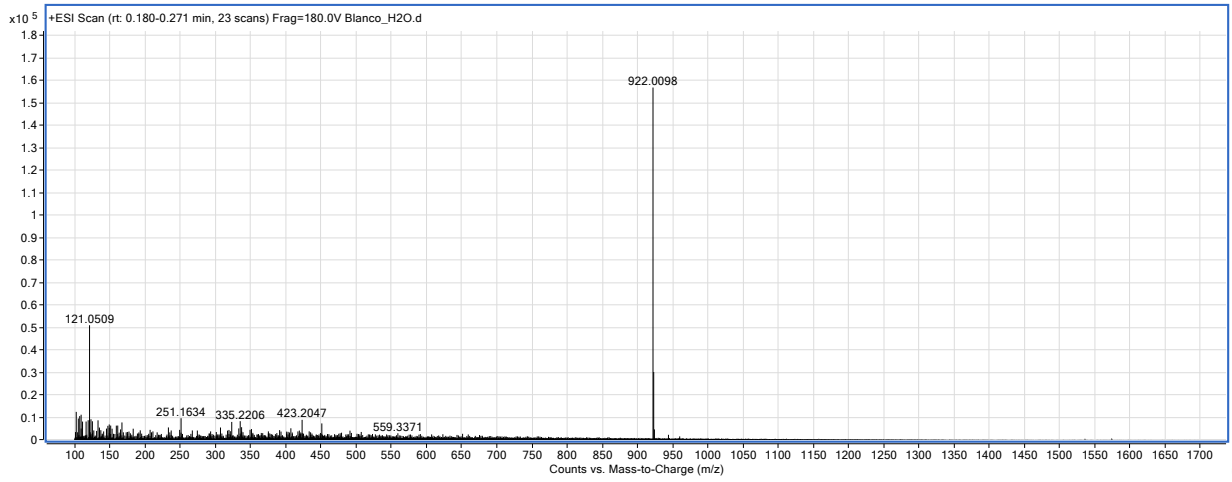

(b)

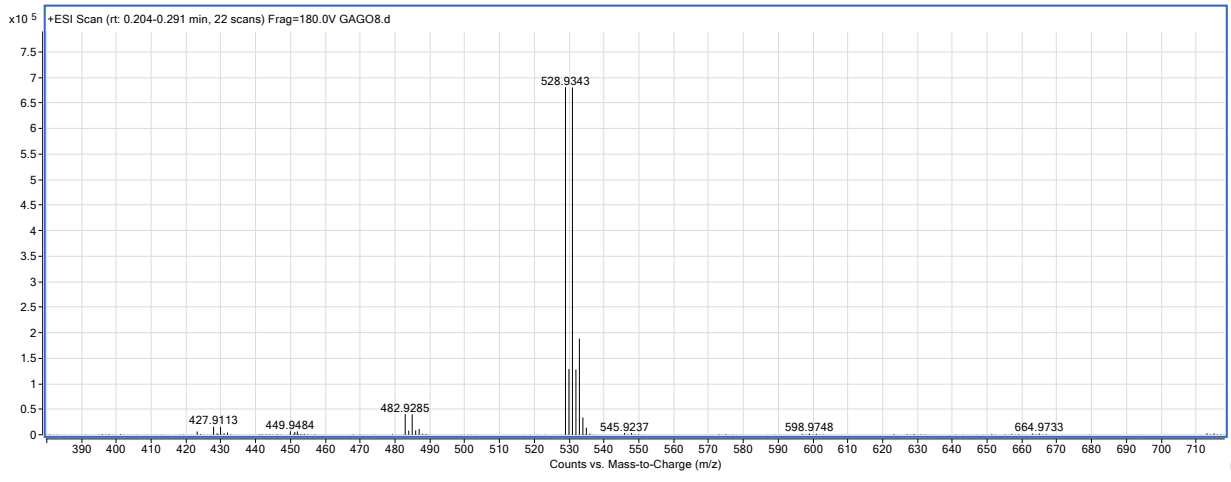

(c)

Figure S3.5. ESI^+ mass spectra of sample at pH = 2.0 (a), the blank (b) and a magnification (c).

Sample at pH = 4.0. 0.267 g. Experimental: C, 27.91; H, 2.32; N, 22.98; S, 10.90%. Calculated for [CuL(NO_3)], $C_7H_7CuN_5O_3S$, C, 27.59; H, 2.32; N, 22.98; S, 10.52%.

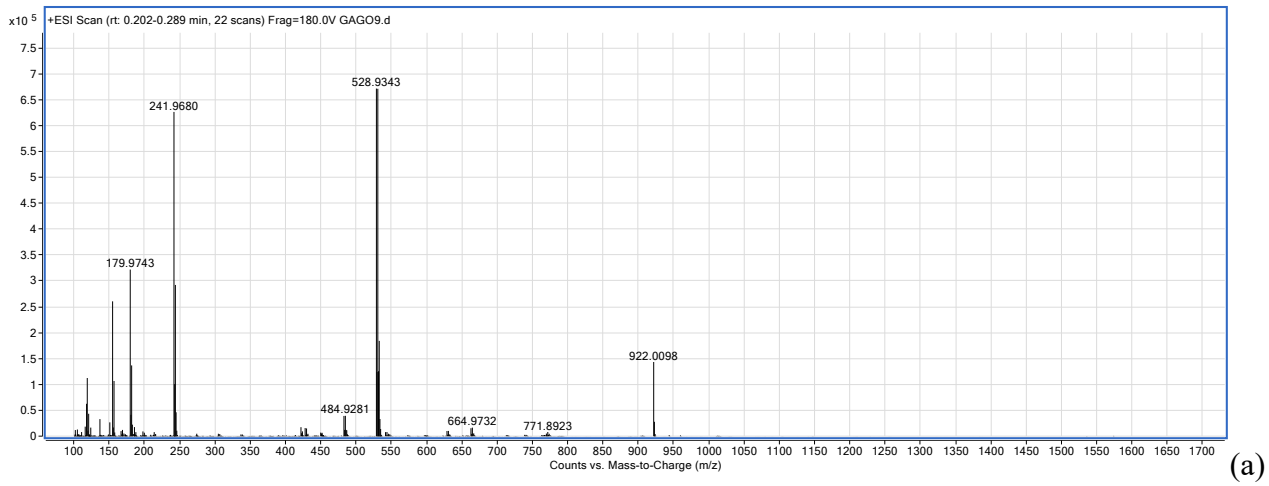

(a)

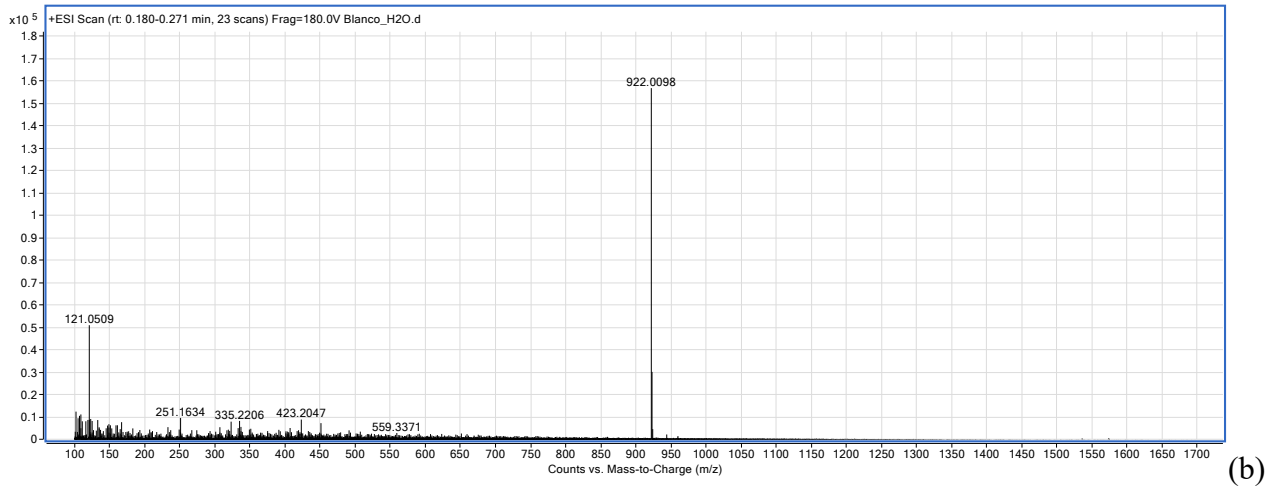

(b)

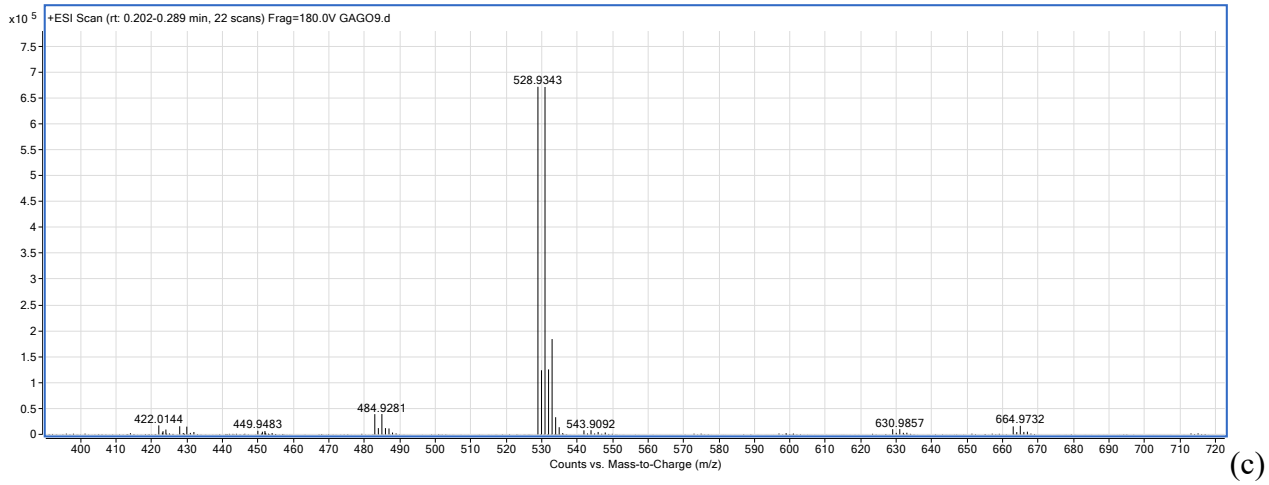

(c)

Figure S3.6. ESI^+ mass spectra of sample at pH = 4.0 (a), the blank (b) and a magnification (c).

Sample at pH = 7.4. 0.092 g. Experimental: C, 28.68; H, 2.54; N, 22.27; S, 11.45%.

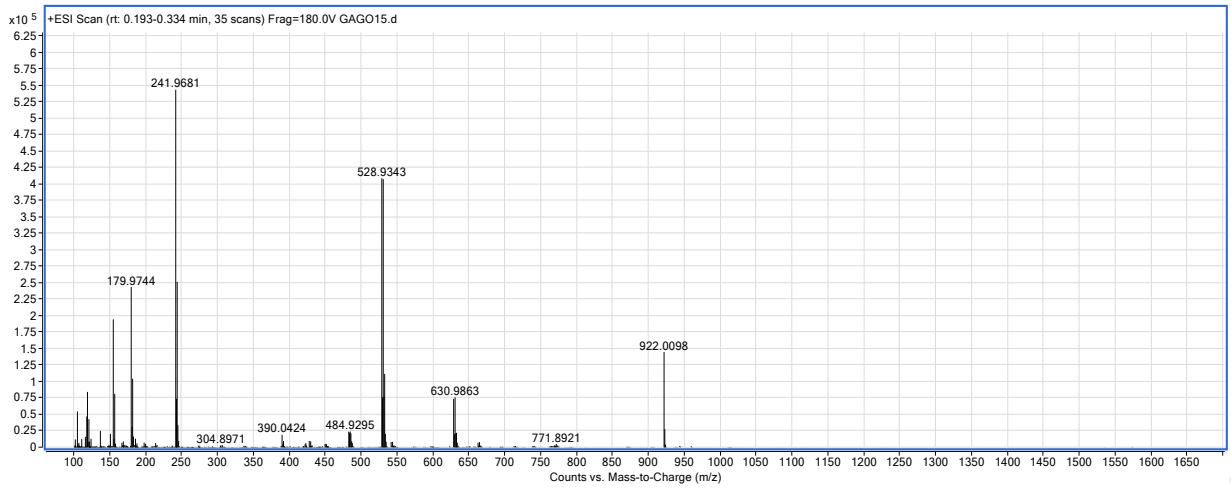

(a)

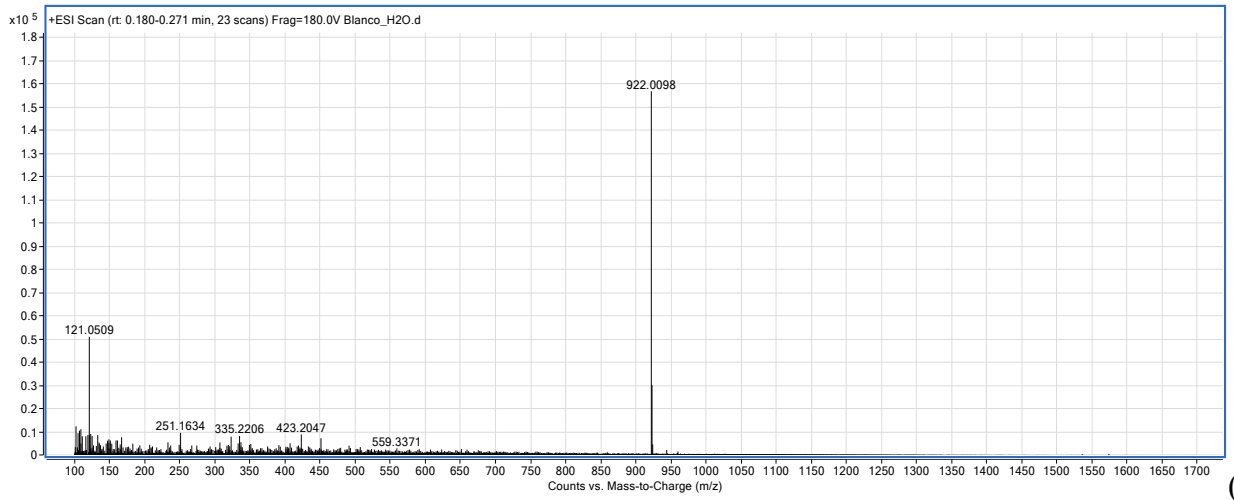

(b)

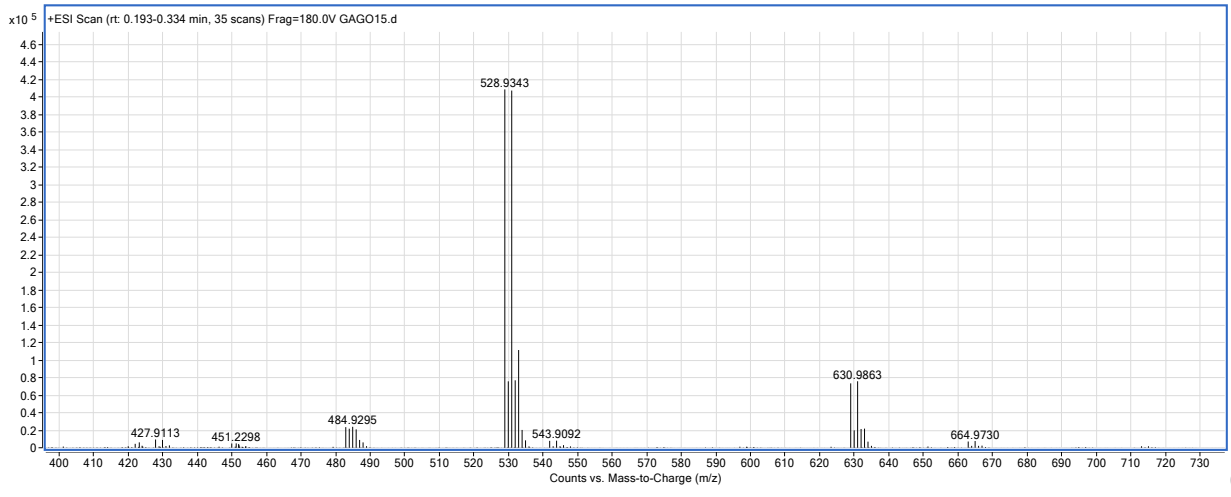

(c)

Figure S3.7. ESI$^+$ mass spectra of sample at pH = 7.4 (a), the blank (b) and a magnification (c).

Sample at pH = 9.0. 0.182 g. Experimental: C, 28.53; H, 2.68; N, 21.8; S, 11.75%. Close to a nominal $Cu_2L_2(NO_3)(OH)$ formula. Calculated for $Cu_2L_2(NO_3)(OH)$, $C_{14}H_{15}Cu_2N_9O_4S_2$, C, 28.86; H, 2.94; N, 21.64; S, 11.01%.

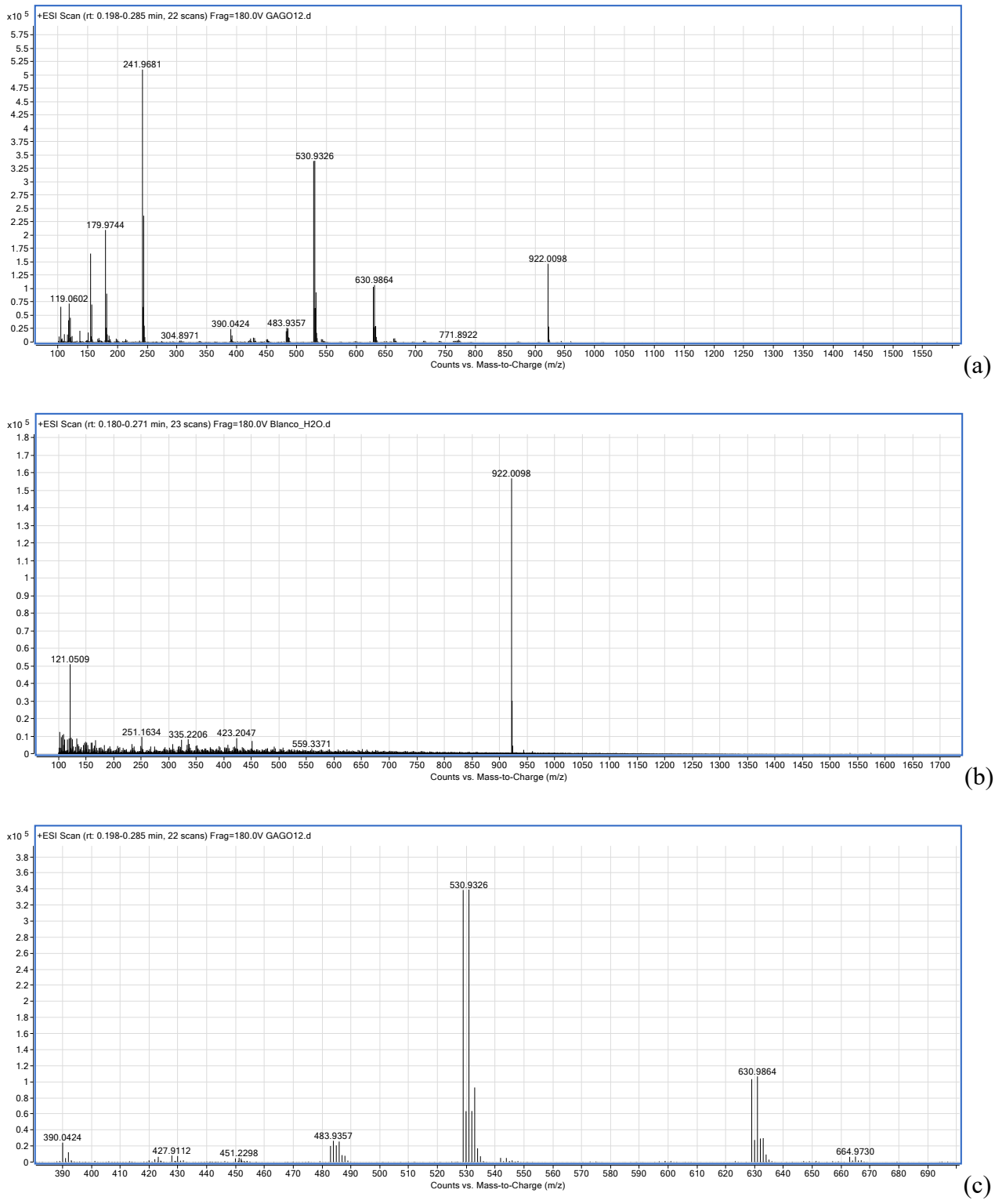

Figure S3.8. ESI^+ mass spectra of sample at pH = 9.0 (a), the blank (b) and a magnification (c).

Summary of the main peaks in the mass spectra depicted in Figures 3.5−3.8. ESI^+ mass spectrometry (m/z): 154.98 $[Cu(NO_3)(MeOH)]^+$, 179.97 $[CuNa(NO_3)(MeOH)]^+$, 241.84 $[CuL]^+$, 422.01 $[Cu(HL)L]^+$, 482.92 $[Cu_2L(NO_3)_2(H_2O)_3]^+$, 528.93 $[Cu_2L_2(HCOO)]^+$, 530.93 $[Cu_2(HL)_2(HCOO)]^+$, 628.99 $[Cu_2L_2(L^{CN})]^+$, 630.99 $[Cu_2(HL)_2(L^{CN})]^+$, 662.97 $[Cu_2L_3]^+$, 664.97 $[Cu_2(HL)_2L]^+$, $[Cu_3L_2(HCOO)(NO_3)_2(H_2O)_3]^+$, 771.89. Note that peaks corresponding to the partially desulfurized $[Cu_2L_2(L^{CN})]^+$ derivatives only appear at pH values above 7.4. In fact, the intensity of these peaks increases with pH in the solids isolated from experiments carried out at 80 ˚C for 3 h (see Figure S3.9). This process depends on time, for the same temperature the longer time the more intense peak of $[Cu_2L_2(L^{CN})]^+$ (Figure S3.10).

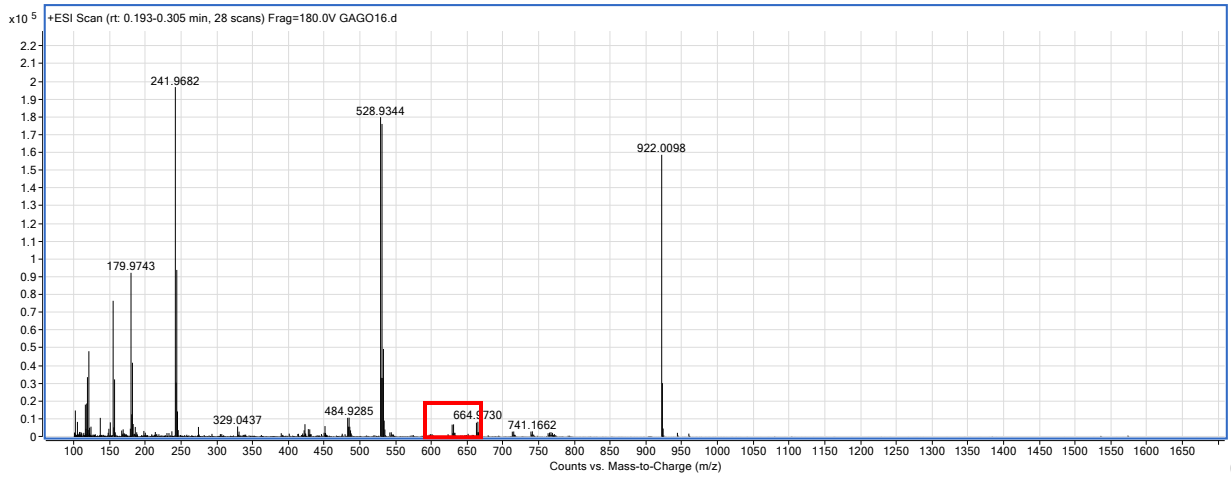

Figure S3.9. ESI^+ mass spectra of samples obtained after 3 h at 80 ˚C and pH 7.4 (a) and 9.0 (b).

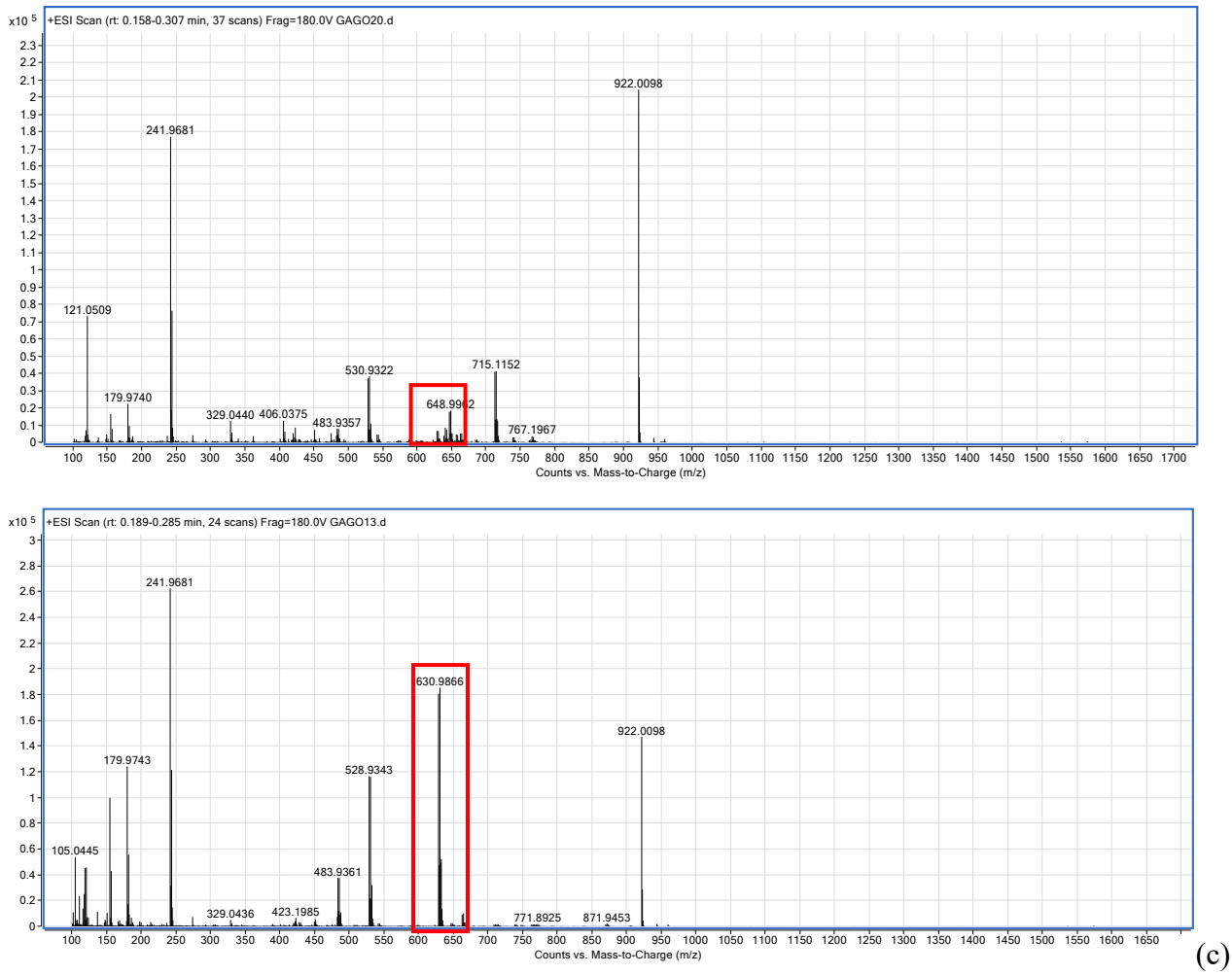

Figure S3.10. ESI^+ mass spectra of samples obtained after treatments at pH = 9.0 in reactions maintained at 80 ˚C for (a) 1 h and (b) 3 h.

Comparative IR studies have been performed on solid mixtures obtained at different pH values. It must be highlighted that the addition of base to solutions of preformed TSC-Cu(II) complexes yield solid mixtures that evidence the appearing of a bands in the 2120−2070 cm^{-1} region. Thus, the sample at pH 7.4 shows the most intense band at 2116 cm^{-1}. This absorption is also present in the compound at pH 9.0 (resolved as a weak and broad in the 2117−2079 cm^{-1} region) and, perhaps, in the spectrum of the complex at pH 4. Note the lack of this band in the spectrum of **[CuL_2]** in spite of being attained at pH 13. This feature could be attributed to the different preparative method where the stoichiometry is (1:2) metal/ligand and addition of base is carried out before the formation of the TSC-Cu(II) complex. In the last conditions, no breakage of the ligand was observed.

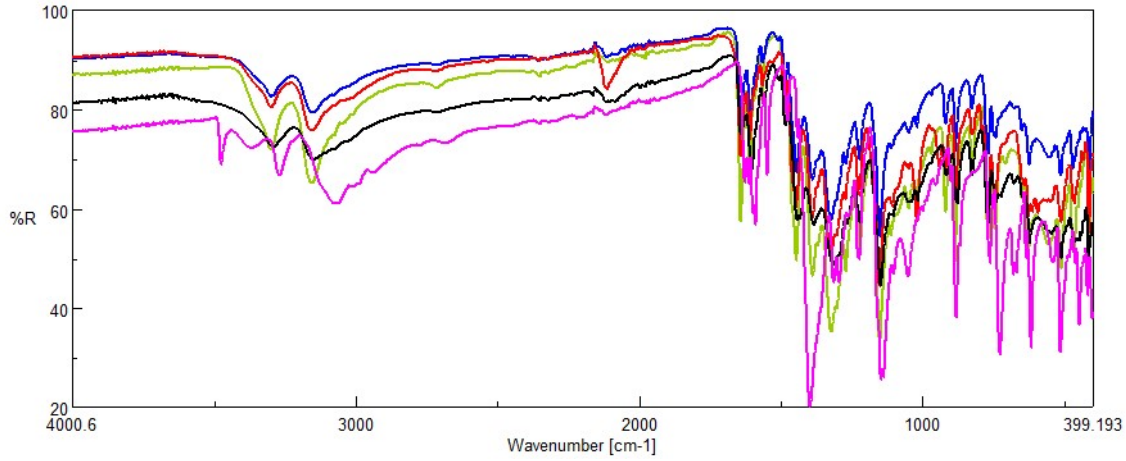

(a)

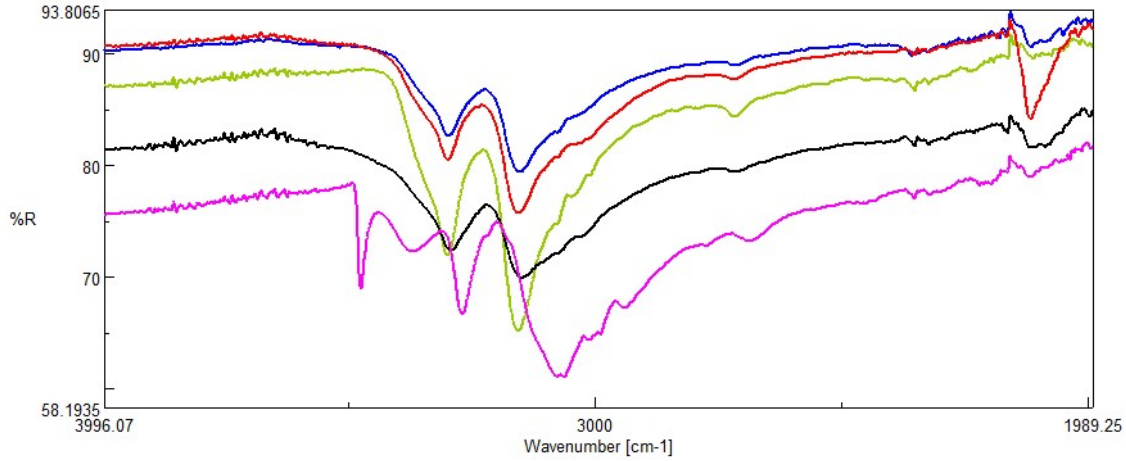

(b)

Figure S3.11. (a) Low pH (~2) light green, pH 4.0 blue, pH 7.4 red, pH 9.0 black and pH 13.0 (**[CuL_2]** ratio 1:2 Cu-ligand) pink spectrum. (b) A magnification is given below.

The processes related with the transformation of the ligand seem to be quite complex. For instance, the bands in the pseudohalide region (2150−2050 cm^{-1}) are often shifted and it is not clear if the origin is really the same (Figure S3.12). On the other hand, an increase in the duration of the treatment at 80 ˚C for the samples at pH 9.0 implies an increment in the intensity of the bands in this region (Figure S3.13).

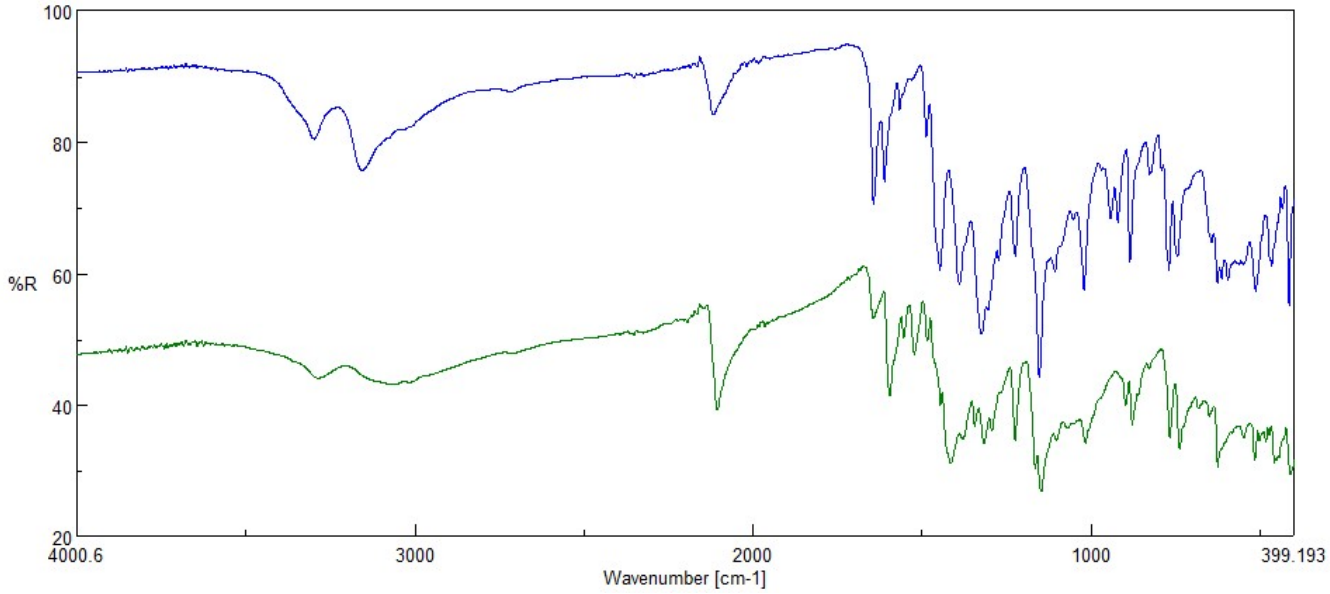

(a)

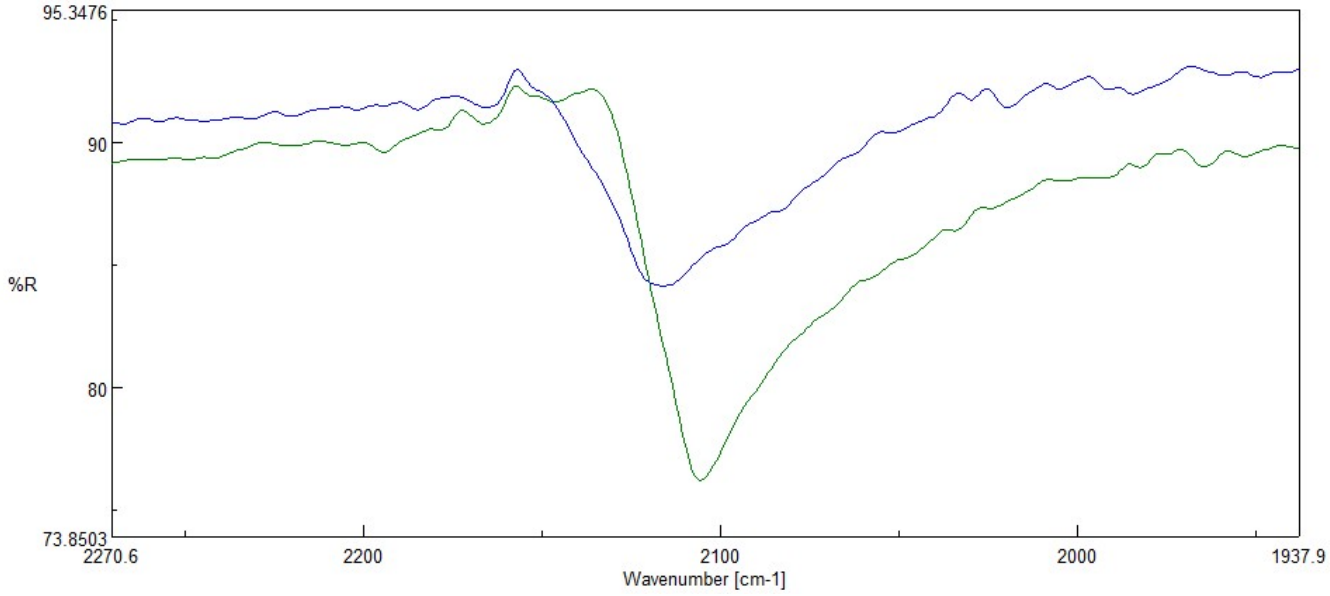

(b)

Figure S3.12. (a) Comparison of IR spectra of the sample obtained at RT and pH 7.4 (in blue) and that at 80 ˚C for 3 h (green). (b) Minima at 2116 (7.4, RT) and 2106 cm^{-1} (9.0, 80 ˚C).

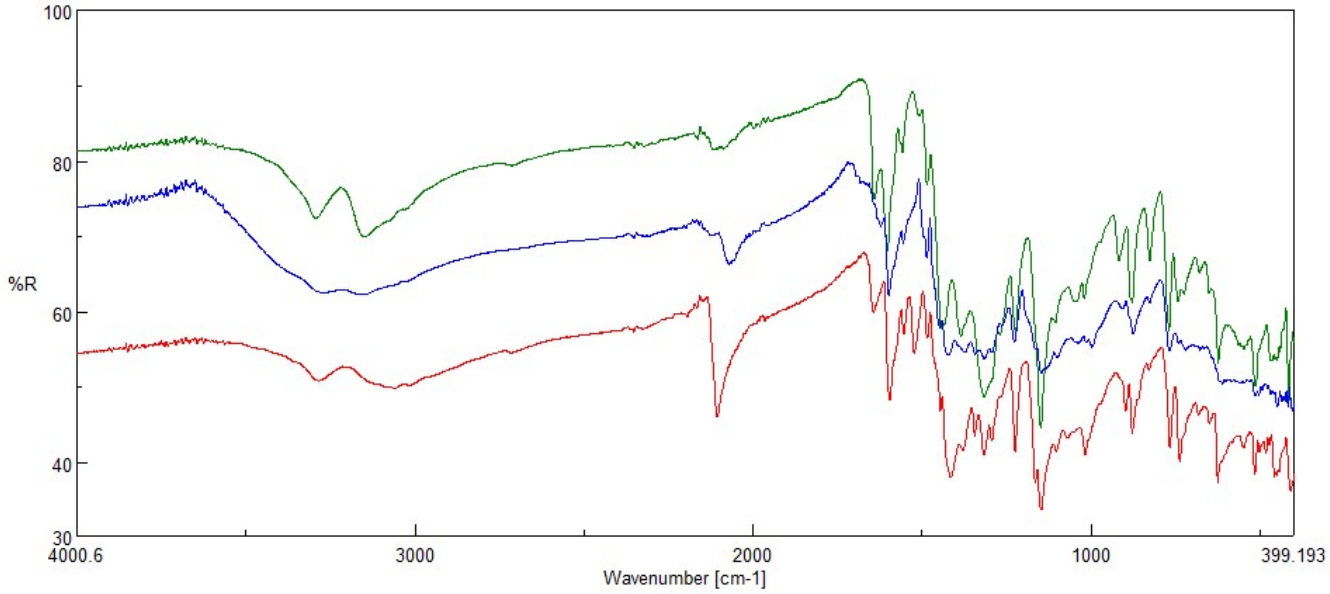

(a)

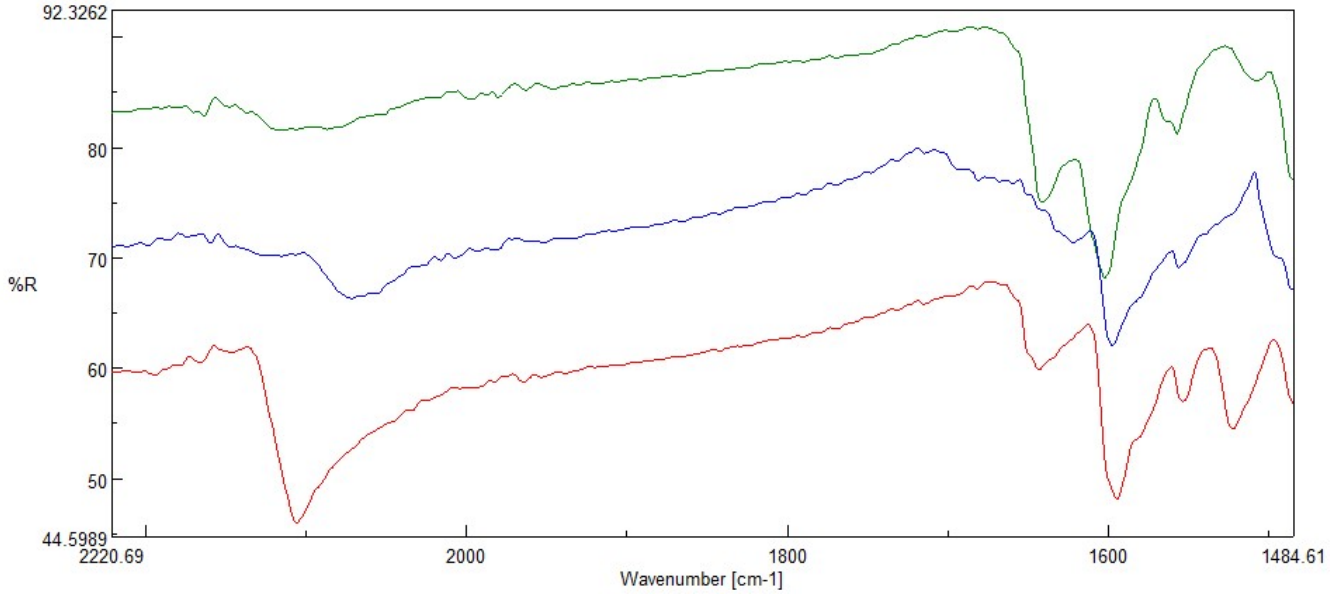

(b)

Figure S3.13. (a) IR spectra of the samples obtained at pH 9.0 and RT (green), 80 ˚C for 1 h (blue) and 80 ˚C for 3 h (red). (b) A magnification is given below.

4. Computational studies

1.- Thermochemistry

Table S4.1.1. Calculated values of thermochemical parameters.

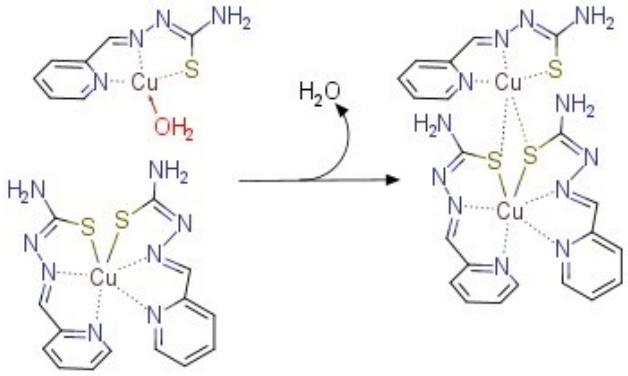

I II

	Structure I			Structure II		Thermochemistry	
	Cu_Oh	Cu_tricoord_aq	Reactants	Oh+PC	water	a.u.	kcal/mol
E+ZPE	-2685,51784	-1873,49348	-4559,01132	-4482,71584	-76,398367	-0,10289	-64,5644636
Et	-2685,49779	-1873,47931	-4558,9771	-4482,68384	-76,395532	-0,10228	-64,1816827
H	-2685,49684	-1873,47837	-4558,97521	-4482,6829	-76,394588	-0,10228	-64,1816827
G	-2685,566	-1873,53509	-4559,10109	-4482,77737	-76,416024	-0,0923	-57,9191368

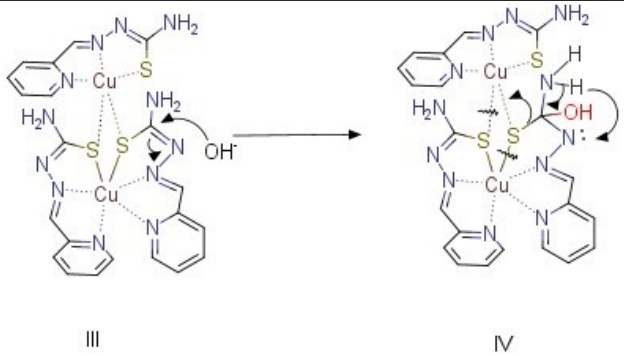

III IV

	Structure III			Structure IV	Thermochemistry	
	Oh+PC	OH-	Reactants	IV	a.u.	kcal/mol
E+ZPE	-4482,71584	-75,718319	-4558,43416	-4558,68374	-0,249581	-156,614475

Et	-4482,68384	-75,715959	-4558,3998	-4558,65116	-0,251361	-157,731443
H	-4482,6829	-75,715015	-4558,39792	-4558,65022	-0,252305	-158,323812
G	-4482,77737	-75,734608	-4558,51197	-4558,74487	-0,232896	-146,144478

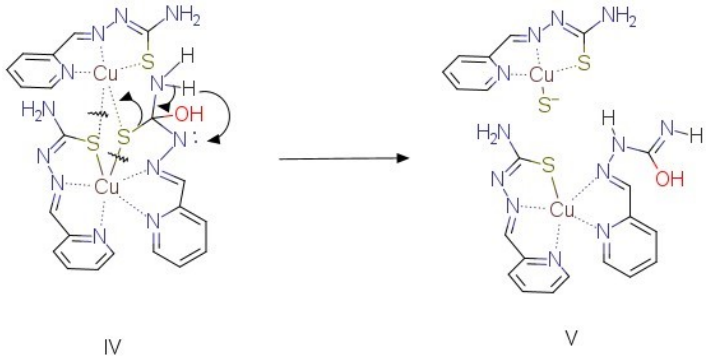

IV V

	Structure IV	Structure V	Thermochemistry	
	IV	V	a.u.	kcal/mol
E+ZPE	-4558,68374	-4558,7079	-0,024164	-15,1631422
Et	-4558,65116	-4558,67546	-0,024299	-15,247856
H	-4558,65022	-4558,67452	-0,024299	-15,247856
G	-4558,74487	-4558,76976	-0,024886	-15,6162041

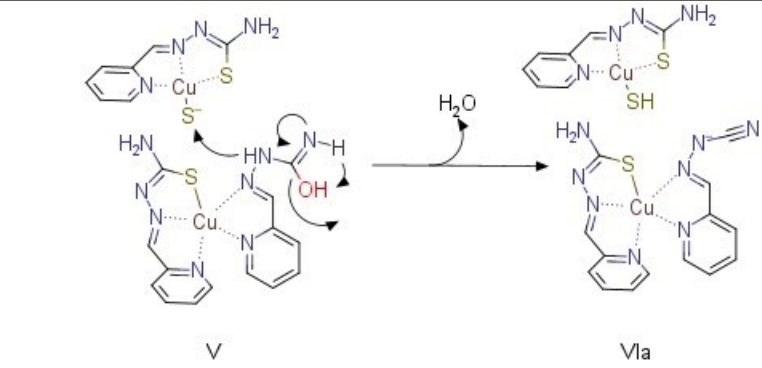

V VIa

	Structure V	Structure VIa		Thermochemistry	
	V	VIa	water	a.u.	kcal/mol
E+ZPE	-4558,7079	-4482,23291	-76,398367	0,076624	48,0822962
Et	-4558,67546	-4482,20114	-76,395532	0,078794	49,4439921
H	-4558,67452	-4482,20019	-76,394588	0,079738	50,0363611
G	-4558,76976	-4482,29418	-76,416024	0,059552	37,3694522

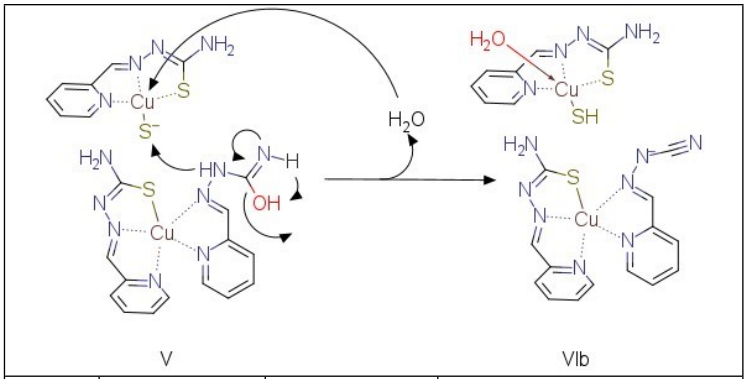

V VIb

	Structure V	Structure VIb	Thermochemistry	
	V	VIb	a.u.	kcal/mol
E+ZPE	-4558,7079	-4558,72544	-0,017541	-11,007146
Et	-4558,67546	-4558,69252	-0,017056	-10,7028039
H	-4558,67452	-4558,69158	-0,017056	-10,7028039
G	-4558,76976	-4558,78781	-0,018052	-11,3278034

2

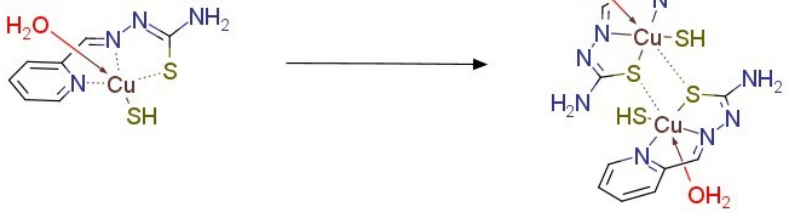

	Monomer	Dimer	Thermochemistry	
	Cu_NNS_SH_aq	Dímero_Rubén_hidrat	a.u.	kcal/mol
E+ZPE	-2272,59266	-4545,28729	-0,10197	-63,9871547
Et	-2272,57785	-4545,25799	-0,102277	-64,1798002
H	-2272,57691	-4545,25704	-0,103221	-64,7721693
G	-2272,63446	-4545,34405	-0,075127	-47,1429143

2.- Cartesian coordinates of the structures

Table S4.2.1. Cartesian coordinates of $[CuL(OH_2)_n]^+$.

	X	Y	Z
Cu	0.38231	0.83653	0.00003
C	-281.981	109.711	-0.00015
C	-185.902	-101.572	-0.00006
C	-411.092	0.57534	-0.00005
H	-264.496	216.896	-0.00021
C	-312.055	-161.929	0.00014
C	-425.767	-0.81315	0.00011
H	-496.830	123.854	-0.00012
H	-319.994	-270.123	0.00027
H	-524.549	-126.270	0.00019
C	-0.64535	-183.386	0.00002
H	-0.71252	-292.065	0.00037
N	-172.632	0.33158	-0.00016
N	0.49516	-122.802	-0.00017
N	165.942	-188.272	-0.00003
C	271.277	-105.811	-0.00002
N	392.632	-161.489	0.00015
H	475.294	-103.817	-0.00003
H	401.331	-262.276	0.00013
S	265.995	0.71150	-0.00015
H	174.421	314.086	0.00127
H	0.32699	376.492	-0.00027
O	0.80109	291.917	0.00017

Table S4.2.2. Cartesian coordinates of [CuL_2].

	X	Y	Z
Cu_Oh			
Cu	-0.60532	0.00063	-0.00019
C	151.543	-203.877	-0.54373
C	138.788	-0.20649	-191.861
C	265.466	-250.241	-117.425
H	106.491	-264.786	0.22647
C	254.073	-0.60304	-261.435
C	320.449	-175.220	-222.865
H	308.739	-345.137	-0.87774
H	288.524	-0.00462	-345.195
H	410.294	-207.949	-274.193
C	0.64477	0.95867	-224.641
H	0.85878	160.223	-309.379
N	0.90221	-0.86574	-0.80801
N	-0.30798	124.976	-139.798
N	-110.621	231.186	-164.081
C	-196.750	254.132	-0.65389
N	-281.124	359.792	-0.82840
H	-362.644	364.858	-0.23888
H	-287.907	397.441	-176.384
S	-207.959	165.857	0.86170
C	138.735	0.20451	191.911
C	151.871	203.621	0.54390
C	254.076	0.59896	261.507
C	265.864	249.786	117.467
H	106.940	264.601	-0.22643
C	320.674	174.681	222.934
H	288.391	0.00005	345.289
H	309.327	344.596	0.87820
H	410.573	207.250	274.268
C	0.64198	-0.95929	224.673
H	0.85435	-160.318	309.427
N	-111.060	-230.978	164.063
C	-197.208	-253.812	0.65350
N	-281.744	-359.324	0.82835
H	-363.229	-364.339	0.23836
H	-288.597	-396.938	176.387
S	-208.244	-165.579	-0.86233
N	0.90332	0.86434	0.80820
N	-0.31072	-124.902	139.781

Table S4.2.3. Cartesian coordinates of Oh+SP (Structure II).

	X	Y	Z
Cu	105.863	-0.00279	-0.03746
C	275.299	0.54837	235.248
C	296.752	-147.652	129.490
C	379.272	0.26814	321.598
H	219.710	146.161	250.470
C	402.895	-184.574	213.804
C	447.443	-0.95623	309.460
H	404.673	0.96976	400.206
H	447.541	-282.844	202.758
H	529.944	-120.698	375.254
C	246.527	-232.220	0.27788
H	281.982	-332.902	0.08745
N	236.953	-0.23189	131.591
N	161.244	-174.124	-0.53253
N	111.454	-245.953	-157.121
C	0.30200	-179.078	-234.784
N	-0.21907	-238.706	-344.367
H	-0.92846	-192.345	-398.660
H	-0.09371	-338.401	-355.139
S	-0.17391	-0.06258	-210.187
C	306.131	179.507	-0.67471
C	353.887	-0.20425	-167.403
C	428.294	234.247	-108.269
C	476.844	0.25254	-211.419
H	322.114	-118.713	-198.409
C	517.242	155.497	-179.298
H	451.014	337.626	-0.84492
H	539.020	-0.38518	-273.196
H	613.269	194.285	-211.510
C	210.121	252.778	0.07294
H	220.438	357.097	0.35186
N	0.17404	241.565	128.081
C	-0.77837	159.835	168.426
N	-171.418	208.706	252.030
H	-251.564	152.655	276.100
H	-172.582	307.959	270.961
S	-0.87004	-0.13656	132.317
N	269.510	0.48400	-0.87271
N	111.732	180.381	0.52743
Cu	-204.932	-0.49775	-0.59203
C	-200.264	252.003	-118.496
C	-374.465	164.071	0.09442

C	-260.269	375.640	-125.552
H	-104.607	236.355	-167.228
C	-442.444	287.711	0.03790
C	-385.741	394.040	-0.62958
H	-211.095	456.554	-178.272
H	-539.060	296.250	0.52528
H	-436.532	489.780	-0.68082
C	-427.529	0.49939	0.74716
H	-523.782	0.48847	124.908
N	-252.201	144.791	-0.52831
N	-354.902	-0.60089	0.64344
N	-404.543	-175.666	112.496
C	-331.612	-280.201	0.79327
N	-372.430	-402.721	118.703
H	-322.235	-484.989	0.89928
H	-461.649	-412.081	165.002
S	-181.365	-274.190	-0.14376

Table S4.2.4. Cartesian coordinates of water.

	X	Y	Z
O	0.00000	0.00000	0.11919
H	0.00000	0.75929	-0.47675
H	0.00000	-0.75929	-0.47675

Table S4.2.4. Cartesian coordinates of OH^-.

	X	Y	Z
O	0.00000	0.00000	0.10927
H	0.00000	0.00000	-0.87412

Table S4.2.5. Cartesian coordinates of Structure IV.

Cu	103.907	0.09098	0.00270
C	260.121	0.90208	240.252
C	278.263	-124.312	163.556
C	358.094	0.71020	336.315
H	207.796	184.473	238.195
C	377.164	-153.875	258.950
C	419.603	-0.54263	344.964
H	382.950	150.693	405.444
H	417.793	-254.324	263.727
H	496.690	-0.73912	418.886

C	231.385	-220.470	0.70216
H	267.758	-322.469	0.65999
N	224.108	0.00055	147.177
N	154.875	-173.652	-0.26008
N	114.017	-254.069	-120.025
C	0.50043	-192.738	-232.583
N	-0.41620	-286.060	-287.101
H	-0.92238	-247.116	-365.810
H	-104.457	-325.133	-217.524
S	-0.27305	-0.14668	-195.636
C	310.422	179.896	-0.68801
C	362.971	-0.31744	-143.557
C	436.708	228.336	-110.702
C	488.131	0.07366	-185.539
H	331.309	-132.650	-164.725
C	527.363	142.071	-166.942
H	458.941	333.855	-0.98148
H	553.110	-0.63080	-236.150
H	625.142	176.757	-198.954
C	212.521	260.465	-0.09925
H	222.705	366.949	0.07738
N	0.10258	263.810	100.234
C	-0.85133	189.002	148.274
N	-183.844	248.039	223.292
H	-270.825	197.033	229.168
H	-193.225	347.806	208.884
S	-0.90010	0.11203	138.143
N	274.924	0.45649	-0.75980
N	109.075	193.207	0.38937
Cu	-200.990	-0.53924	-0.50494
C	-214.089	239.732	-141.784
C	-385.632	156.072	-0.07086
C	-276.388	361.755	-155.199
H	-119.145	222.533	-191.177
C	-456.014	278.515	-0.19160
C	-401.910	381.515	-0.92219
H	-229.358	440.084	-213.465
H	-552.456	287.962	0.29873
H	-454.468	475.995	-102.235
C	-433.382	0.46355	0.67049
H	-528.476	0.45736	119.351
N	-262.279	136.039	-0.68355
N	-355.250	-0.61333	0.67472
N	-401.722	-173.653	127.038
C	-322.408	-276.400	111.102

N	-355.917	-395.476	169.570
H	-312.423	-478.644	132.830
H	-451.464	-403.831	201.534
S	-169.032	-272.475	0.22910
O	141.248	-155.347	-334.408
H	177.963	-239.886	-365.142

Table S4.2.6. Cartesian coordinates of Structure V.

	X	Y	Z
Cu	-0.99296	-0.07854	0.02057
C	-231.803	-162.760	220.482
C	-303.455	0.51465	180.106
C	-329.895	-184.308	314.695
H	-157.866	-240.101	206.046
C	-407.282	0.37573	275.451
C	-423.109	-0.81409	341.777
H	-332.531	-277.499	369.954
H	-471.881	122.661	294.498
H	-502.143	-0.94956	414.923
C	-278.914	168.780	109.455
H	-336.182	259.495	125.048
N	-220.038	-0.51907	143.594
N	-181.628	167.573	0.17325
N	-158.399	299.283	-0.24459
C	-140.448	338.914	-157.089
N	-110.599	460.755	-179.821
H	-100.907	473.433	-280.448
S	0.22937	0.13451	-186.347
C	-278.556	-187.862	-110.556
C	-354.728	0.24391	-143.443
C	-392.974	-243.652	-167.844
C	-472.985	-0.21821	-199.972
H	-333.858	129.963	-144.029
C	-494.232	-159.056	-211.103
H	-400.408	-351.302	-178.826
H	-545.315	0.49034	-238.650
H	-585.353	-198.694	-254.776
C	-169.394	-266.316	-0.62925
H	-163.842	-374.414	-0.71015
N	0.21764	-272.306	0.53135
C	109.497	-199.419	120.753
N	206.623	-267.250	185.926
H	287.200	-214.574	216.338
H	221.228	-363.458	158.194

S	105.764	-0.25028	139.886
N	-260.445	-0.54533	-0.88937
N	-0.78725	-199.435	0.00490
Cu	197.724	0.61288	-0.54878
C	244.888	-223.187	-160.813
C	406.627	-128.699	-0.21622
C	320.676	-336.459	-181.126
H	148.926	-211.090	-209.731
C	490.246	-241.841	-0.39569
C	447.507	-346.177	-118.066
H	283.288	-415.491	-245.199
H	587.665	-242.819	0.08453
H	510.212	-433.539	-133.234
C	443.922	-0.15868	0.54005
H	539.341	-0.06395	104.885
N	280.833	-119.939	-0.80352
N	355.815	0.83355	0.57840
N	391.848	197.226	121.742
C	301.029	291.118	112.422
N	322.497	410.513	176.010
H	271.425	489.924	140.432
H	417.841	427.753	205.105
S	149.481	273.096	0.24249
O	-166.819	245.429	-251.779
H	-109.806	165.460	-234.373
H	-104.323	355.502	0.40308

Table S4.2.7. Cartesian coordinates of Structure VIa.

	X	Y	Z
Cu	-108.399	0.07921	-0.06563
C	-269.897	-0.93161	221.443
C	-312.251	117.744	145.383
C	-376.339	-0.88432	310.039
H	-204.811	-179.052	223.453
C	-421.609	131.807	231.845
C	-456.272	0.26213	314.418
H	-394.303	-171.647	377.124
H	-476.416	225.383	233.068
H	-540.929	0.33429	381.959
C	-270.195	220.207	0.57756
H	-316.354	318.237	0.54437
N	-240.243	0.03067	131.653
N	-173.980	191.573	-0.26853
N	-139.334	298.767	-0.99805

C	-0.45386	296.243	-191.605
N	0.39626	329.088	-267.004
S	0.19693	-0.03009	-192.286
C	-302.717	-169.205	-0.96183
C	-346.226	0.41015	-179.492
C	-422.894	-218.835	-151.432
C	-464.597	0.00397	-236.779
H	-311.754	141.585	-199.134
C	-506.462	-133.667	-219.645
H	-446.284	-324.228	-140.010
H	-522.121	0.69179	-297.670
H	-599.788	-169.011	-262.348
C	-208.433	-248.341	-0.29225
H	-217.108	-355.493	-0.14797
N	-0.16364	-252.694	0.93515
C	0.78149	-181.533	148.765
N	170.248	-245.963	227.673
H	257.679	-197.209	240.732
H	178.158	-345.414	210.439
S	0.93817	-0.04725	140.414
N	-267.921	-0.35152	-0.99531
N	-109.283	-180.577	0.25648
Cu	189.812	0.39183	-0.66109
C	216.528	-261.649	-120.068
C	389.248	-156.060	-0.03855
C	282.515	-383.187	-118.114
H	120.367	-250.017	-168.790
C	463.241	-277.058	0.00411
C	409.431	-390.484	-0.55903
H	237.374	-469.883	-164.905
H	561.392	-277.460	0.46823
H	464.221	-484.252	-0.53885
C	434.341	-0.33841	0.48095
H	531.816	-0.21195	0.93868
N	263.917	-149.785	-0.61411
N	352.756	0.72399	0.37903
N	409.806	189.602	0.78328
C	336.399	294.877	0.68456
N	381.393	418.207	109.196
H	334.029	498.781	0.71164
H	481.966	426.363	116.882
S	161.384	284.027	0.24172
H	169.795	317.212	-108.767

Table S4.2.8. Cartesian coordinates of Structure VIb.

	X	Y	Z
Cu	-123.921	-0.00856	-0.01987
C	-319.404	-0.04880	219.966
C	-336.869	162.315	0.64668
C	-436.198	0.34386	283.197
H	-260.137	-0.83959	263.121
C	-455.351	209.492	122.414
C	-508.086	143.065	232.032
H	-468.564	-0.16362	373.354
H	-503.433	297.472	0.80998
H	-600.407	176.288	278.426
C	-275.057	223.689	-0.47119
H	-311.814	314.686	-0.93258
N	-272.136	0.49205	105.854
N	-170.655	162.232	-0.97429
N	-112.431	230.867	-197.804
C	-0.02242	189.918	-255.526
N	0.99714	186.604	-316.188
S	0.27324	-0.71856	-147.183
C	-321.252	-192.916	-0.42370
C	-337.413	-0.30934	-204.943
C	-439.225	-255.065	-0.88245
C	-452.504	-0.86279	-256.909
H	-292.438	0.52575	-256.942
C	-507.658	-200.261	-194.460
H	-472.763	-346.494	-0.40292
H	-497.204	-0.45263	-346.750
H	-598.952	-245.749	-231.609
C	-238.480	-244.563	0.58954
H	-252.418	-341.256	106.198
N	-0.44900	-218.022	176.949
C	0.46579	-133.411	216.463
N	154.267	-179.494	287.910
H	234.131	-117.877	289.010
H	174.594	-277.985	276.560
S	0.43877	0.43426	188.056
N	-275.434	-0.72565	-0.92457
N	-139.834	-165.020	0.94796
Cu	181.222	0.20437	-0.30431
C	224.721	-274.245	-0.43992
C	408.850	-144.529	0.02588
C	299.201	-390.838	-0.41426
H	117.667	-279.229	-0.57649
C	493.537	-258.274	0.03327
C	438.618	-382.054	-0.20588

H	250.219	-486.625	-0.54585
H	599.002	-245.524	0.25704
H	500.554	-471.290	-0.20419
C	448.696	-0.15352	0.36647
H	548.569	0.10368	0.69979
N	276.018	-150.119	-0.33692
N	354.920	0.80224	0.30962
N	399.333	199.484	0.78779
C	321.973	301.579	0.66011
N	349.190	420.813	129.894
H	325.623	504.693	0.78556
H	440.227	422.829	174.283
S	161.779	297.538	-0.18725
H	207.660	264.018	-142.357
H	226.603	0.70346	-267.307
H	372.962	0.34774	-211.520
O	278.739	0.27683	-193.115

Table S4.2.9. Cartesian coordinates of Monomer [$CuL(OH_2)(SH)$].

	X	Y	Z
H	0.68295	330.721	-0.97509
S	-0.19463	277.689	-0.09623
C	-272.190	0.76080	-0.14695
C	-169.375	-132.584	-0.02623
C	-398.263	0.20567	-0.09194
H	-260.424	183.372	-0.24795
C	-295.797	-196.242	0.01447
C	-410.381	-120.344	-0.00354
H	-485.612	0.84659	-0.12470
H	-299.270	-304.697	0.05582
H	-508.183	-167.345	0.03401
C	-0.47487	-203.300	-0.03700
H	-0.41092	-311.625	-0.00634
N	-156.559	0.05583	-0.07669
N	0.61999	-129.083	-0.09065
N	182.655	-190.648	-0.15577
C	281.202	-104.808	-0.09253
N	410.412	-149.842	-0.12513
H	481.123	-0.83206	-0.39421
H	423.288	-244.898	-0.44557
S	256.312	0.68819	0.10468
H	103.654	0.79062	194.118
H	-0.23844	-0.06489	227.011
O	0.20176	0.43832	158.231

Cu	0.33630	0.60599	-0.32624

Table S4.2.10. Cartesian coordinates of Dimer [{CuL(OH_2)(SH)}$_2$].

Cu	-132.499	0.00466	-0.83251
S	0.82847	-0.55708	-136.197
N	-0.43303	-274.433	-0.39087
N	160.387	-314.256	-145.374
H	156.430	-405.790	-101.885
H	252.890	-273.227	-145.460
C	-246.970	-217.144	0.47293
H	-254.319	-316.316	0.90261
N	-315.479	-0.06655	-0.23928
C	-475.624	-136.704	109.410
H	-495.718	-227.993	164.636
C	-349.232	-122.032	0.46299
C	0.61679	-229.222	-101.143
C	-411.239	0.89253	-0.31658
H	-381.716	177.461	-0.87701
N	-137.015	-178.752	-0.16680
C	-536.053	0.80665	0.25474
H	-606.982	161.856	0.14238
C	-568.904	-0.36706	0.99120
H	-666.104	-0.46699	146.468
S	-144.859	209.403	-197.455
H	-201.261	138.195	-297.110
Cu	132.507	-0.00453	0.83286
S	-0.82874	0.55728	136.248
N	0.43300	274.434	0.39109
N	-160.392	314.291	145.372
H	-156.421	405.814	101.862
H	-252.899	273.271	145.450
C	246.965	217.153	-0.47259
H	254.319	316.338	-0.90194
N	315.462	0.06642	0.23892
C	475.605	136.718	-109.423
H	495.710	228.036	-164.599
C	349.221	122.039	-0.46299
C	-0.61685	229.239	101.171
C	411.193	-0.89307	0.31521
H	381.661	-177.538	0.87523
N	137.013	178.754	0.16709
C	535.989	-0.80725	-0.25650
H	606.892	-161.950	-0.14493

C	568.861	0.36690	-0.99219
H	666.054	0.46687	-146.581
S	144.878	-209.402	197.499
H	201.351	-138.235	297.144
H	198.897	124.380	325.330
H	299.692	110.628	205.451
H	-299.512	-110.884	-205.421
H	-198.742	-124.410	-325.325
O	208.257	0.96207	233.591
O	-208.130	-0.96207	-233.598

5. References

[1] R. Gil-García, R. Zichner, V. Díez-Gómez, B. Donnadieu, G. Madariaga, M. Insausti, L. Lezama, P. Vitoria, M. R. Pedrosa and J. García-Tojal, *Eur. J. Inorg. Chem.*, 2010, 4513–4525.

[2] J. C. Bonner and M. E. Fisher, Phys. Rev., 1964, **A 135**, 640–658.

[3] O. Kahn, Molecular Magnetism, VCH Publishers, Weinheim, 1993.

[4] A. G. Bingham, H. Bögge, A. Müller, E. W. Ainscough and A. M. Brodie, *J. Chem. Soc. Dalt. Trans.*, 1987, 493–499.

[5] J. García-Tojal, R. Gil-García, V. I. Fouz, G. Madariaga, L. Lezama, M. S. Galletero, J. Borrás, F. I. Nollmann, C. García-Girón, R. Alcaraz, M. Cavia-Saiz, P. Muñiz, Ò. Palacios, K. G. Samper and T. Rojo, *J. Inorg. Biochem.*, 2018, **180**, 69–79.

[6] P. Gómez-Saiz, R. Gil-García, M. A. Maestro, J. L. Pizarro, M. I. Arriortua, L. Lezama, T. Rojo and J. García-Tojal, *Eur. J. Inorg. Chem.*, 2005, 3409–3413.

[7] J. García-Tojal, M. K. Urtiaga, R. Cortés, L. Lezama, M. I. Arriortua and T. Rojo, *J. Chem. Soc., Dalt. Trans.*, 1994, 2233–2238.

[8] R. Gil-García, P. Gómez-Saiz, V. Díez-Gómez, G. Madariaga, M. Insausti, L. Lezama, J. V. Cuevas and J. García-Tojal, *Polyhedron*, 2014, **81**, 675–686.